U.S.NRC
United States Nuclear Regulatory Commission
Protecting People and the Environment

Technical Letter Report

TLR-RES/DE/CIB-2020-05

BENCHMARKS AND SENSITIVITY STUDIES FOR SUBCRITICAL CRACK GROWTH ANALYSES USING XFEM IN ABAQUS/STANDARD

Date:

August 21, 2020

Prepared in response to Task B3 in User Need Request NRR-2020-004, by:

L. T. Hill
Engineering Mechanics Corporation of Columbus

F.W. Brust
Engineering Mechanics Corporation of Columbus

S. Kalyanam
Engineering Mechanics Corporation of Columbus

NRC Project Manager:

Giovanni Facco
Materials Engineer
Component Integrity Branch

Division of Engineering
Office of Nuclear Regulatory Research
U.S. Nuclear Regulatory Commission
Washington, DC 20555–0001

DISCLAIMER

This report was prepared as an account of work sponsored by an agency of the U.S. Government. Neither the U.S. Government nor any agency thereof, nor any employee, makes any warranty, expressed or implied, or assumes any legal liability or responsibility for any third party's use, or the results of such use, of any information, apparatus, product, or process disclosed in this publication, or represents that its use by such third party complies with applicable law.

This report does not contain or imply legally binding requirements. Nor does this report establish or modify any regulatory guidance or positions of the U.S. Nuclear Regulatory Commission and is not binding on the Commission.

Final Report

On

Support for XFEM Component Integrity Analysis: Task 2

Benchmarks and Sensitivity Studies for Subcritical Crack Growth Analyses using XFEM in Abaqus/Standard

U.S. Nuclear Regulatory Commission
Prime Contract No.: NRC-HQ-25-14-E-0004
Task Order No. 31310019F0075
Emc^2 Project Number: 19-G121-01
As a Subcontractor to NUMARK Associates, Inc.

to

U.S. Nuclear Regulatory Commission
Washington, D.C. 20555-0001

By

L.T. Hill, F.W. Brust and S. Kalyanam

Engineering Mechanics Corporation of Columbus
3518 Riverside Drive, Suite 202
Columbus, OH 43221
Phone/Fax (614) 459-3200/6800

August 21, 2020

As a Subcontractor to
NUMARK Associates, Inc.
1220 19th Street, NW, Suite 500
Washington, DC 20036

EXECUTIVE SUMMARY

This report represents the second of four total tasks associated with the *Support for XFEM Component Integrity Analysis* program. The other reports are completed or undergoing final review at present. Task 1 (Literature Survey) provides a literature review of the eXtended Finite Element Method (XFEM) which summarizes the capabilities and limitations for current codes which have implemented XFEM based crack growth. This Task 2 report discusses the Abaqus XFEM implementation coupled with a simplified fatigue procedure which allowed exploration of optimum parameter definitions to provide the most appropriate solutions for constant-amplitude fatigue and PWSCC (Primary Water Stress Corrosion Crack) crack growth analyses. This Task 2 report explores five crack geometry cases, from simple two-dimensional constant-amplitude fatigue cases to the VC Summer hot leg dissimilar metal weld (DMW) PWSCC analysis for three-dimensional axial PWSCC growth and leakage. The Task 3 report (Evaluation of PWSCC-type crack growth in Abaqus XFEM for Complex geometries) provides detailed solutions for the VC Summer and control rod drive mechanism (CDRM) XFEM based crack growth to leakage solutions. The Task 3 report summarizes the best ABAQUS based XFEM solution parameter definitions and compares the solutions to crack growth analyses performed in the past using other methods. The Task 3 report also identifies limitations in the analysis process and pitfalls possible. Task 4 provides a summary of solutions performed by the NRC and contractors, and other organizations that may be used in the future for further benchmarking. The Benchmark solutions presented provide references along with other data necessary to perform XFEM based solutions and predicted results using other PWSCC growth methods for benchmark comparisons.

In this current Task 2 report, the conditions and assumptions of the Abaqus simplified fatigue procedure were used to define a relationship between the Abaqus Paris-like fatigue crack growth law and a general PWSCC growth rate relation. So, in addition to readily available constant-amplitude fatigue benchmarks, PWSCC Abaqus XFEM crack growth analyses were executed to determine those parameters that control the accuracy, repeatability of analysis results and computational resources for this capability.

Specifically, 2-D and simple 3-D models were evaluated in a systemic approach as highlighted by the activities listed below:

- Evaluation Parameters – The crack growth rate and crack shape were used as the fundamental evaluation criteria for the geometries evaluated with results compared to results using traditional finite element crack results or other acceptable analytical solutions.
- Geometries Studied – Four basic geometries were used to evaluate the capabilities with a focus on different crack front shapes (curved versus straight) and crack extension (planar versus curvilinear).
- Input Parameters Studied – In addition to mesh parameters (mesh size and mesh type), element formulation, fatigue procedure and crack growth parameters were studied. Overall, over forty analysis models were completed in this study.

It has been found that even performing basic crack growth problems will be a challenge without significant benchmarking of results for a given problem class. With that stated, general modeling recommendations are summarized below:

- Software Version: Abaqus/Standard 2020 or later
- Minimum Mesh Refinement of XFEM Enriched Region in Key Structural Dimensions:
  - Thickness (crack growth depth direction): 50-elements
  - Width (crack growth length direction): Use Thickness mesh seed
  - Height (perpendicular to initial crack plane): 10-elements with Thickness mesh seed
- Mesh Type: Structured
- Element Formulation: Quad/Hex with Reduced integration

The analysis parameters for calculating crack growth under these conditions (growth tolerance, fracture criteria, general solution controls) should be set to default values. However, with careful evaluation and benchmarking, non-default parameters could be utilized to obtain robust, accurate solutions in a timely fashion. As an example, for applications with nonplanar curvilinear crack growth, the nonlocal averaging option may be required along the crack front to ensure proper crack propagation directions are calculated.

To provide some assurance that these recommendations were transferrable to more complex geometries, a VC Summer hot leg dissimilar metal weld (DMW) axial flaw assessment was successfully analyzed.

This report documents the models, parameters studied, and other supporting evidence associated with providing these general recommendations.

ACKNOWLEDGEMENTS

The authors gratefully acknowledges the helpful comments provided by the NRC staff during the preparation of this report. In particular, the extensive comments, edits, and contributions from the Office of Nuclear Reactor Regulation and the Component Integrity Branch are gratefully appreciated.

TABLE OF CONTENTS

1 INTRODUCTION

The extended finite element method (XFEM) is a Finite Element Analysis (FEA) method that allows for mesh independent analysis of discontinuities and singularities and can be used to simulate crack growth in complex geometries in a simplified manner. This capability is available in several commercial FEA codes, including Abaqus [1], and is potentially a powerful tool for representing cracks and simulating crack growth in industry relevant models. In addition to its XFEM capabilities, Abaqus can simulate fatigue crack growth using a Paris Law type relationship. Furthermore, Abaqus is capable of modeling this fatigue behavior via a simplified analysis, where a multi-cycle fatigue process is modeled in a single static step. This approach to fatigue may allow for other types of subcritical crack growth, like PWSCC (primary water stress corrosion cracking), to be modeled. By taking advantage of both the XFEM and this simplified fatigue approach in Abaqus, the purpose of this report was then to determine those parameters that control the accuracy, repeatability of analysis results and computational resources for simplified subcritical crack growth applications.

Section 2 provides an overview of the XFEM and the subcritical crack growth capabilities within Abaqus. By understanding the implementations, it is possible to gain insight into the strengths and weaknesses of the techniques as it relates to our applications. Section 3 defines the evaluation criteria and the five geometries studied. Section 4 then provides the detailed sensitivity study where the parameters are defined, and results presented. Sections 5 and 6 summarize the key observations and provides the general modelling recommendations. Appendices are also provided for finite element modeling details for each of the five geometries studied.

2 ABAQUS CAPABILITIES UTILIZED FOR EVALUATION

2.1 XFEM Implementation within Abaqus

XFEM allows for discontinuities that are not aligned with the finite element mesh to simulate crack propagation without remeshing. In essentially all XFEM stationary crack implementations, including Abaqus/Standard [1], the standard displacement (shape) interpolation function is augmented for the crack jump (via the Heaviside enrichment term) and the crack tip enrichment term as shown below:

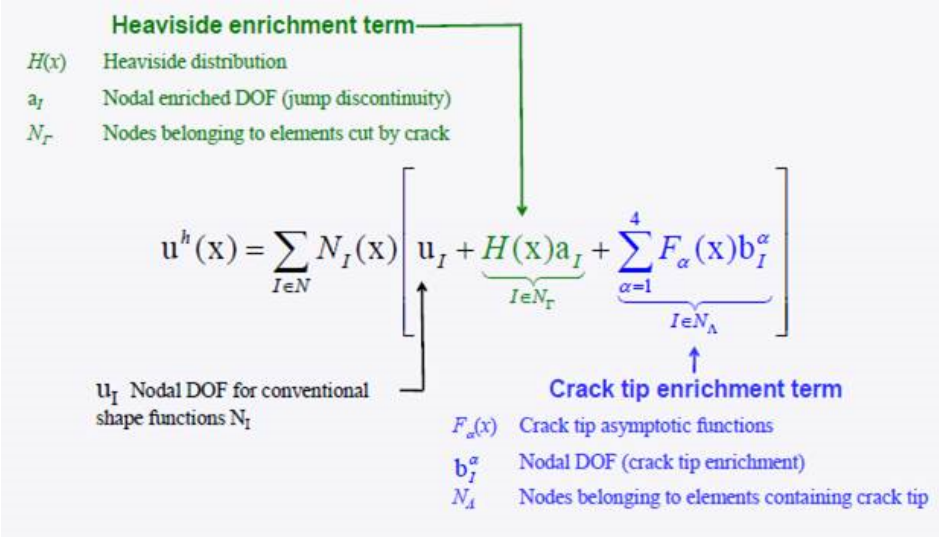

Figure 1 – Standard Displacement Interpolation Function Augmented for XFEM. Adapted from [1].

To better appreciate the terms of this function, consider a 2D finite element model of a cracked body shown in Figure 2. The set of nodes of elements completely cut by the stationary crack, N_Γ, are enriched by the Heaviside (jump discontinuity) enrichment term as denoted by the green circles while the set of nodes of elements around the crack tip (or crack front in three-dimensions), N_Λ, is denoted by the purple squares. Usually, one element, as shown at Crack Tip B in Figure 2 is sufficient but accuracy improvements can be expected by using several elements as seen at Crack Tip A. It should be noted that this is a local partition of unity as the enrichment is added only where it is useful. This substantially reduces the computational efficiency. More details on the enrichment coefficient determination are provided by Belytschko [3].

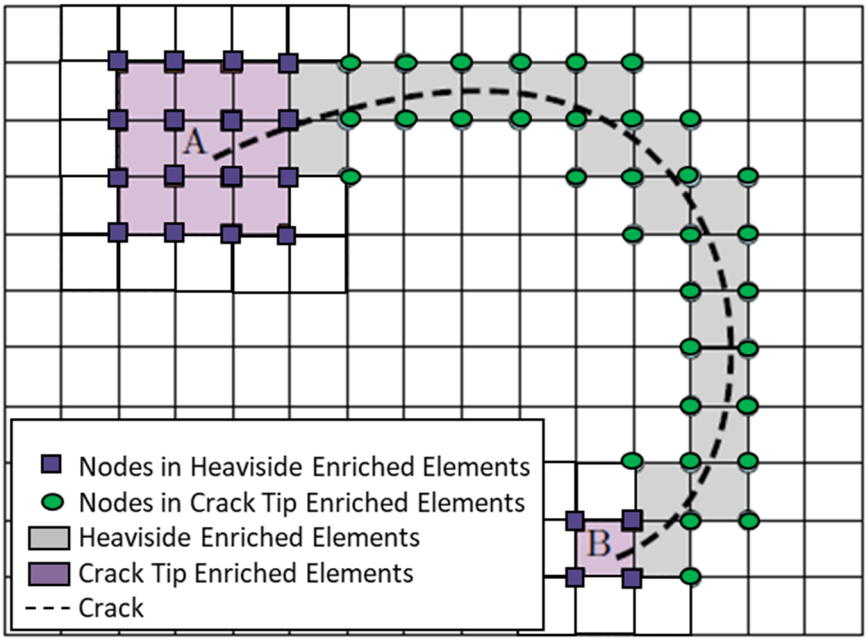

Figure 2 – Arbitrary XFEM Stationary Crack Line in a 2D Structured Mesh with Heaviside (Displacement Jump) Enriched and Crack Tip Enriched Elements. Adapted from [3].

In the original XFEM formulation [2], the numerical integration of elements cut by the discontinuity required special treatment and additional degrees of freedom were introduced which would make the implementation of XFEM into available commercial FE codes difficult. At first, the most commonly adopted method was to divide the element into subdomains on two sides of the line of discontinuity. This method is flexible but not appropriate for history-dependent material where the projection of variables from old Gauss points to new ones are inevitable. As an improvement on this method, Belytschko [3] proposed the 'phantom node' method. In this formulation an overlaid element and 'phantom nodes' were added to cracked elements avoiding the need for additional degrees of freedom. It is this 'phantom node' method that is implemented in Abaqus/Standard. However, this method is limited to elements completely cut by the discontinuity.

To state very clearly, for subcritical crack growth analyses in the Abaqus XFEM implementation using a Paris type relationship that will be discussed in Section 2.2, the near-tip asymptotic singularity is not considered, and only the displacement jump across a cracked element is considered. Therefore, the crack has to propagate across an entire element at a time to avoid the need to model the stress singularity [1]. Further, the strain energy release rate at the crack tip is calculated based on the modified Virtual Crack Closure Technique (VCCT) [1]. Unlike the stationary crack contour integral (J-Integral) and interaction integral (stress intensity factor, K) where fairly coarse meshes are able to capture path independent driving force values, the propagating crack linear-elastic strain energy release rate, G, values are calculated locally and directly for each crack front element.

The Abaqus XFEM capability when combined with the subcritical crack growth procedure has implementation nuances that will be seen to greatly influence mesh refinement requirements in order to obtain accurate and timely results.

Another interesting topic involved in the development of the XFEM is the method used to represent the geometry of discontinuities as they are not meshed in XFEM. It is the Level Set Method (LSM) [46] that makes this possible as the description of cracks is strictly in terms of nodal data. This is accomplished through the use of two orthogonal level set functions. The ψ level set is used to track the crack surface, while the φ level set is used to track the crack tip. For the case when there are multiple crack tips, multiple φ level set functions are used. Therefore, the use of the fast-marching LSM is utilized for capturing crack propagation.

Abaqus simulates time- or cycle-dependent subcritical crack growth in XFEM using a Paris Law type relationship that will be discussed in Section 2.2.

To summarize, mesh independent crack modeling is implemented in Abaqus/Standard using the following methodology:

1. Incorporate the discontinuous geometry (i.e. crack) and the discontinuous solution field into the finite element basis functions
    - eXtended Finite Element Method (XFEM)
2. Quantify the magnitude of the discontinuity – the displacement jump across the crack faces.
    - Heaviside Functions
    - Phantom Nodes
3. Locate the Discontinuity.
    - LSM
4. Define Crack Propagation Criteria
    - Subcritical Crack Growth Law (described in Section 2.2)

In addition to Abaqus (/Standard solver with /CAE pre- and post-processing), XFEM has also been implemented as a core implementation in such DOE-sponsored research codes such as Grizzly developed at Idaho National Laboratory [7], and commercial finite element software codes as Ansys [8] and VirFac Crack/Morfeo[9]. Implementation details will likely vary within and between each code. As an example for the former, Ansys offers both 'phantom node' and 'singularity-based' XFEM methods for stationary crack evaluation. For the latter, Abaqus supports distributed pressure on the crack face while Ansys does not currently support this option.

To provide additional capability for both research and commercial usage, user element and associated subroutines have been coded to further develop capabilities in the basic XFEM methods, level sets and discontinuity abstractions. This current work has been performed in Abaqus using built-in capabilities, but other codes have similar capabilities for method development and structural evaluations. As an example, Spencer [10] demonstrates the 3D XFEM crack propagation capability in Grizzly to simulate the burst behavior of nuclear fuel rod cladding during a loss-of-cooldown accident scenario.

As another approach, 'Morfeo/Crack for Abaqus' [9] utilizes the built-in XFEM capability in Abaqus/Standard along with the user interface of Abaqus/CAE. After initial model setup in Abaqus/CAE, this method is based on calling Abaqus/Standard at each propagation step. Between each step, it reads the Abaqus solution, recovers an XFEM stationary crack solution, accurately computes the Stress Intensity Factors (SIF) which determine the crack advance and updates the Abaqus input file with the new crack position.

2.2 Creation and Considerations for an Abaqus XFEM Subcritical Crack Growth Model

The development of an Abaqus XFEM subcritical crack growth model is performed in three primary steps that are described below. Context of how different modeling aspects for each step can affect the solution results, stability of solution and computation resources are introduced.

Further, the interactive pre-processor Abaqus/CAE makes defining the enrichment region, locating the initial crack and selecting special purpose output variables very straightforward. However, as the *FATIGUE is a relatively new Abaqus capability, the input deck must be hand-edited to incorporate the *FATIGUE procedure and related subcritical crack growth criteria fatigue criteria (*FRACTURE CRITERION,TYPE=FATIGUE). Section 2.2.3 will address converting fatigue constants to those related to PWSCC while Section 2.2.4 provides a complete input file template for this workflow.

2.2.1 Define Enrichment Region

As was conceptually shown in Figure 2, the enrichment regions in an XFEM analysis should consist of elements that are intersected by any initial crack and those that are likely to be intersected by the cracks as they propagate. For the current discussion, a single existing crack will be assumed in the model.

Even though XFEM is said to be mesh independent, it remains nevertheless a finite element method for which the mesh needs to be fine enough to get accurate results. The enriched portion of the finite element mesh needs to be sufficiently refined, as would be the case in a conventional stress analysis. If the mesh is too coarse, the crack propagation process may not be captured in detail. If the mesh is excessively refined, the crack propagation may be computationally slow.

To provide some level of context, normally, analyses of finite element models of components subject to combined membrane and bending loads requires mesh refinement of only four first-order reduced integration continuum elements to obtain accurate displacement and resultant stress fields.[1] For the XFEM, this report will show that an order of magnitude more elements is required to capture a propagating crack in terms of crack growth rate and crack shape.

Knowing the level of refinement needed, if the regions expected to crack are known in advance and limited, the geometry can be partitioned so that the refined regions are be kept to a reasonable size. If needed, tie constraints can then be introduced to join the finely meshed enriched regions to the rest of the model.

The element type and the mesh type used when modeling XFEM cracks are known to impact the results of the analyses. Element types supported by Abaqus include first-order 2D and 3D continuum elements (CPE4, CPS4, CAX4, C3D8, and C3D4), second order tetrahedral 3D continuum elements (C3D10) along with reduced integration/incompatible mode/hybrid formulations. When using a 2D quadrilateral (CPE4) or 3D hexahedral (C3D8) mesh, a structured or unstructured approach can be specified. A structured mesh predominantly consists of regular hexahedral elements in 3D and quadrilateral elements in 2D. Structured mesh types are preferred over free unstructured meshes as structured meshes typically give a more accurate prediction of stress and strain fields ahead of the crack tip.[11] It is noted that due to geometric and/or time constraints that an unstructured mesh may be required. In terms of element type, the focus in this study was on plane strain 2D quadrilateral (CPE4) and first-order 3D continuum hexahedral elements (C3D8); second order tetrahedral elements (C3D10) were not investigated in the enriched region.

With these definitions to consider, the enrichment region itself is simply an element set that can be created in any FEA pre-processor. In the case of Abaqus/CAE, this element set is combined with the initial crack location within the Interaction module. More details are provided in the next section.

2.2.2 Define Initial Crack

As discussed previously, the crack surface and the crack front are defined in Abaqus by means of two level set functions, φ and ψ. If performed manually, it would be difficult to identify, locate and specify these values for the initial flaw. Fortunately, Abaqus/CAE has a very elegant interface using the Special Menu in the Interaction module.

Using the semi-elliptical flaw in a flat plate as an example, Figure 3 shows the initial crack is defined using a part (depicted in the figure as the red-colored area) constructed in the elliptical shape of the crack and instanced in the assembly at the desired location. The crack geometry is defined as the intersection of the crack and component parts from which the appropriate φ and ψ values are written to the Abaqus input deck via the *INITIAL CONDITIONS,TYPE=ENRICHMENT keyword. Note that the crack part need not be meshed or assigned material properties; it is a dummy part present only for the purpose of defining the initial crack.

The XFEM method does not require the mesh to conform to the crack geometry; however, the method does not permit a crack plane to lie parallel and coincidence with element faces.[11] Therefore, in simple problems where the crack is expected to propagate along a straight plane (such as seen in Figure 3) the mesh should be designed such that the expected crack propagation path lies between element faces in the plane perpendicular to the crack propagation direction. While the Abaqus XFEM capability does allow for damage initiation from an initially uncracked structured, sharp cracks will be assumed to be pre-existing for this study.

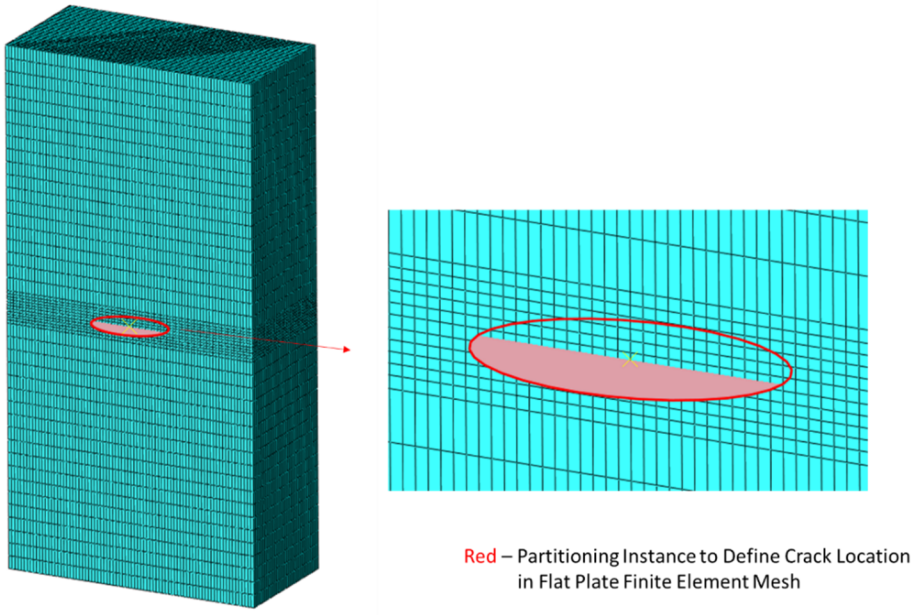

Figure 3 Usage of an Elliptical Crack-Shaped Part in Abaqus/CAE to Locate an Initial XFEM Semi-Elliptical Surface Flaw in a Flat Plate

2.2.3 Define Fatigue Procedure with Associated Constants

Beginning in the Abaqus 2020 release, Abaqus/Standard can simulate linear elastic subcritical crack growth by using XFEM with a Paris Law type relationship defined as:

$$\frac{da}{dN} = C_3 \, \Delta G^{C_4}$$

This relationship calculates a crack growth rate in terms of crack extension (da) per cycle (dN) using the change in strain energy release rate, ΔG, over the course of one loading cycle at the crack tip to determine the crack extension for that cycle, using empirically derived growth rate constants (C_3 and C_4). In the Abaqus fatigue model Paris regime growth only occurs when the maximum energy release rate (G_{max}) during a cycle is greater than the threshold energy release rate (G_{thresh}) and less than the energy release rate upper limit for stable growth (G_{pl}), or $G_{thresh}<G_{max}<G_{pl}$. These values can be defined by the user and default to 10% and 85% of the critical energy release rate (G_c). Using this method, the crack can only grow in increments where it can extend from one element boundary to another in a single time step.

Therefore, the crack grows across an element only on the cycle where $G_{max}>G_{thresh}$, and the length of the crack extension segment is greater than the length of the segment which spans the element in the crack growth direction.. Finally, if $G_{pl}<G_{max}< G_c$, then Abaqus treats the crack as "unstable" and the element in front of the crack will always fracture in the next cycle. [1]

The simplified fatigue step procedure in Abaqus (*FATIGUE, TYPE=SIMPLIFIED) can model subcritical crack growth under static loading. This is meant as a way to simplify subcritical crack growth models and allows for subcritical crack growth without modeling cycles or time directly, only the loading state at G_{max}. . In addition to these conditions the following three assumptions are made in simplified subcritical crack growth models:

1. Contact conditions within or between bodies, if present, are assumed to remain unchanged
2. G is proportional to the square of the applied load, P^2
3. G_{max} occurs at maximum load, P_{max}

It is due to these simplifications and assumptions used in a simplified fatigue procedure in Abaqus that it becomes possible to adapt this type of analysis procedure for use in PWSCC growth analyses. This modification of the simplified fatigue analysis is achieved through a straightforward transformation of the fatigue input parameters, without the need for external algorithms, post-processing, or user subroutines.

To explain further, for PWSCC growth in dissimilar weld metals (DMW) at constant temperature the rate equation can be simplified to [12]:

$$\frac{da}{dt}_{PWSCC} = \alpha \cdot K^b$$

where α is the crack growth coefficient and is the product of the power law constant for the given material at the reference temperature and the correction factor at the operating temperature, while *b* is the crack growth exponent and *K* is the stress intensity factor.

The conditions and assumptions of the simplified fatigue function can be used to define a relationship between the Abaqus Paris-like fatigue crack growth law and the PWSCC relation. First, because the simplified analysis does not explicitly model cycles and instead uses step time in lieu of cycles, cycles and unit time are interchangeable. Next, taking the condition that the ΔG equals the G_{max} and the assumption that *G* is proportional to P^2, then using the relationship between *G* and *K*, it is shown that *G* is directly proportional to K^2. From which, by applying modification factors to the coefficient and exponent inputs for the fatigue crack growth definitions in Abaqus, the simplified fatigue function can be adjusted for use in PWSCC growth models. Expressing K in terms of G results in the following:

$$\frac{da}{dt}_{PWSCC} = \alpha \cdot (E')^{(\frac{b}{2})} \cdot G^{(\frac{b}{2})}$$

where $E' = E/(1-\upsilon^2)$ for plane strain and $E' = E$ for plane stress with *E* being the elastic modulus. From simple substitutions, the relationships between the fatigue growth rate constants and the PWSCC relation are defined as follows:

$$C_3 = \alpha \cdot (E')^{(\frac{b}{2})}$$

$$C_4 = \frac{b}{2}$$

Further, this transformation of crack growth parameters results in the simulation step time being equivalent time, where normally the step time would be associated with cycles. If a more sophisticated $\frac{da}{dt}_{PWSCC}$ relations is required (e.g. have a minimum threshold for the strain energy release rate), the use of the UMIXMODEFATIGUE will be required to code the desired relation.

Since PWSCC is the primary application of interest, the simplified fatigue analysis procedure will be utilized throughout the sensitivity study. As detailed in Appendix F and provided in the Supplemental Files, a unit and parameter conversion Excel spreadsheet tool for driving force (K-to-G and G-to-K) and Paris Law (ΔK-to-ΔG and ΔG-to-ΔK) coefficients has been developed. This tool can be used for cycle-dependent (i.e. fatigue) and time-dependent (e.g. PWSCC) Paris-like crack growth relations.

In the following description on crack growth, the discussion will utilize the Abaqus terminology of cycles as it relates to the *FATIGUE,TYPE=SIMPLIFIED nomenclature. It should be realized that the same methodology applies to PWSCC applications where one fatigue cycle is equal to unit time.

Once the criterion for crack growth is satisfied at any crack tip location in an enriched element at the end of a completed cycle, N, Abaqus extends the crack length, a_n, from the current cycle over a number of cycles, ΔN, to $a_{N+\Delta N}$ by fracturing one enriched element ahead of the crack tip. The crack extension occurs orthogonal to the maximum tangential stress when the crack growth criterion is met. [1] Given the Paris Law form combined with the known element length and propagation direction ($\Delta a_{Nj} = a_{N+\Delta N} - a_N$), the number of cycles necessary to fail each enriched element ahead of the crack tip can be calculated as ΔN_j where *j* represents each enriched element ahead of the crack tip along the length of the crack. The analysis procedure is set up to advance the crack by one enriched element per increment of each loading cycle is completed. The element with the fewest cycles is identified to be failed, and its $\Delta N_{min} = \min(\Delta N_j)$ is represented as the number cycles to grow the crack equal to its element length, $\Delta a_{Nmin} = \min(\Delta a_{Nj})$.

While this capability precisely accounts for the number of cycles needed to cause fatigue crack growth over that length, it may be computationally intensive. To accelerate the fatigue crack growth analysis and to provide a smooth solution for the crack front, you can specify a nonzero tolerance, ΔD_{Ntol}, for the least number of cycles to fracture an enriched element. The default value for ΔD_{Ntol} is 0.1:

$$\frac{Log\Delta N_j - Log\Delta N_{min}}{Log\Delta N_{min}} \leq \Delta D_{Ntol}$$

In addition to the enriched element that takes the fewest cycles, ΔN_{min}, to fracture with zero constraint and a zero stiffness immediately after fracture, all of the other adjacent enriched elements satisfied by the above condition are also fractured.

To help understand the importance of the ΔD_{Ntol} parameter, Figure 4 provides an illustration of a 2D planar mesh with a surface flaw one element deep by three-elements long using ΔD_{Ntol} values of 0.1 and 0.01. At time zero, the crack front is identified and the predicted number of cycles until failure (ΔN_j) is provided for each element ahead of the crack front. Using the ΔN_{min} of 1000 cycles, the solution is advanced to the 1000 cycle increment where the center element is fractured. For the analysis with ΔD_{Ntol} = 0.1, the elements adjacent to the failed element are also failed as each element falls within the ΔD_{Ntol} tolerance value ($\frac{1060-1000}{1000} = 0.06 \leq 0.10$). For the ΔD_{Ntol} = 0.01 analysis, the side elements are not failed using the same criteria. From there, the algorithm is repeated. This example demonstrates that the larger ΔD_{Ntol} value can allow some elements to fail sooner which results in higher (conservative) crack growth.. This, in turn, may affect the crack shape and corresponding strain energy release rate.

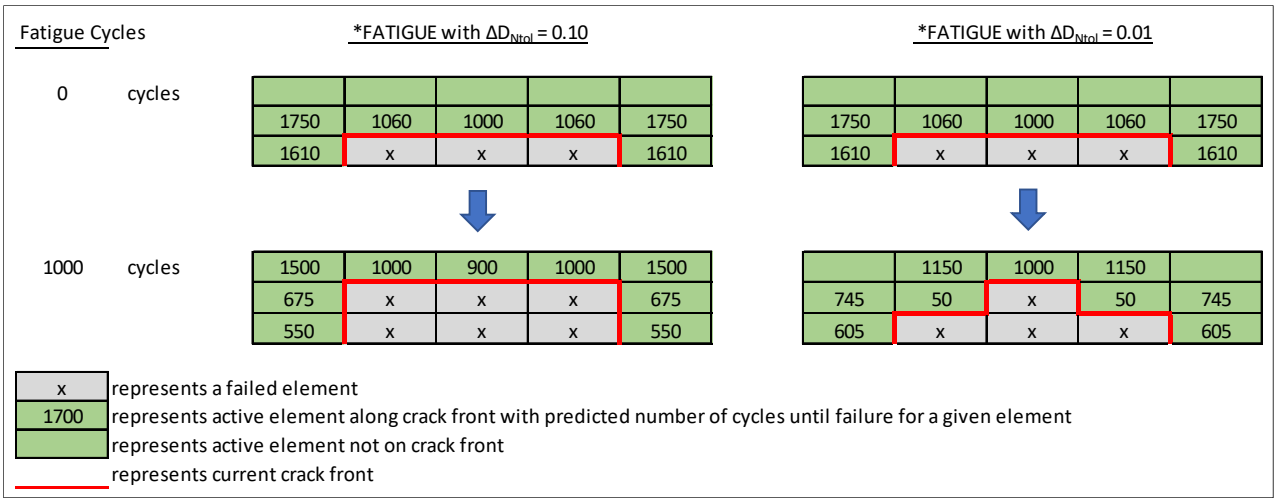

Figure 4 – 2-D Planar Example Illustrating the Importance of ΔD_{Ntol} in the Abaqus *FATIGUE, TYPE=SIMPLIFIED Capability

2.2.4 Abaqus Input Deck Template

In the following description on the Abaqus/Standard input deck, the discussion will utilize the Abaqus terminology of crack growth parameters and cycles as it relates to the *FATIGUE,TYPE=SIMPLIFIED nomenclature. It should be realized that the same methodology applies to PWSCC applications where one fatigue cycle is equal to one unit time and the Paris-law coefficients are modified from fatigue to PWSCC in Section 2.2.3.

The Abaqus/CAE pre-processing capabilities allow definition for the vast majority of the required simplified fatigue crack XFEM modeling details including location of the initial flaw within the enrichment region and specification of key output variable requests. However, as highlighted in **red** below, for the keyword components of a typical linear elastic fatigue crack growth model workflow, two items require hand-editing of the input deck. The *FATIGUE procedure and its data line need to be added as this procedure is not currently supported in Abaqus/CAE. Typically, a dummy *STATIC procedure would be defined in the Abaqus/CAE model which is then replaced in the input deck via a text editor. Also, the *FRACTURE CRITERION, TYPE=FATIGUE is not supported in Abaqus/CAE. The input deck must be hand-edited to include this keyword and the associated data lines which are a sub option of the *SURFACE INTERACTION definition.

A summary of the key parameters are described below that were utilized in various combinations within the sensitivity studies completed:

*FRACTURE CRITERION – Used to specify the criterion for crack propagation

Required Option:

TYPE=FATIGUE - Defines fatigue crack growth option

Options

ANGLEMAX=xx	to set the maximum allowed change in the crack propagation angle (in degrees) between the new crack propagation direction and the previous crack propagation direction. Default is 85 degrees.
POSITION=NONLOCAL	to use a moving least-squares approximation by polynomials to smooth out the individual crack front facet normals in elements

that satisfy the fracture criterion to obtain the crack propagation direction along the crack front. This is not the default option.

R CRACK DIRECTION =xx used in conjunction with POSITION=NONLOCAL, set this parameter equal to the radius around the crack tip within which the elements along the crack front are included for smoothing out the normals of the individual crack facets to obtain the crack propagation direction. The default value is three times the typical element characteristic length along the crack front in the model.

NPOLY = xx used in conjunction with POSITION=NONLOCAL, is used to specify the number of terms in the polynomial used for the moving least-squares approximation. The default is 7.

MIXED MODE BEHAVIOR = POWER – is a parameter that is used to specify final fracture and is not used for subcritical crack growth. In this study, the mixed mode fracture criterion is based on a simple power law as follows:

$$\frac{G_{equiv}}{G_{equivC}} = \left(\frac{G_I}{G_{IC}}\right)^{a_m} + \left(\frac{G_{II}}{G_{IIC}}\right)^{a_n} + \left(\frac{G_{III}}{G_{IIIC}}\right)^{a_o}$$

where $a_m = a_n = a_o = 1$ with G_{equiv} being used in the fatigue crack growth relation along with the critical energy release rate for each fracture mode, G_{IC}, $G_{IIC}$and G_{IIIC}, respectively.

In addition to the constants defined above, the required data parameters for *FRACTURE CRITERION,TYPE-FATIGUE are as follows:

- C_1 – material constant for fatigue crack initiation [set to zero for this study]
- C_2 – material constant for fatigue crack initiation [set to zero for this study]
- C_3 – material constant for fatigue crack growth [defined in Section 2.2.3]
- C_4 – material constant for fatigue crack growth [defined in Section 2.2.3]
- GT_GC – Ratio of energy release rate threshold used in the Paris Law over the equivalent critical energy release. [Set to value of 0.001 for this study]
- GP_GC –Ratio of energy release rate upper limit used in the Paris Law over the equivalent critical energy release rate. [Set to value of 0.999 for this study]

*FATIGUE,TYPE SIMPLIFIED - Uses a constant load to simplify the subcritical crack growth loading.

In Abaqus, at least two increments are required for each single loading cycle in this case.

Hence, the data line for the initial time increment (first data line, 1st entry) is set to one-half of the time for a loading cycle (first data line, second data entry).

The second data line specifies the minimum increment in number of cycles over which the damage is extrapolated forward (mincycle), the maximum increment in number of cycles over which the damage is extrapolated forward (maxcycle), the total number of cycles allowed in a step (totalcycle) and the damage extrapolation term, ΔD_{Ntol}, which was fully described in 2.2.3.

*AMPLITUDE needs to be defined to ensure that each loading is applied with maximum value for the simplified fatigue procedure.

*STEP,UNSYMM=NO|YES – While the default is set to NO, the unsymmetric solver may need to be specified to aid convergence of the solution.

*CONTROLS displacement correction

An XFEM crack propagation analysis can sometimes fail to converge due to the displacement jump and the sudden increase in local compliance. The usage of the C_n^{α} parameter (largest correction to displacement in the model divided by the largest increment of displacement for a given global degree-of-freedom) is used to control the displacement accuracy of the Newton-Raphson nonlinear algorithm. The default value is 0.01.

The visualization module of Abaqus/CAE (or Abaqus/Viewer) is recommended for post-processing of XFEM flaws as this post-processor has the ability to visualize the crack surface throughout the analysis. To aid this activity, the following XFEM-specific crack propagation field output variables are available for request within the Step Module of Abaqus/CAE or via direct inclusion in the Abaqus input deck:

- PHILSM - Signed distance function to describe the crack surface.
- PSILSM - Signed distance function to describe the initial crack front.
- STATUSXFEM - Status of the enriched element (0.0 (uncracked) or 1.0 (completely cracked)).
- CYCLEXFEM - Number of cycles to fracture at the enriched element.
- ENRRTXFEM - All components of strain energy release rate (e.g. Mode I).
- LOADSXFEM - Distributed pressure loads applied to the XFEM-based crack surface.

The key input file components for a given model are provided below:

```
*HEADING
…
*NODE
…
*ELEMENT,TYPE=C3D8R,ELSET=REGULAR
…
*ELEMENT,TYPE=C3D8R,ELSET=ENRICHED
…
*SOLID SECTION, ELSET=REGULAR, MATERIAL=STEEL
*SOLID SECTION, ELSET=REGULAR, MATERIAL=STEEL
*MATERIAL, NAME=STEEL
…
*ENRICHMENT, NAME=CRACK-1, TYPE=PROPAGATION, ELSET=ENRICHED,INTERACTION=INTPROP-1
*SURFACE INTERACTION, NAME=INTPROP-1
*SURFACE BEHAVIOR
*FRACTURE CRITERION,TYPE=FATIGUE,MIXED MODE BEHAVIOR=POWER,POSITION=<DEFAULT OR
NONLOCAL>(,ANGLEMXAX=85)(,RCRACKDIRECTION=5.)
<C1>, <C2>, <C3>, <C4>, <GT_GC>, <GP_GC>, <GIC >, <GIIC>
<GIIIC>, <A_M>, <A_N>, <A_O>
**
*INITIAL CONDITIONS, TYPE=ENRICHMENT
901, 1, Crack-1, 0.25, -1.5
901, 2, Crack-1, 0.25, -1.0
901, 3, Crack-1,-0.25, -1.5
901, 4, Crack-1,-0.25, -1.0
```

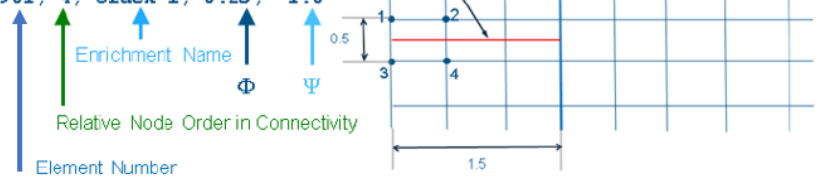


```
...
*AMPLITUDE,NAME=AMP2
0,1,1,1
*STEP(,UNSYMM=YES|NO)
*FATIGUE,TYPE=SIMPLIFIED
0.5, 1.
<MINCYCLE>, <MAXCYCLE>, <TOTALCYCLE>,, ΔD_Ntol
**
*CONTROLS, PARAMETERS=FIELD, FIELD=DISPLACEMENT
, C_n^α
**
*DSLOAD,AMP=AMP2
*BOUNDARY
**
*OUTPUT, FIELD,VAR=PRESELECT
*NODE OUTPUT
PHILSM, PSILSM
*ELEMENT OUTPUT, DIRECTIONS=YES
ENRRTXFEM, STATUSXFEM, LOADSXFEM, CYCLEXFEM
*END STEP
```

3 APPROACH IN EVALUATION OF CAPABILITY

3.1 Evaluation Criteria

The crack growth rate and crack shape were selected as the fundamental evaluation criteria for the geometries evaluated with results compared to traditional finite element crack analysis results or other acceptable analytical solutions. Within these two criteria, a focus was maintained on different crack front shapes (initially curved versus straight) and crack extension (planar versus curvilinear).

While this may seem obvious, crack growth rates and crack shape evolution will be shown to depend on a number of parameters within the modeling capability including mesh refinement, size of enrichment zone, element formulation, mesh type (structured or unstructured), crack growth controls and general FEA solution controls.

3.2 Models Selected for Sensitivity Study

As shown in Figure 5, four basic geometries along with a relatively complex assessment were studied to show that reasonable SIF and crack growth rates and shapes for both applied load and residual stress configurations, using subcritical crack growth relations, could be obtained using Abaqus XFEM:

- Two cracks emanating from a hole in plate under uniform tension
- Semi-elliptical surface flaw in a flat plate under uniform tension
- Modified Compact Tension (CT) specimen with Miss and Sink Hole configuration
- Compact Tension specimen utilizing PWSCC constants and loading
- Internal semi-elliptical surface flaw for the VC Summer hot leg dissimilar weld metal joint assessment subjected to a PWSCC environment.

In the preceding list, the first three configurations represent readily available constant-amplitude fatigue benchmarks while the last two configurations consistent of PWSCC growth analyses. Due to the similarity of physics between these two application groups as demonstrated in Section 2, learnings from the two groups of analyses will be used to inform and verify sensitivity parameter results that control the accuracy, repeatability of analysis results and computational resources for this capability.

The 2D hole in plate was used to compare planar, straight crack growth with analytical solutions for stress intensity factor and fatigue crack growth rates. Based on learnings from this model, it was determined that a curvilinear crack growth model was needed to explain some of the initial findings regarding element formulation and mesh type. The modified CT specimen with the additional hole to perturb the crack path was used for this purpose. This model was particularly useful since experimental validation results were available.

The standard CT specimen was evaluated using the developed methodology for PWSCC. As a transition to more complex geometries, the semi-elliptical surface flaw in a flat plate serves as an excellent benchmark for axial and circumferential flaws in piping systems with the obvious analogy to a pipe with infinite radius. Finally, the VC Summer hot-leg DMW axial flaw assessment was utilized to provide some assurance that more complex problems could also be studied.

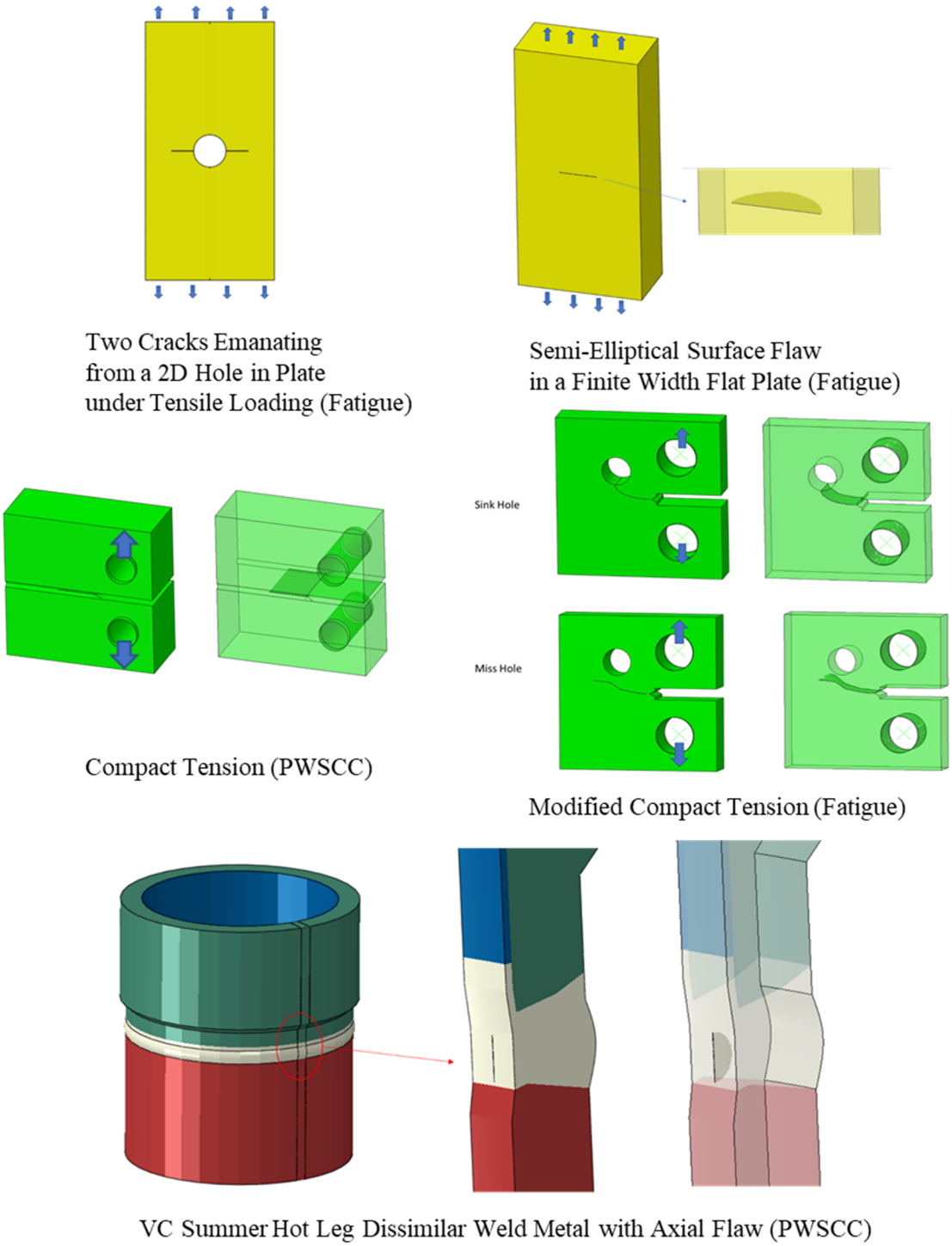

Figure 5– Problems Utilized to Understand Built-In Abaqus XFEM with Simplified Subcritical Crack Growth Capabilities

3.3 Parameters Selected for Sensitivity Study

In addition to mesh parameters (mesh size, mesh type, enrichment zone width), element formulation and crack growth parameters were studied. Overall, over forty analysis models were studied. The following sections provide background and an overview of the parameters studied. The Appendix associated with each XFEM model provides the complete modeling details.

3.3.1 Mesh Parameters

The three meshing parameters investigated were element type and formulation, mesh type, and mesh size. Additionally, it was found that how the crack is defined relative to the mesh can be important in order to obtain accurate results.

The models introduced in the previous section and described in detail in the Appendices have a large range in terms of absolute dimensions. In order to provide general mesh refinement recommendations, terms needed to be defined that would allow nondimensional guidance to be provided. Shown in Figure 6, three structural dimensions (height, width and thickness) are defined. The structural thickness is aligned with the crack depth growth direction. The structural width follows the crack length, while the structural height is defined to be the direction perpendicular to the initial crack plane.

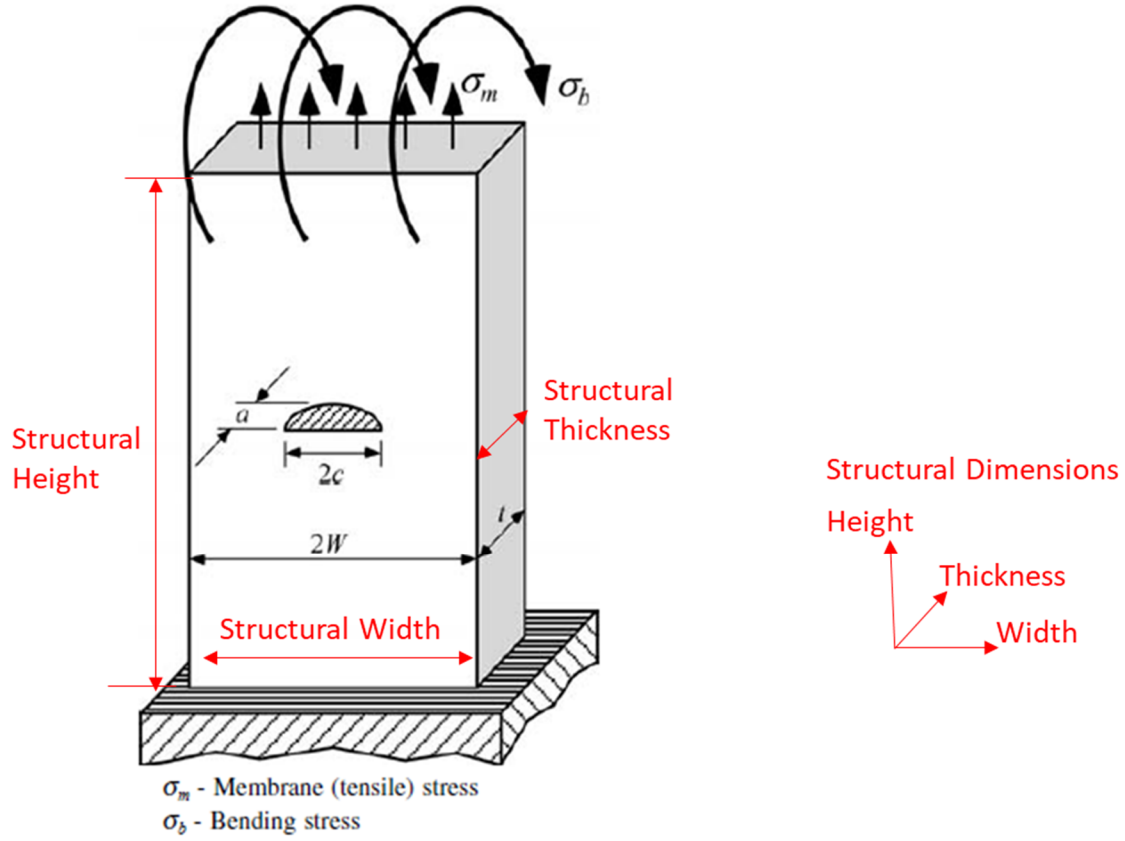

Figure 6 - Definitions for Structural Dimensions (Thickness, Width and Height) used in this Study. Adapted from Anderson 4th Edition Table 9A.1 [13]

Figure 7 provides a visual representation of the enriched regions and the structural dimensions within each XFEM model studied. It is noted that the structural dimensions do not always match the enrichment region size. As the crack regions are known in advance for some of the models, the geometry was partitioned such that the enriched regions are kept to a reasonable size.

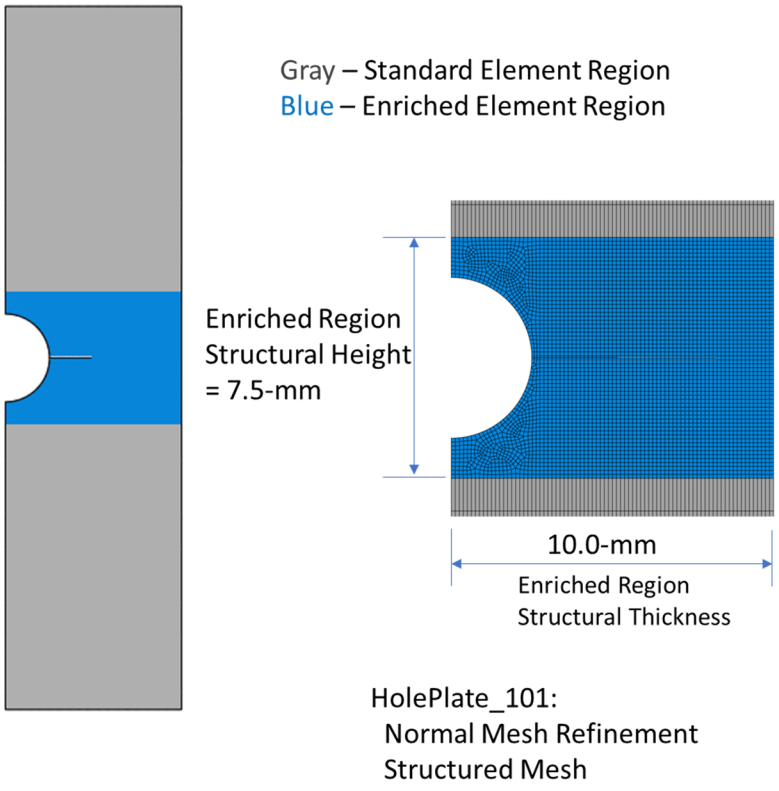

(a) Two cracks emanating from a hole in plate under uniform tension (Constant-Amplitude Fatigue)

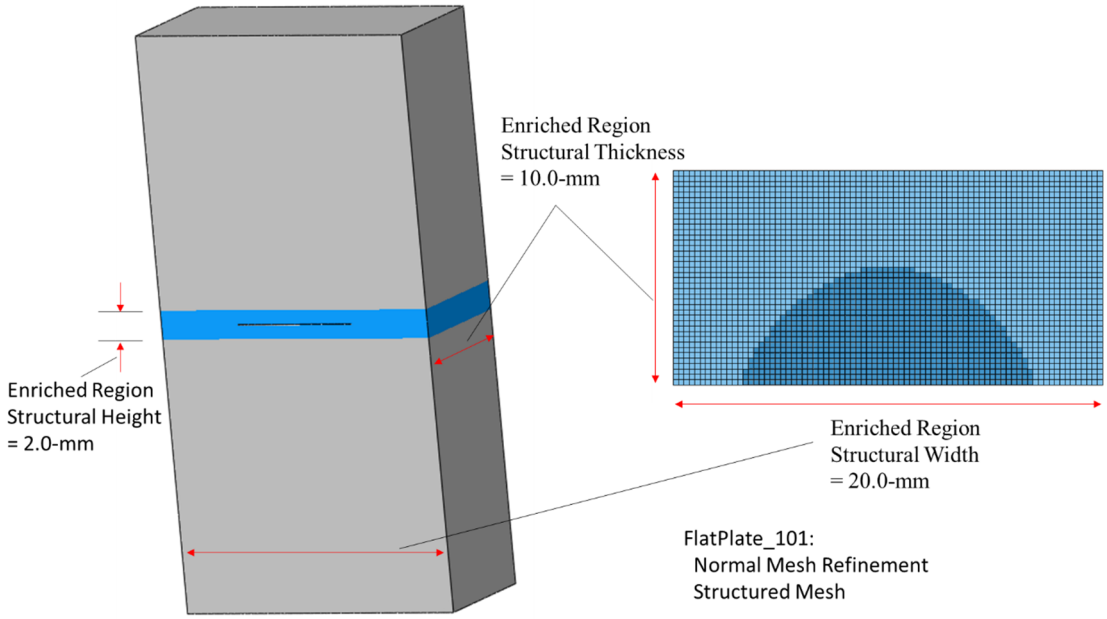

(b) Semi-elliptical surface flaw in a flat plate under uniform tension (Constant-Amplitude Fatigue)

Figure 7 Structural Dimension (Depth, Width and Height) and Enriched Region Definitions for Each XFEM Model Studied

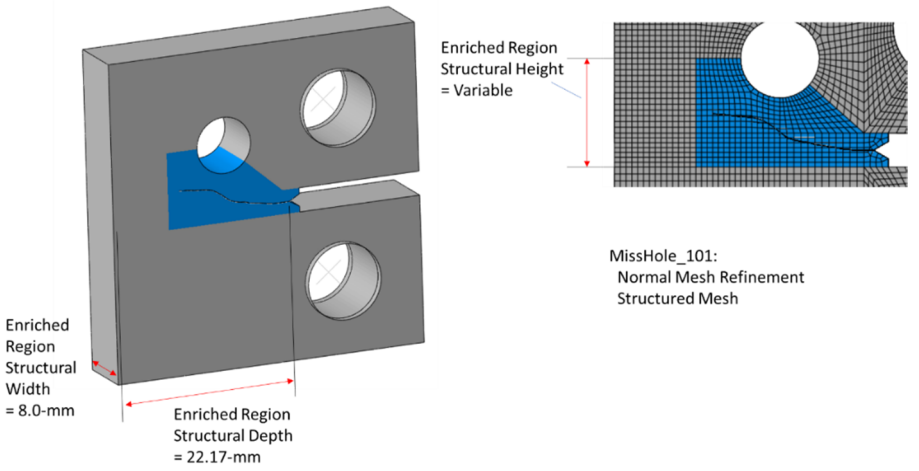

(c) Modified Compact Tension (CT) specimen with Miss and Sink Hole configuration (Constant-Amplitude Fatigue)

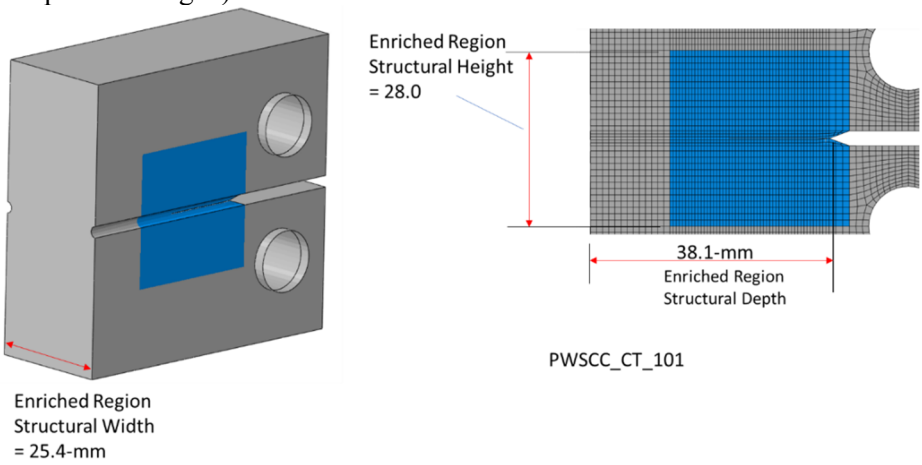

(d) Compact Tension specimen utilizing PWSCC constants and loading (PWSCC)

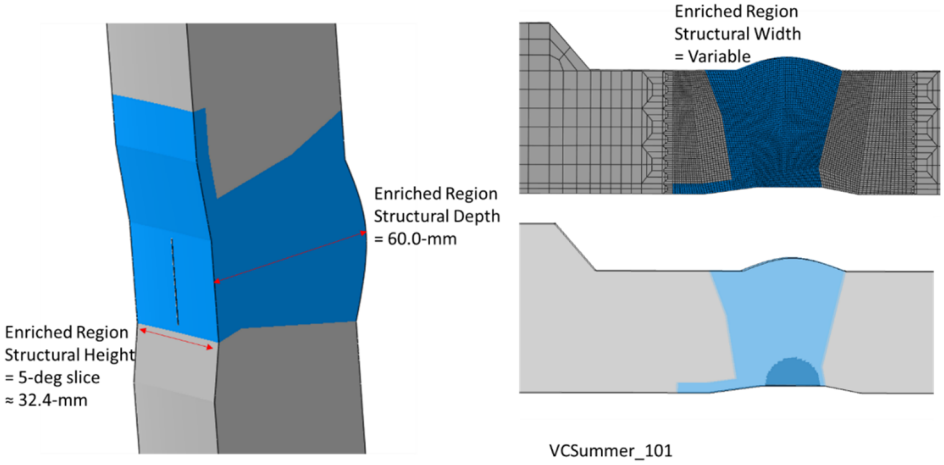

(e) Internal semi-elliptical surface flaw for the VC Summer hot leg dissimilar weld metal joint assessment subjected to a PWSCC environment (PWSCC)

Figure 7 (continued) Structural Dimension (Depth, Width and Height) and Enriched Region Definitions for Each XFEM Model Studied

Table 1 provides a summary of the parameter variations for the mesh refinements in terms of the structural dimensions within each XFEM model studied. In order to reduce dimensionality in this study, the key parameter will be the structural thickness. The structural width uses the same mesh seed required to define the structural thickness element number specification and the structural height is correlated to a fraction of the structural thickness while still using the structural thickness mesh seed. In so doing, the intent is to create an enriched region mesh with the best formed elements to minimize mesh bias in any direction.

Table 1 Overview of Baseline Meshing Parameters used In XFEM Sensitivity Study

Baseline Properties	**Refinement**	**Structural Dimension**			**Enriched Region Mesh Seed (mm)**	**Number of Elements in Structural Thickness Direction**
		Thickness (mm)	**Height (mm)**	**Width (mm)**		
Hole_in_Plate (Constant-Amplitude Fatigue)		10.0	7.5	N/A		
	Coarse				0.25	29
	Normal				0.125	58
	Fine				0.0625	116
Flat_Plate (Constant-Amplitude Fatigue)		10.0	2.0	20.0		
	Normal				0.25	40
	Fine				0.125	80
Sink_Hole (Constant-Amplitude Fatigue)		22.17	Variable	8		
	Coarse				0.6x1.0mm (height)	45
	Normal				0.6	45
	Fine				0.3	90
PWSCC_CT (Steady-State PWSCC)		38.1	28	25.4		
	Normal				0.5	58
PWSCC_VC_Summer (Steady-State PWSCC)		60	~32.4 (5-deg)	Variable		
	Normal				1.0	60

In addition to the mesh refinement, analysis runs were made to determine the influence of the structural height and the usage of *TIE between the enriched and standard element regions. The usage of the *TIE allows dissimilar meshes to be "glued" together. In this case, a 3D simple to generate coarse tetrahedral-like mesh in the far-field is tied to a fine hex mesh in the enrichment region. It is a known issue that when stationary crack J-Integral contour integrals have paths crossing this tied interface that inaccurate values result. [1] This current study was to verify whether any similar issues exist with VCCT-extracted strain energy release rate values for a propagating XFEM crack in the subcritical critical crack growth procedure. To accomplish this, separate hole in plate analysis runs were made with the structural height set to be 75%, 25% and 10% of the structural depth while utilizing a *TIE between the enriched and standard element regions.

Figure 8 shows the structured and unstructured meshes utilized for the 2D hole in plate (Appendix A) and the 3D Flat Plate (Appendix B) model in the enriched regions. The same mesh seed was used within a model class for both the structured and unstructured meshes. For the Flat Plate model, two unstructured mesh classes were studied. The in-plane unstructured mesh had a prescribed free mesh perpendicular to the thumbnail crack plane which was then swept through-the-thickness. The out-of-plane unstructured mesh refers to an unstructured mesh parallel to the crack plane which is then extruded through the enriched region of the model.

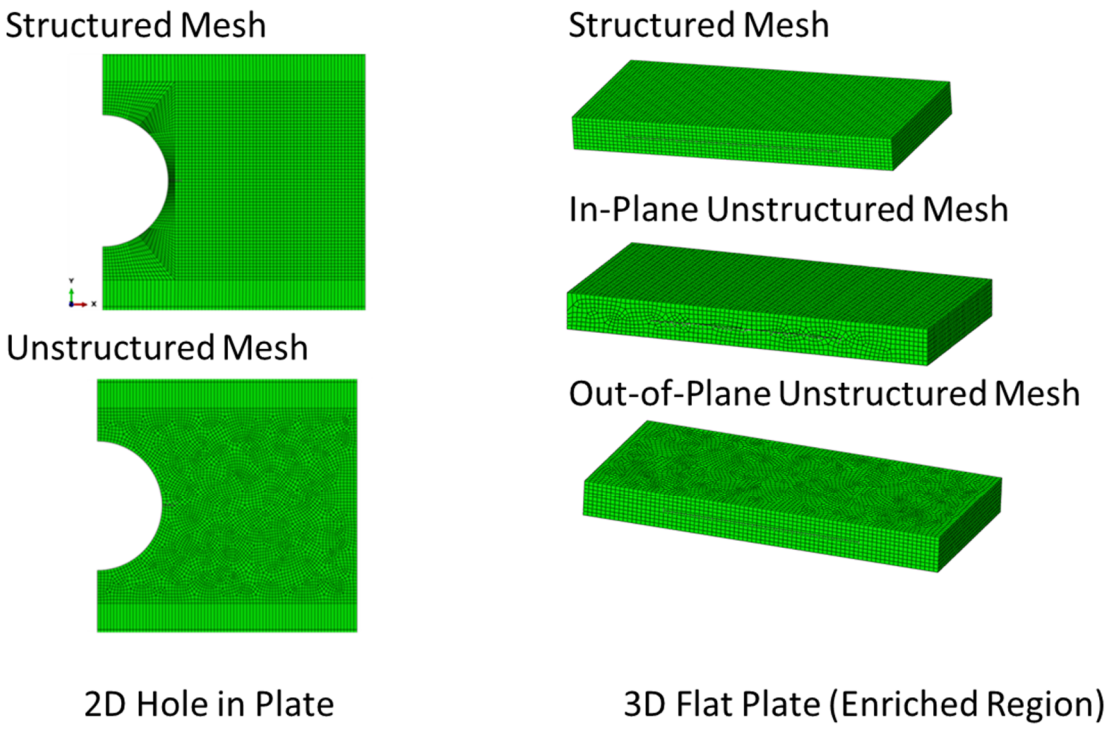

Figure 8 Structured and Unstructured Mesh Types Utilized the 2D hole in plate and 3D Flat Plate XFEM Models in the Enriched Regions

The element integration rule was also studied. One of the most important aspects and difficulties of the XFEM implementation is the integration of the XFEM augmented shape functions. While the difference between full- and reduced integration would be expected to be small for such finely meshed standard regions in linear elastic problems, significant differences were noted in initial scoping analyses for the hole in plate geometry. As a result, full- and reduced integration analysis runs were made for the hole in plate, Flat Plate, Sink Hole and CT geometries.

In addition to these primary sensitive parameters, the ability to assess the stress intensity factor and crack propagation with XFEM was studied for flaws that were not initially aligned to be perpendicular to the principal stress (hole in plate). Further, small initial flaw sizes (down to crack depth / structural thickness = 0.05) were investigated while still using a normal mesh for the Flat Plate geometry.

Following the guidance of Chen[11], the meshes were designed such that the initial flaws did not lie along the element boundaries. For the majority of the problems, at least some non-planar curved crack growth was observed. Finally, while the Abaqus XFEM capability does allow for damage initiation from an initially uncracked structure, sharp cracks were assumed to be pre-existing for this study.

3.3.2 Crack Growth Control Options

The XFEM-based Linear Elastic Fracture Mechanics (LEFM) subcritical crack growth approach can be used to simulate crack propagation along an arbitrary, solution-dependent path in the bulk material with an initial crack. Various options are available when defining the behavior of the crack extension. Listed below are the parameters that were studied that could influence the quality of the results, stability of the model and computational resources.

3.3.2.1 Crack Tip Strain Averaging Control

An accurate and efficient evaluation of the stress/strain fields ahead of the crack tip is important for both evaluating the crack initiation criterion and computing the crack propagation direction. By default, the stress/strain computed at the element centroid ahead of the crack tip is used to determine if the fracture criterion is satisfied for crack extension and to determine the crack propagation direction. The crack propagation direction occurs orthogonal to the maximum tangential stress when the crack growth criterion is met. In the case of unstructured or relatively coarse meshes, it becomes extremely challenging to maintain a smooth, continuous three-dimensional crack front during nonplanar crack propagation with the current XFEM method. By setting the parameter POSITION=NONLOCAL on *FRACTURE, the XFEM-based nonlocal approach includes both nonlocal stress/strain averaging and crack normal smoothing to improve the computed crack propagation direction.

The radius around the crack tip within which the elements along the crack front are included for smoothing out the normals of the individual crack facets to obtain the crack propagation direction is controlled by the *FRACTURE, POSITION=NONLOCAL,RCRACKDIST= parameter. The default value is three times the typical element characteristic length along the crack front in the model. The *FRACTURE, POSITION=NONLOCAL, NPOLY= is used to specify the number of terms in the polynomial used for the moving least-squares approximation. The NPOLY default is 7. These two optionally parameters were found not to affect solution quality or convergence rates for the relatively simple geometries evaluated in this study. For more complex geometries, these parameters may require modification to obtain accurate and converged solution results.

The influence of default and *FRACTURE,POSITION=NONLOCAL was studied for the modified CT (Sink Hole and Miss Hole), Flat Plate and VC Summer DWM Hot Leg geometries.

3.3.2.2 Crack Propagation Direction Control

The new crack propagation direction can be limited with the *FRACTURE, POSITION=NONLOCAL option to within a certain angle (in degrees) of the previous crack propagation direction. Using the default crack direction normal (maximum tangential stress), the new crack propagation direction can be limited relative to the previous crack propagation direction using the ANGLEMAX parameter. This number limits the maximum change in the crack propagation direction in a single increment in degrees. If no ANGLEMAX value is specified, a default value of 85°is used. The ANGLEMAX parameter was studied using the Flat Plate and Miss Hole geometries.

3.3.2.3 Damage extrapolation tolerance

As described in Section 2.2.3, the *FATIGUE damage extrapolation tolerance term (ΔD_{Ntol}) was found to be one of the most important parameters for balancing solution accuracy with computational time. Using the default value of 0.1 for ΔD_{Ntol} along with values of 0.01 (more accurate but slower computational time), 0.175 and 0.25 were used to evaluate crack growth rates and shapes. The PWSCC CT and Flat Plate geometries were tested with the default and the more stringent value of 0.01. For longer running practical problems such as the VC Summer Hot Leg DWM axial flaw assessment, relaxed (looser) tolerance values (0.175 and 0.25) were set to obtain a conservative crack growth rate in a shorter amount of computational time.

3.3.3 General Solution Control Options

An XFEM crack propagation analysis can sometimes fail to converge, in spite of reasonable damage properties and a suitably refined mesh in the enriched region. Two analysis settings were studied to facilitate convergence.

3.3.3.1 Unsymmetric Solver

The stiffness matrix for enriched elements is unsymmetric; therefore, unsymmetric matrix storage and solution scheme is recommended for XFEM analysis to improve convergence behavior.[11]

The convergence rate influence of the *STEP,UNSYMM=YES and *STEP,UNSYMM=NO (default) was evaluated on the five models in this study.

3.3.3.2 Displacement Correction

An XFEM crack propagation analysis can sometimes fail to converge due to the displacement jump and the sudden increase in local compliance. For example, as the fracture criterion is achieved, the crack front is released with typically small displacements and displacement corrections.

The usage of the C_n^α parameter (largest correction to displacement in the model divided by the largest increment of displacement for a given global degree-of-freedom) is used to control the displacement accuracy of the Newton-Raphson nonlinear algorithm:

```
*CONTROLS, PARAMETERS=FIELD, FIELD=DISPLACEMENT
,C_n^α
```

To study this parameter, the C_n^α was varied between the default (0.01) and an order of magnitude higher value (0.1) for the Flat Plate model.

4 SENSITIVITY STUDY RESULTS

In addition to mesh parameters (mesh size, mesh type, enrichment region height), element formulation and crack growth parameters were examined. Overall, over forty analysis models were studied. The modeling details, parameters varied and results are provided for each model class in Appendices A through F. This section is intended to provide context and observations in the pursuit of providing general modeling recommendations. Due to the similarity of physics between constant-amplitude fatigue and PWSCC crack growth applications as demonstrated in Section 2, learnings from the two groups of analyses will be used to inform and verify sensitivity parameter results that control the accuracy, repeatability of analysis results and computational resources for this capability.

4.1 Mesh Parameters

The three meshing parameters investigated were element type and formulation, mesh type and mesh size. While these topics are intertwined in terms of evaluating the crack growth rate and shape, an attempt is to provide a logical flow in discussion of the results. To aid in this conversation, unless otherwise specified, the general modeling recommendations discussed in Section 5 serve as the baseline for which a sensitivity variation run is made.

4.1.1 Element Type and Formulation

The study began with an evaluation of the stress intensity factor for geometries with published analytical solutions. For propagating XFEM flaws in the Abaqus simplified subcritical crack growth procedure, the strain energy release rate at the crack tip is calculated based on the modified Virtual Crack Closure Technique (VCCT). [1] Unlike the stationary crack contour integral (J-Integral) and interaction integral (stress intensity factor, K) where fairly coarse meshes are able to capture path independent driving force values, the propagating crack values are calculated for each crack front element with the linear-elastic strain energy release rate, G, being calculated directly which implies that mesh density and element formulation are important.

As a matter of observation, for the 3D Flat Plate and PWSCC CT models, the reduced integration formulation was a better match for the analytical crack driving results at constrained (interior) crack tip points within a specimen. As an example, Figure 9 shows the strain energy release rate (Abaqus output variable ENRRTXFEM) for the initial crack depth along the crack front from back to front and also a plot of the strain energy release rate as a function of crack depth at the center-width location of the specimen at the initial crack length. The reduced integration results differ by less than 2% from the analytical solution. For these linear elastic models, it is not clear why reduced and full-integration vary in such refined models. However, it is appreciated that one of the most important aspects and difficulties of the XFEM implementation is the integration of the XFEM augmented shape functions. In the end, these results imply that the element integration rule should be included in future benchmarking.

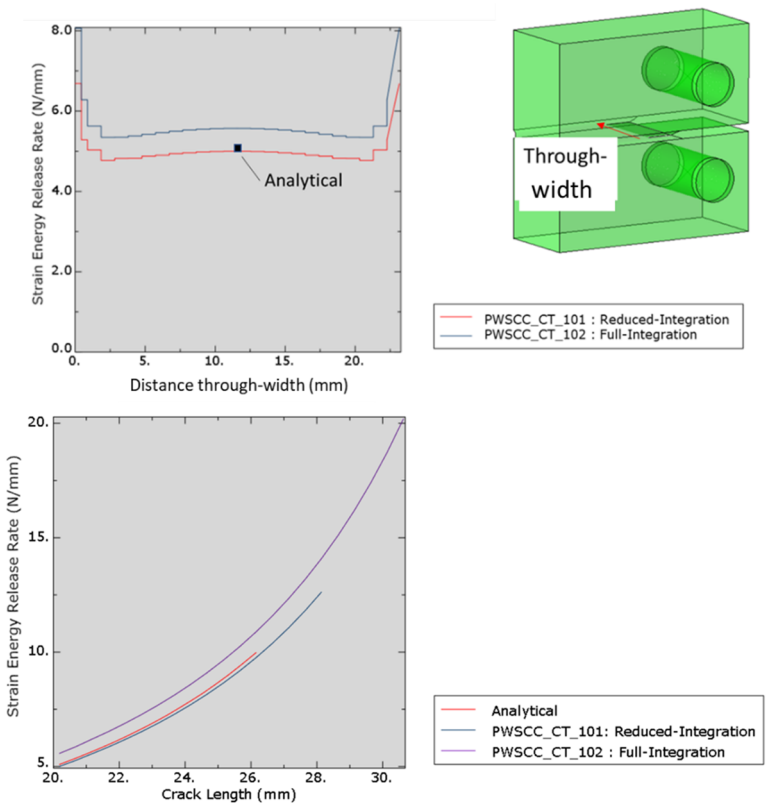

Figure 9 Strain Energy Release Rate Comparisons for the PWSCC Compact Tension utilizing Full- and Reduced Integration Compared to Analytical Results (Analytical Solution Provided in [19] and Detailed in Appendix D)

Shown in the Figure 10, the 2D plane strain hole in plate model with the full integration formulation was the better match with less than a 2% variation as compared to the published analytical solution [22]. (Note that these results are shown in the form of the nondimensional geometrical correction factor, $\beta = \frac{K}{\sigma\sqrt{\pi a}}$ where K is the stress intensity factor, σ is the applied stress and a is the crack depth). For the 2D and 3D models evaluated, the two element formulations differed by less than 10% and bounded the analytical result for the crack driving force.

One of the most surprising results of this study was that full integration, and to a lesser extent, reduced integration element formulations result in inaccurate crack turning and can lead to unconservative crack growth rates. Illustrated in Figure 10 for the hole in plate model, curvilinear cracks propagate up to an element interface, turn and then extend further along the element boundary that is parallel to the original crack orientation. In this way, the anticipated crack trajectory is not obtained. As long as a crack propagates from one element edge to the opposite edge and is away from the side edges, the XFEM approach using the full-integrated element formulation is shown in Figure 10 to match published benchmark [22] and values obtained from traditional focused-mesh stationary cracks (see Appendix A) for a given crack shape, geometry and loading up to a/b=0.7. The deviation occurs when there is a crack tip propagates to the element "top edge" boundary at approximately a/b=0.7. To a lesser extent, the same observation can be made for reduced integration at a/b=0.9. These findings are consistent with results provided with the 3D Sink Hole (Appendix C) XFEM model in Figure 11.

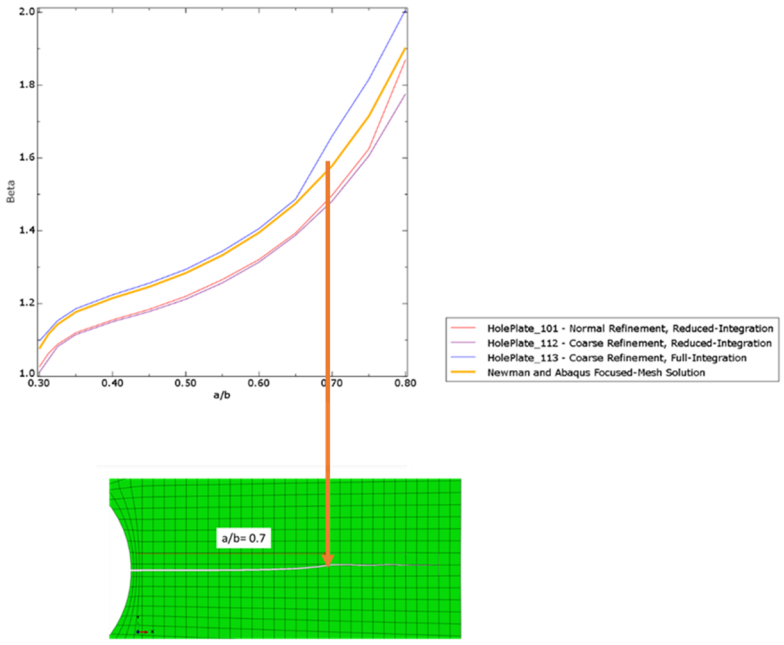

Figure 10 Nondimensional Geometric Correction Factor as a nondimensional function of crack depth for the hole in plate model comparing analytical results (see Newman [16] and Appendix A Figure A1).

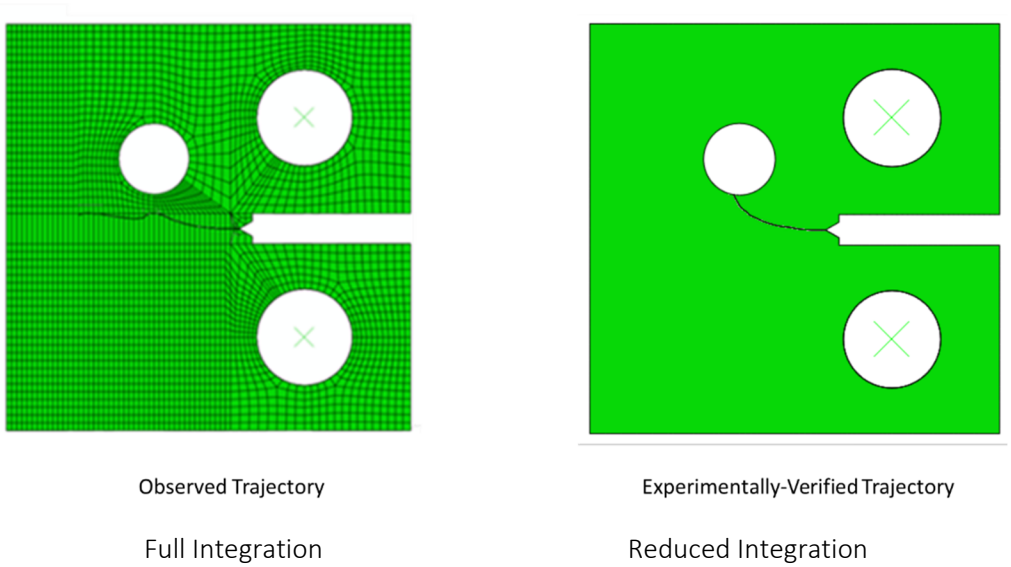

Figure 11 Influence of Element Formulation for Structured Mesh Sink Hole Model

For 3D models, a structured, hexahedral first-order continuum element with a reduced integration formulation was the best match for the analytical crack growth and crack shape results along the crack fronts. To support this statement, Figure 12 shows the PWSCC CT specimen results using the baseline reduced integration and full integration element models along with the analytical solution ([19] is detailed in Appendix D). (A more stringent fatigue damage extrapolation term, ΔD_{Ntol}, will be discussed later in the crack growth controls results section). In both cases, a conservative bounding solution for crack growth is seen with the crack propagating in a uniform, straight front.

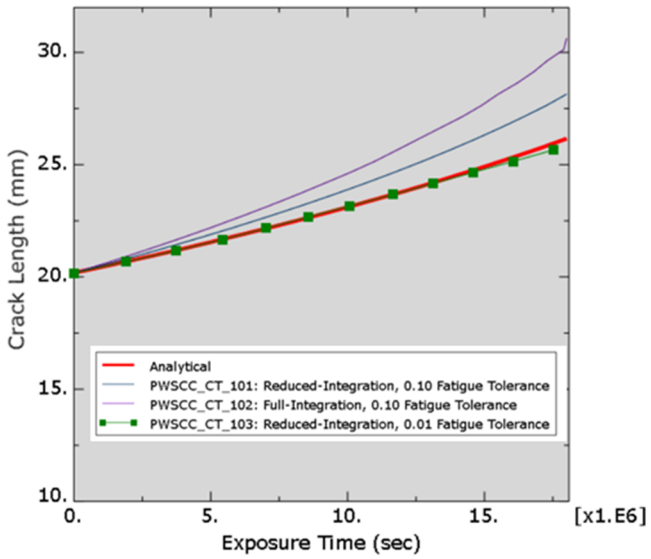

Figure 12 PWSCC CT Crack Length as a Function of Exposure Time for Full- and Reduced Integration Elements (Analytical Solution Provided in [19] and Detailed in Appendix D)

Despite the overall positive behavior observed in the study for reduced integration structured hexahedral meshes, it should be noted that asymmetric deformation may be observed (e.g. Miss Hole geometry) despite having no physical or mesh-dependent mechanism that should have led to this oscillating wavy crack path behavior. Figure 13 shows these numerical artifacts where non-symmetric results occurred for the Miss Hole geometry in the thickness direction and nonplanar growth was observed during the VC Summer DMW assessment. Careful review of all results is required with the XFEM capability.

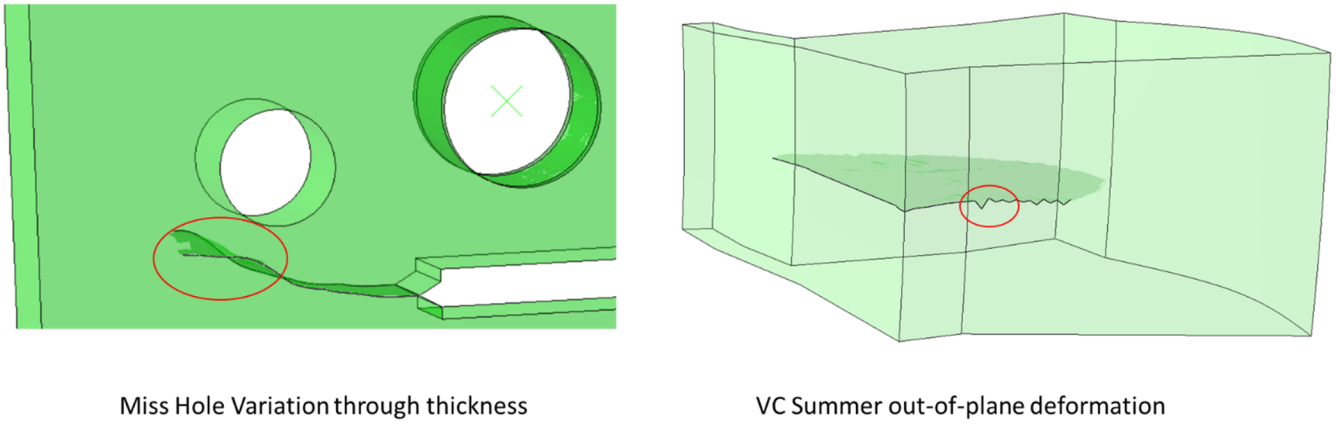

Figure 13 Examples of Unexpected Asymmetric Deformation and Oscillating Crack Paths Observed with Reduced Integration, Structured Hexahedral Meshes

4.1.2 Mesh Type

The crack growth rate and crack shape were run for structured and unstructured meshes using a common mesh seed for each model class. Figure 14 shows results for the crack growth rates at the surface and deepest crack locations for two unstructured meshes (in-plane unstructured and out-of-plane unstructured) along with the baseline structured mesh and analytical results for the semi-elliptical flaw in the Flat Plate. A top view of the crack profile is also shown at 50000 cycles. A similar approach is seen in Figure 15 for the hole in plate model where unstructured and structured meshes were compared. Overall, the unstructured mesh results were found to be somewhat erratic as higher crack growth rates were observed

at shallow depths and slower rates as the cracks progressed. As compared with analytical solutions([16] as detailed in Appendix B), the most consistent crack growth results were obtained with structured meshes.

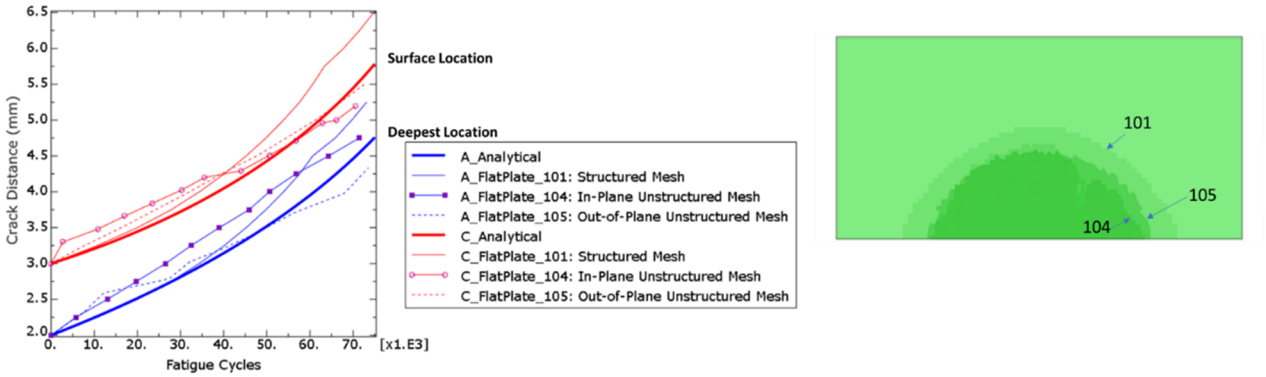

Figure 14 Influence of Mesh Type on Crack Growth Rate and Shape for Semi-Elliptical Surface Flaw in a Finite Width Flat Plate under Uniform Uniaxial Far-Field Pressure Loading (Reduced Integration) (Analytical Solution Provided in [16] and Detailed in Appendix B)

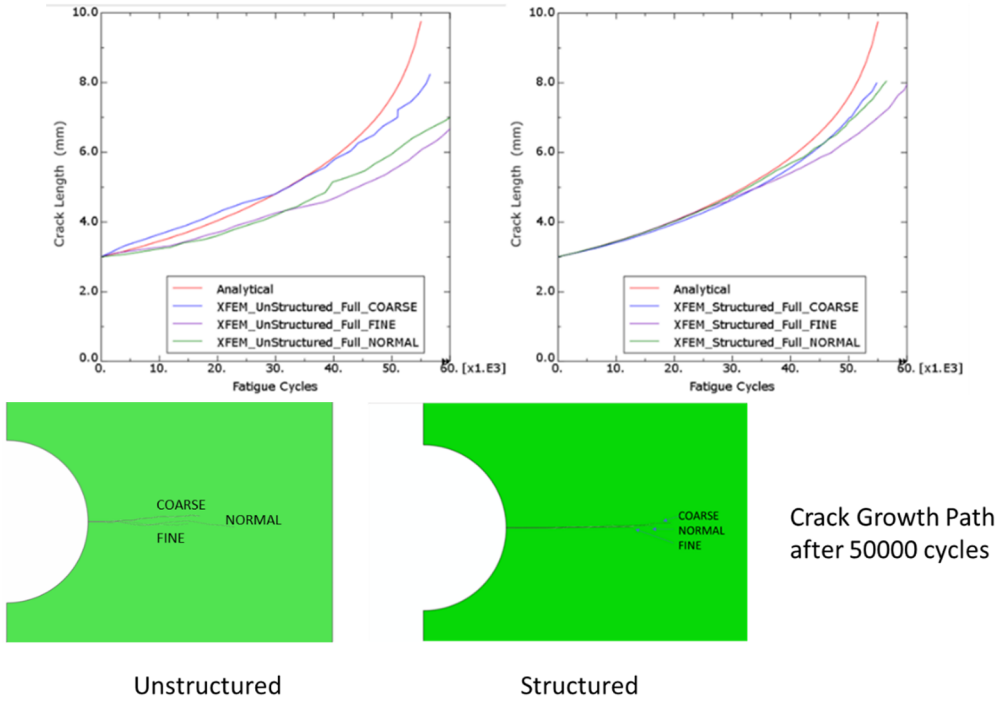

Figure 15 Influence of Mesh Type and Mesh Size on Crack Growth Rate and Shape for Two Cracks Emanating from a Hole in a Finite Plate under Uniform Uniaxial Far-Field Pressure Loading (Full Integration Elements) (Analytical Solution Provided in [22] and Detailed in Appendix A)

4.1.3 Mesh Size

In order to reduce dimensionality in this mesh refinement study, the key parameter will be the structural thickness. The structural width uses the same mesh seed required to define the structural thickness element number specification and the structural height is correlated to a fraction of the structural thickness while still using the structural thickness mesh seed. In so doing, the intent is to create an

enriched region mesh with the best formed elements to minimize mesh bias in any direction. This also allows nondimensional recommendations to be made for the enriched region mesh refinement.

As previously delineated in Table 1, mesh refinement studies were completed for the 2D hole in plate model (shown previously in Figure) and the 3D Flat Plate (Figure 16) model where results could be compared to analytical results. It was found that a minimum structural thickness refinement of ~50 elements was found to conservatively capture the crack growth rates and provide reasonable crack shape predictions. This guideline was then successfully applied to the other analysis models. Of course, additional refinement does provide more accurate results but will require more computational time (4.9x slower wall clock time for the fine (80-elements in thickness direction) Flat Plate refinement compared to the normal (40-elements in the thickness direction) mesh).

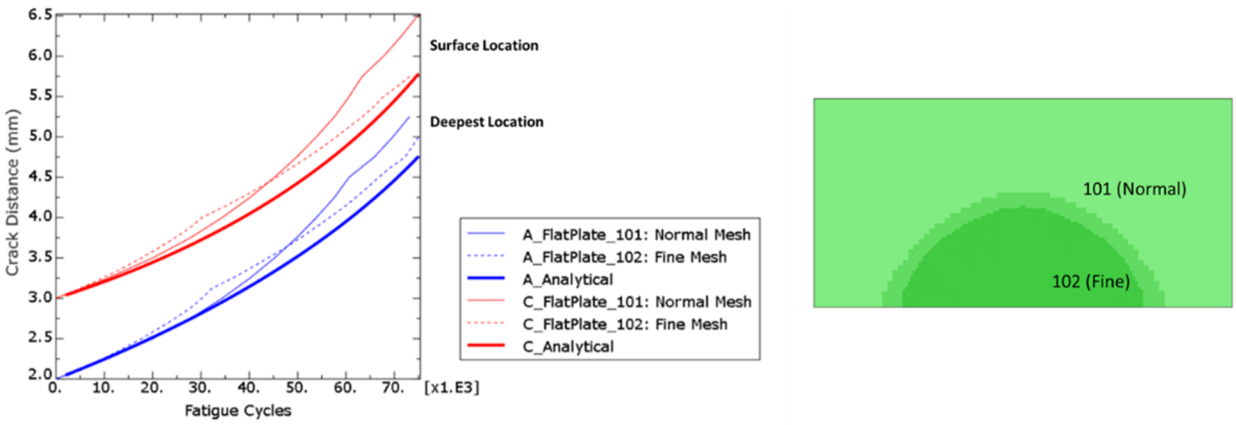

Figure 16 Influence of Mesh Refinement on Crack Growth Rate and Crack Shape (at 50000 cycles) for Semi-Elliptical Surface Flaw in a Finite Width Flat Plate under Uniform Uniaxial Far-Field Pressure Loading (Reduced Integration) (Analytical Solution Provided in [16] and Detailed in Appendix B)

To ensure that the structural height was sufficient, a series of analysis runs were made varying the height as a function of the structural thickness for the hole in plate geometry. Shown in Figure 17, the structural thickness for this geometry is 10.0 mm. In addition to the baseline zone height being 75% of the structural height, analysis runs were made with the height set to 25% and 10% of the structural thickness. Further, these analysis runs were made with the structured quadrilateral element mesh for the enriched region tied to a triangular standard element region mesh. This was used to simulate a 3D simple to generate coarse tetrahedral-like mesh in the far-field with a fine hex mesh in the enrichment region.

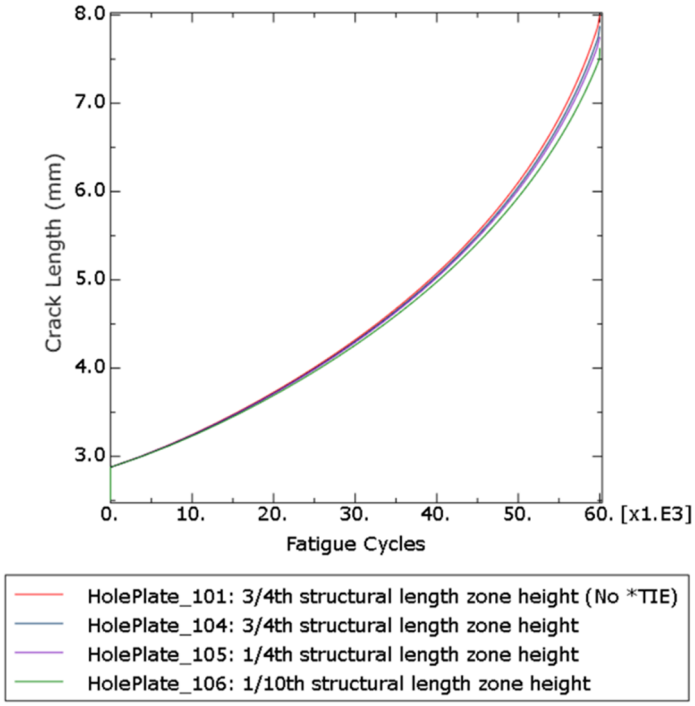

Figure 17 Influence of Enrichment Region Height on Crack Growth Rate for Two Cracks Emanating from a Hole in a Finite Plate under Uniform Uniaxial Far-Field Pressure Loading (Structured Mesh, Normal Mesh Refinement, Reduced Integration Formulation)

The influence of the enrichment region structural height on the calculated crack growth was found to be insignificant down to and including the height set to 10% of the in-plane structural depth. It was found that the strain energy release rate (Abaqus output variable ENTTRXFEM for propagating XFEM cracks) was not as sensitive to tie interfaces as the standard contour integral approach. The computational cost for the different enriched zone sizes was found to be minimal due to the high level of parallelization in the Abaqus XFEM implementation.

A logical question could be asked whether small initial flaw sizes could be utilized with reasonable mesh refinements. To address this concern, a sensitivity study was developed to include a_i/t values of 0.2 (baseline), 0.1, and 0.05 using the normal mesh refinement (40-elements in structural thickness direction) with the Flat Plate model. Shown below in **Error! Reference source not found.** 18, it is quite obvious that for both the initial a_i/t flaws of 0.1 and 0.05 that the crack shape is rather poorly captured with this level of refinement. However, by the time that the crack reaches an a/t=0.4 that the crack shape is reasonably captured and at the end of the simulation that crack front is captured quite well. This is expected as the crack front is passing through more and more elements. In these cases, the crack growth rates are conservatively captured compared to the analytical solution([16] as detailed in Appendix B) shown in Figure 19.

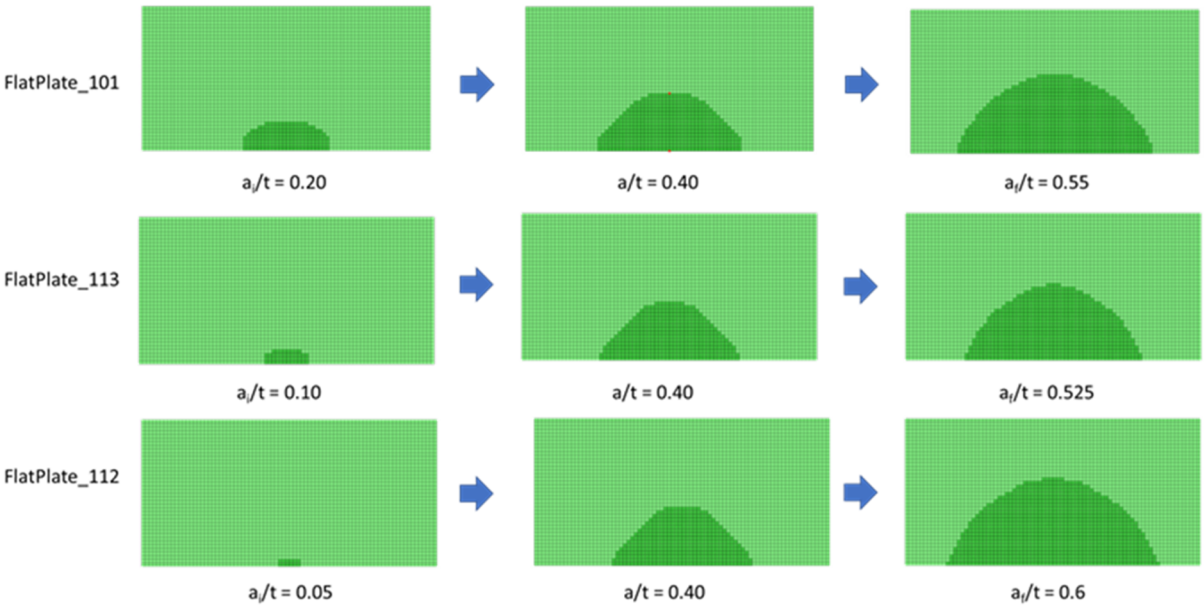

Figure 18 Effect of Initial Flaw Size on Crack Growth Shape while using Normal Mesh Refinement (40-elements in structural thickness direction) for the Flat Plate Model

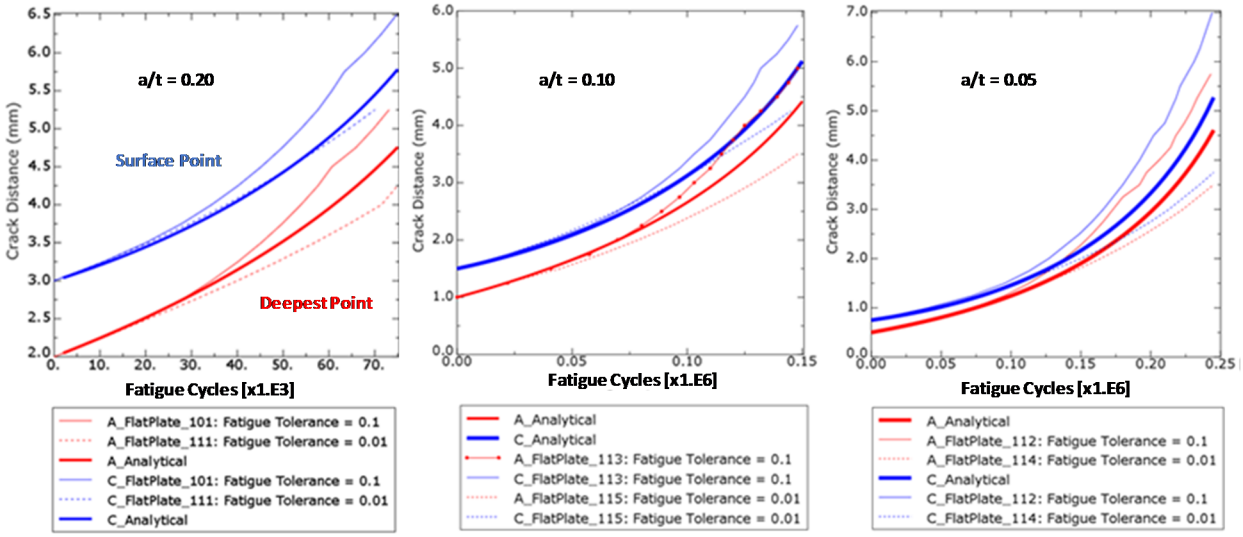

Figure 19 Effect of Initial Flaw Size on Crack Growth Rate while using Normal Mesh Refinement (40-elements in structural thickness direction) for the Flat Plate Model (Analytical Solution Provided in [16] and Detailed in Appendix B)

4.2 Crack Growth Control Options

4.2.1 Crack Tip Strain Averaging Control

As expected for true simple in-plane crack extension geometries (e.g. Flat Plate), Figure 20 shows no appreciable difference in the crack growth shape between the local and nonlocal crack tip stress field location parameters.

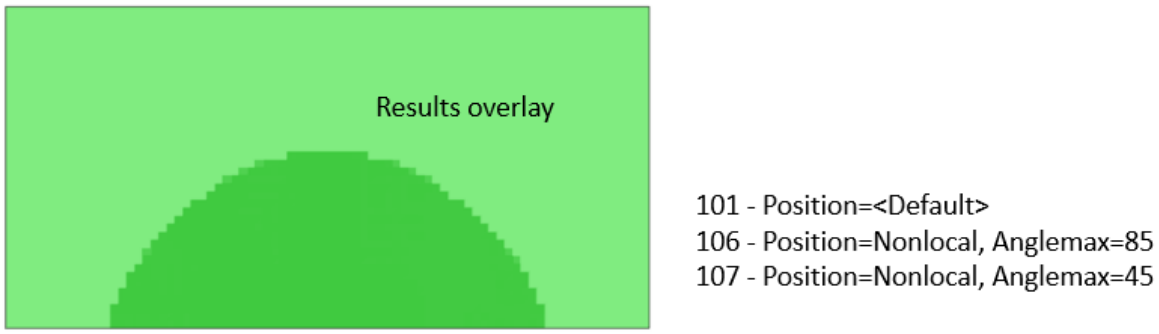

Figure 20 Influence of Crack Growth POSITION Parameter on Crack Shape at 50000 cycles for Semi-Elliptical Surface Flaw in a Finite Width Flat Plate

For practical problems (e.g. VC Summer DWM axial flaw) which are intended to see planar crack extension, the POSITION=NONLOCAL was observed to cause only minimal changes in the crack shape and crack growth rates where limited out-of-plane crack growth is noted. Alongside the Advanced Finite Element Analysis (AFEA) solution results that are described in Appendix D, Figure 21 shows only a slight change between the two settings for the VC Summer DWM axial flaw assessment.

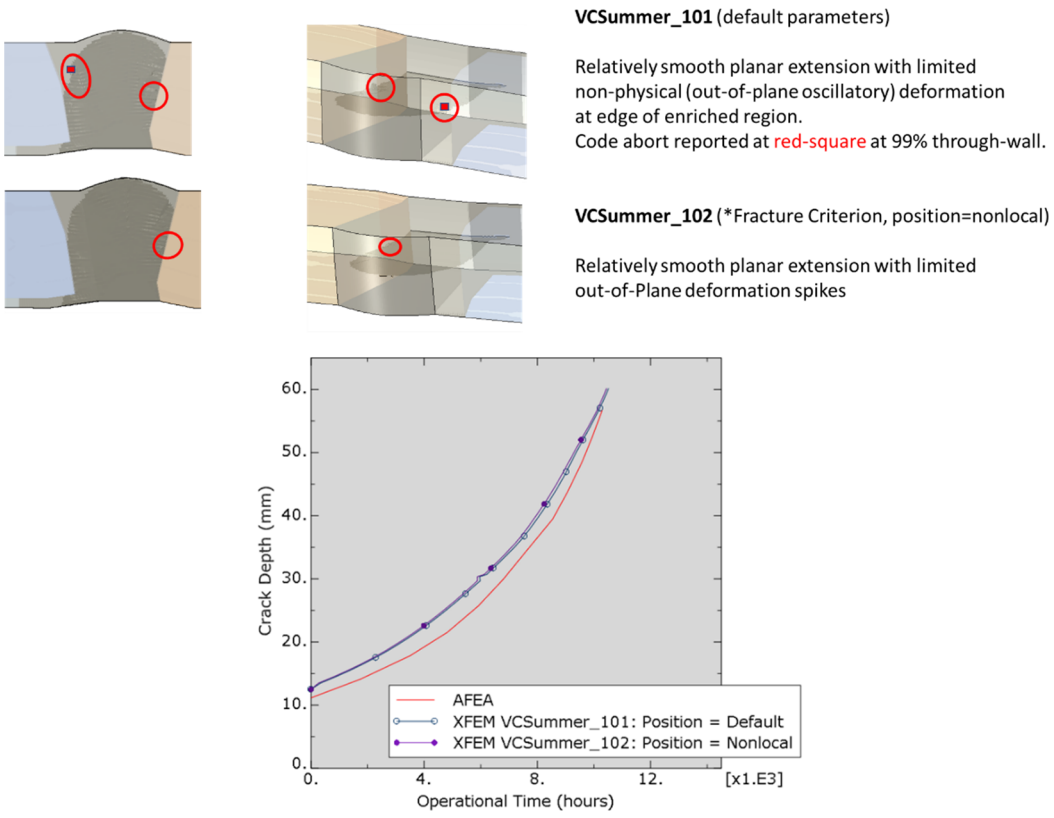

Figure 21 Influence of Crack Growth POSITION Parameter on Crack Growth at Deepest Point as a Function of Time and Overall Crack Shape for PWSCC VC Summer Axial Surface Flaw in DWM Hot Leg. (The Advanced Finite Element Analysis (AFEA) benchmark solution is described in Appendix E.)

Perhaps most importantly, for the curvilinear crack growth Miss Hole geometry, an incorrect crack trajectory is seen when an unstructured mesh is used with reduced integration elements with the default

POSITION option. However, with the POSITION=NONLOCAL option which allows for a smoother crack propagation direction projection, an unstructured reduced integration mesh is able to obtain the desired crack trajectory as depicted below in Figure 22.

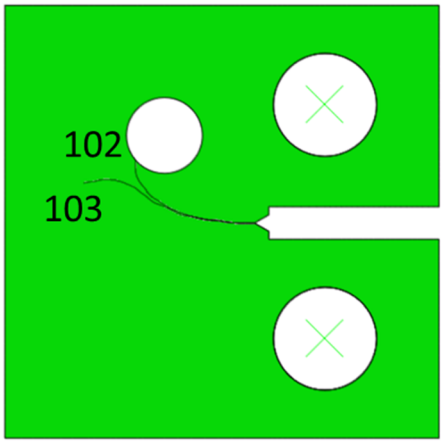

Figure 22 Influence of Crack Growth POSITION Parameter (102 for Default, 103 for Nonlocal) on Crack Growth Shape for Reduced Integration "Miss Hole" Unstructured Mesh Models

4.2.2 Crack Propagation Direction Control

For true planar crack extension geometries (e.g. Flat Plate), no appreciable difference was noted in Figure 20 for the crack growth shape or crack growth rates when the ANGLEMAX is set to smaller angles less than the default of 85 degrees. For the curvilinear crack growth Miss Hole geometry, controlling the maximum crack turn within one element from the default of 85 degrees to values as low as 30 degrees were found to cause no appreciable difference in results as seen in **Error! Reference source not found.** 23. ANGLEMAX seems hard to use effectively for general purposes as it might inhibit both "corrective" crack path incremental advances as well as detrimental ones for low ANGLEMAX values (e.g. less than 30 degrees for the Miss Hole geometry).

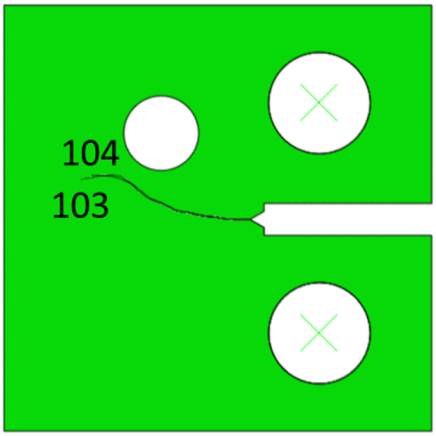

Figure 23 Influence of Crack Growth ANGLEMAX Parameter (103 = 85°, 104 = 30°) on Crack Growth Shape for Reduced Integration "Miss Hole" Unstructured Mesh Models

4.2.3 Damage Extrapolation Tolerance

As described in Section 2.3.2, the *FATIGUE damage extrapolation tolerance term, ΔD_{Ntol}, was found to be one of the most important parameters for balancing solution accuracy with computational time. Using the default ΔD_{Ntol}= 0.1, conservative bounding results were found for the 3D analysis models studied

(PWSCC CT (see **Error! Reference source not found.** below) and Flat Plate (Figure 25) with reduced ntegration elements in structured meshes. More accurate solutions were found by lowering the ΔD_{Ntol} to 0.01. However, it could be seen for deeper cracks that the crack growth rates could be slightly underpredicted.

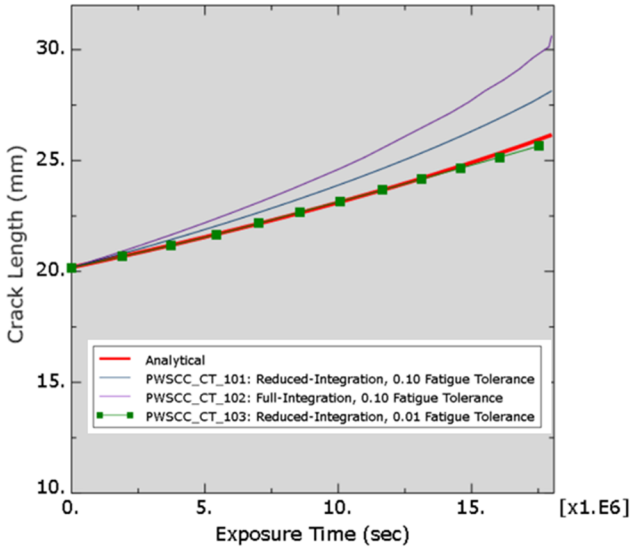

Figure 24 Crack Length as a Function of Exposure Time for Fatigue Damage Extrapolation Tolerance Parameters for the PWSCC CT Specimen Geometry (Analytical Solution Provided in [19] and Detailed in Appendix D)

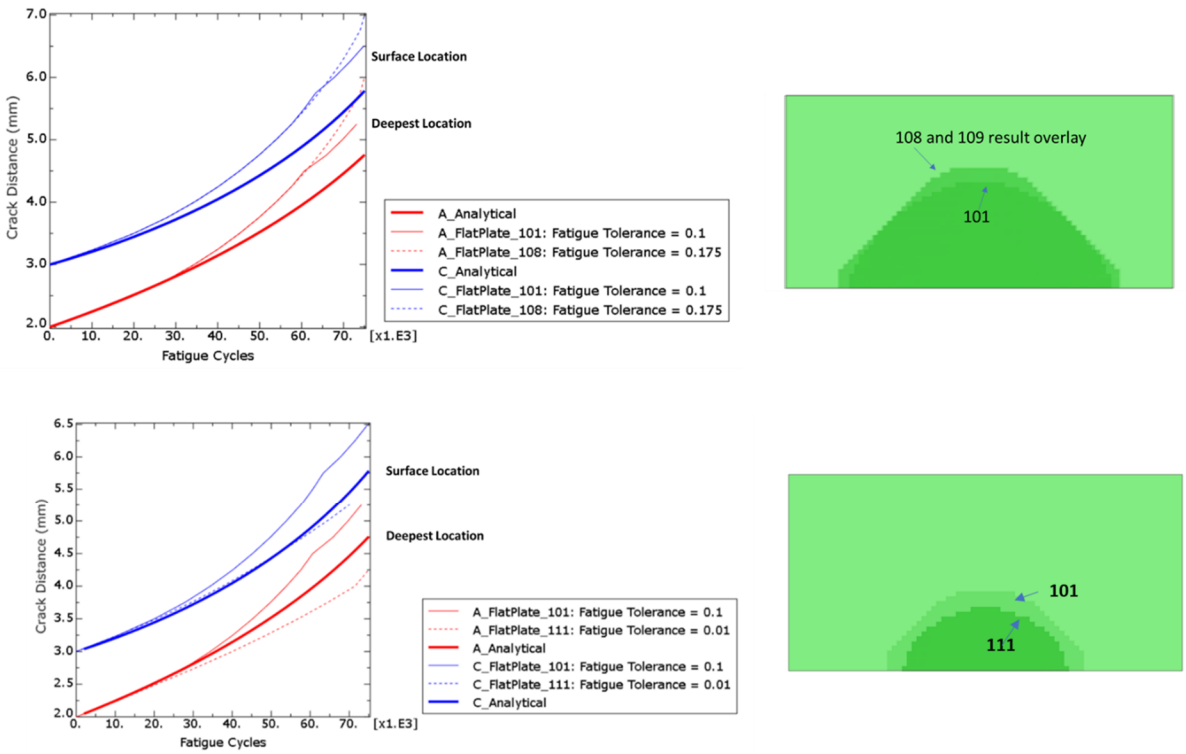

Figure 25 Influence of Subcritical Damage Extrapolation Tolerance Parameter on Crack Growth Rate and Crack Shape (at 50000 cycles) for Semi-Elliptical Surface Flaw in a Finite Width Flat

Plate under Uniform Uniaxial Far-Field Pressure Loading (Reduced Integration) (Analytical Solution Provided in [16] and Detailed in Appendix B)

For long-running practical problems such as the VC Summer Hot Leg DWM axial flaw assessment, a looser tolerance could be set to obtain a conservative crack growth rate in a shorter amount of computational time. Shown in for the Flat Plate model when the ΔD_{Ntol} is set to 0.175, the crack growth is seen to conservatively increase but with the crack shape becoming more triangular as compared to the expected semi-elliptical shape. Likewise for the VC Summer Hot Leg DWM in **Error! Reference source ot found.** 26, by increasing the ΔD_{Ntol} to 0.175, the solution time was reduced by ~2x. Also, this increased the crack growth rate but the through-wall crack shape was found to deviate significantly from the actual observed crack and baseline XFEM analyses. Further, when ΔD_{Ntol} is set to 0.175, a code abort is observed at an out-of-plane deformation near the edge of the enrichment region.

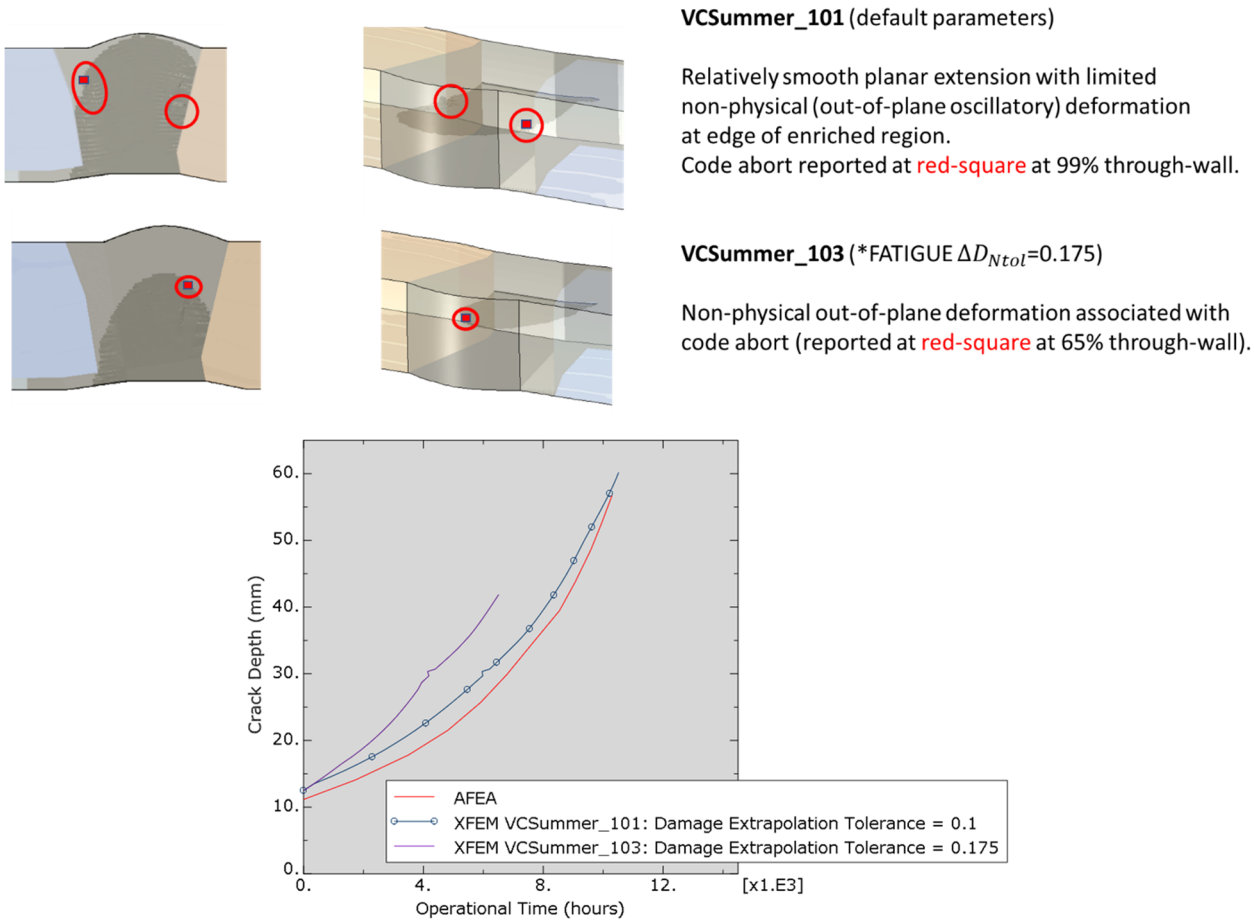

Figure 26 Crack Depth as a Function of Exposure Time for Subcritical Damage Extrapolation Tolerance Parameter for the VC Summer Hot Leg DWM Flaw Assessment

4.3 General Solution Convergence Controls

An XFEM crack propagation analysis can sometimes fail to converge, in spite of reasonable damage properties and a suitably refined mesh in the enriched region. Two analysis settings were studied to facilitate convergence.

4.3.1 Unysmmetric Solver

For all problems studied, no impact on the convergence rate was observed when using the unysmmetric solver (`*STEP,UNSYMM=YES`).

4.3.2 *CONTROLS Displacement Correction

For the linear elastic applications studied, the loosening of the displacement correction `*CONTROLS` displacement correction by an order of magnitude (from 0.01(default) to 0.1) was not found to affect solution quality.

5 RECOMMENDATIONS

It has been found that even performing basic crack growth problems will be a challenge without significant benchmarking of results for a given problem class. With that stated, general modeling recommendations are summarized below:

- Software Version: Abaqus/Standard 2020 or later
- Minimum Mesh Refinement of XFEM Enriched Region in Key Structural Dimensions:
  - Thickness (crack growth depth direction): 50-elements
  - Width (crack growth length direction): Use Thickness mesh seed
  - Height (perpendicular to initial crack plane): 10-elements with Thickness mesh seed
- Mesh Type: Structured
- Element Formulation: Quad/Hex with Reduced Integration

For applications with nonplanar curvilinear crack growth, the nonlocal averaging option may be required along the crack front to ensure proper crack propagation directions are calculated. For all other analyses, other analysis parameters (subcritical damage growth tolerance, subcritical crack extension criteria, general solution controls) should be set to default values. However, with careful evaluation and benchmarking, non-default parameters could be utilized to obtain robust, accurate solutions in a timely fashion.

In these recommendations, the mesh refinement is set via the structural thickness dimension in a nondimensional manner. In line with the implementation requirement that only a single element will "fail" in a given increment, the 50-element recommendation ensures that the depth crack growth rate can be conservatively estimated for simple geometries. The structural width and height values are set to ensure that the hexahedron (or quadrilateral) shape is as close to a perfect cube (or square) as possible. This recommendation is made to minimize crack growth differences in the three principal directions due to mesh refinement. Further, the structural height recommendation is set to 20% of the structural thickness to accommodate the potential for out-of-plane (height-direction) crack growth in practical applications (e.g. VC Summer hot leg DMW axial flaw assessment).

The structured mesh was recommended to minimize mesh bias effects in each direction during crack growth. As compared to full integration, the reduced integration recommendation was made as strain energy release rates were seen to better match the analytical 3D stress intensity factor solutions while also allowing curvilinear crack growth.

Other solution variables should be set to the default settings. This includes the subcritical damage tolerance parameter, ΔD_{Ntol}. While crack growth rates with a tightened ΔD_{Ntol} (=0.01) were initially accurate as compared to analytical benchmark problems, it was found to slightly underpredict growth rates as the solution progressed to higher crack depths. Hence, in order to provide a conservative crack growth rate with reasonable computational cost, the default value of 0.1 is recommended for ΔD_{Ntol}.

6 SUMMARY OF KEY OBSERVATIONS

In support of the following bulleted items, references are provided in parentheses at the end of the statement to the model most closely aligned with the observation.

6.1 Quality of Results

- Using the general XFEM modeling recommendations, the built-in Abaqus XFEM capability has shown to accurately model and analyze relatively complex PWSCC and constant-amplitude fatigue applications.(All models)
- Best results in terms of solution convergence, mesh refinement and mesh type effects involve a refined, structured-mesh using reduced-integration quadrilateral (2D) or hexahedral (3D) elements. (All models)
- Full integration, and to a lesser extent, reduced integration element formulations result in inaccurate crack turning and can lead to unconservative crack growth rates. (Sink Hole)
- Asymmetric results were observed even under nominally symmetric conditions for curvilinear crack growth problems. (Miss Hole)
- The subcritical damage extrapolation tolerance parameter, ΔD_{Ntol}, was found to be one of the most important parameters for balancing solution accuracy with computational time. To obtain solutions that matched benchmark specimen geometries, it was found that a tighter (ΔD_{Ntol} = 0.01) than default tolerance (ΔD_{Ntol} = 0.1) was required. For long-running practical problems, a looser tolerance (ΔD_{Ntol} = 0.175) could be set to obtain a conservative crack growth rate in a shorter amount of computational time. (PWSCC Compact Tension)
- The general minimum mesh refinement is applicable down to practical initial flaw sizes (a_i/t =0.05). Of course, more mesh refinement will lead to more accurate results but this will need to be balanced with additional computational cost. (Flat Plate)

6.2 Stability of Solution

- Using the general XFEM modeling recommendations, the built-in Abaqus XFEM capability was seen to provide converged results for each of the five models examined in this study.
- Some non-physical oscillatory out-of-plane crack propagation was observed in nominally planar crack extension problems. Up to 50% of the time, this behavior led to code aborts, occurring where the crack extended to the boundary of the enriched region. (VC Summer)

6.3 Computational Resources

- Due to the high degree of parallelization of the Abaqus XFEM implementation, solutions can be obtained in reasonable time periods even for relatively complex analyses.
- Using non-default values for fatigue damage extrapolation tolerance parameter ΔD_{Ntol} option of greater than 0.1, solutions can be obtained in a shorter amount of time, but some accuracy loss can be seen in the crack shape while the crack growth rate will be conservative.

7 CONCLUSIONS

This Task 2 report has discussed the Abaqus XFEM implementation coupled with the simplified fatigue procedure which allowed exploration of optimum parameter definitions to provide the most appropriate solutions for constant-amplitude fatigue and PWSCC (Primary Water Stress Corrosion Crack) crack growth analyses. As such, the results are seen to generate reasonable simulation results.

It should be noted that the recommendations are general and heuristic in nature based on previous Abaqus experience and the sensitivity study performed in this study. The recommendations are not absolute and rigid but should be used as a general modeling guide.

In addition to Abaqus (/Standard solver with /CAE pre- and post-processing), XFEM has also been implemented as a core implementation in such DOE-sponsored research codes such as INL's Grizzly and commercial finite element software codes as Ansys and VirFac Crack/Morfeo. Implementation details will likely vary within and between each code. As an example, Ansys offers both 'phantom node' and 'singularity-based' XFEM methods for stationary crack evaluation. For the latter, Abaqus supports distributed pressure on the crack face while Ansys does not support this option.

Regardless of final software and implementation chosen, it has been found that even performing basic crack growth problems will be a challenge without significant benchmarking of results for a given problem class.. With that stated, the general modeling recommendations made here, associated with the built-in Abaqus XFEM implementation, should serve as a reasonable starting point.

For further consideration, the Task 3 report (Evaluation of PWSCC-type crack growth in Abaqus XFEM for Complex geometries) provides detailed solutions for the VC Summer and control rod drive mechanism (CDRM) XFEM based crack growth to leakage solutions. The Task 3 report also summarizes the best Abaqus-based XFEM solution parameter definitions and compares the solutions to crack growth analyses performed in the past using other methods. Finally, Task 4 provides a summary of solutions performed by the NRC and contractors, and other organizations that may be used in the future for further benchmarking. The Benchmark solutions presented provide references along with other data necessary to perform XFEM based solutions and predicted results using other PWSCC growth methods for benchmark comparisons.

REFERENCES

1 Dassault Systèmes (2020). Abaqus/Standard 2020 User's Manual. Providence, RI.

2 Melenk, J. M., & Babuška, I. (1996). The partition of unity finite element method: basic theory and applications. In *Research Report/Seminar für Angewandte Mathematik* (Vol. 1996, No. 01). Eidgenössische Technische Hochschule, Seminar für Angewandte Mathematik.

3 Belytschko, T., Gracie, R. and Ventura, G. (2009), "A review of extended/generalized finite element methods for material modeling." *Modelling and Simulation in Materials Science and Engineering* 17, no. 4:043001.

4 Adalsteinsson, D., Sethian, J.A. (1995),"A fast level set method for propagating interfaces," *Journal of Computational Physics*, 118, 269-277.

5 Stolarska, M., Chopp, D.L., Moes, N., Belytschko, T. (2001), "Modelling crack growth by level sets in the extended finite element method," *International Journal for Numerical Methods in Engineering*, 51, pp943-960.

6 Sukumar, N., et al. (2001), "Modeling holes and inclusions by level sets in the extended finite-element method," Computer methods in applied mechanics and engineering, pp6183-6200.

7 Dolbow, J., Zhang, Z., Spencer, B. and Jiang, W. (2015), "Fracture Capabilities in Grizzly with the eXtended Finite Element Method (X-FEM)," Idaho National Laboratory, INL/EXT-15-36752.

8 Ansys, Inc. (2017), "ANSYS Mechanical APDL Fracture Analysis Guide", Canonsburg, PA.

9 Geonx S.A. (2020), "Virfac© Morfeo/crack for Abaqus", Gosselies, Belgium. http://www.geonx.com/index-112.html.

10 Spencer, B. W., Pitts, S. A., Liu, L., Vyas, M., Jiang, W., Casagranda, A., & McDowell, D. J. (2019). *Summary of Grizzly Development for Advanced Reactor Structural Materials* (No. INL/EXT-19-55958-Rev000). Idaho National Lab.(INL), Idaho Falls, ID (United States).

11 Chen, Y. (2018), "Best Practices in Modeling Crack Propagation with XFEM in Abaqus/Standard", Dassault Systèmes Johnston, RI.

12 Materials Reliability Program (2004) "Crack Growth Rates for Evaluating PWSCC of Alloy 82, 182, and 132 Welds," MRP-115, EPRI, Palo Alto, CA.

13 Anderson, T.L. (2017), Fracture Mechanics: Fundamentals and Applications, Fourth Edition, CRC Press, Boca Raton, FL.

14 Moës, N., Dolbow, J. and Belytschko, T. (1999), "A finite element method for crack growth without remeshing", Int. J. Numer. Meth. Engng., 46: pp131-150.

15 Miranda, A.C.O., Meggiolaro, M.A., Castro, J.T.P., Martha, L.F. and Bittencourt, T.N. (2003), "Fatigue life and crack path predictions in generic 2D structural components", Engineering Fracture Mechanics 70: pp1259-1279.

16 Newman, J.C. and Raju, I.S. (1984), "Stress-Intensity Factor Equations for Cracks in Three-Dimensional Finite Bodies Subjected to Tension and Bending Loads," NASA Technical Memorandum 85793, NASA Langley Research Center, Hampton, VA.

17 Daux, C., Moës, N., Dolbow, J., Sukumar, N., & Belytschko, T. (2000), "Arbitrary branched and intersecting cracks with the extended finite element method", Intl. Journal for Numerical Methods in Engineering, *48*(12), pp1741-1760.

18 Antunes, F. V., Branco, R., Ferreira, J.A.M. and Borrego, L.P. (2019), "Stress Intensity Factor Solutions for CTS Mixed Mode Specimen", Frattura ed Integrità Strutturale, 48, pp. 676-692.

19 Alexandreanu, B, Chopra, O., Shack, W., Crane, S. and Gonzalez, H. (2008), " Crack Growth Rates and Metallographic Examinations of Alloy 600 and Alloy 82/182 from Field Components and Laboratory Materials Tested in PWR Environments", NUREG/CR-6964, US Nuclear Regulatory Commission, Washington, D.C.

20 Scott, P. et al. (2005), "The Battelle Integrity of Nuclear Piping (BINP) Program Final Report", Volumes 1 and 2, NUREG/CR-6837, US Nuclear Regulatory Commission, Washington, D.C.

21 Materials Reliability Program (2004) "Crack Growth Rates for Evaluating PWSCC of Alloy 82, 182, and 132 Welds," MRP-115, EPRI, Palo Alto, CA.

22 Newman, J. C., Jr. (1971), "An Improved Method of Collocation for the Stress Analysis of Cracked Plates with Various Shaped Boundaries," NASA TN D-6376, National Aeronautics and Space Administration, Washington, D.C.

23 Shim, D.-J. Kalyanam, S., Punch, E. Zhang, T., Brust, F. and Wilkowski, G., "Advanced Finite Element Analysis (AFEA) Evaluation for Circumferential and Axial PWSCC Defects,", PVP2010-25162, 2010 ASME Pressure Vessels and Piping Conference, Bellevue, WA.

24 API 579-1/ASME FFS-1 (2016), Fitness for Service, American Petroleum Institute, Washington, DC, USA.

APPENDIX A – XFEM FATIGUE MODEL: HOLE IN PLATE

Description:

This 2D planar problem provides evidence that the Abaqus XFEM can reproduce basic stress intensity factor values from the benchmark defined by Abaqus Benchmark Problem 4.7.5 [1] and Table 7 of Moës [14]. As such, it is based on a 2D plane strain model with two cracks emanating from a central hole in a finite width plate under uniform cyclic pressure loading.

As highlighted below, a slight modification was made such that the boundary conditions along edge AE enforce a plane section remains plane boundary condition which in combination with the uniform pressure applied along edge DF result in a slight non-uniform far-field stress field. This slight modification was made to show that initially the benchmark SIF values were matched but also show that XFEM results in slight crack turning. Further, this modification helps to show the crack turning issue associated with crack extension parallel and near an element boundary. Hence, this boundary condition modification allows us to examine multiple phenomena.

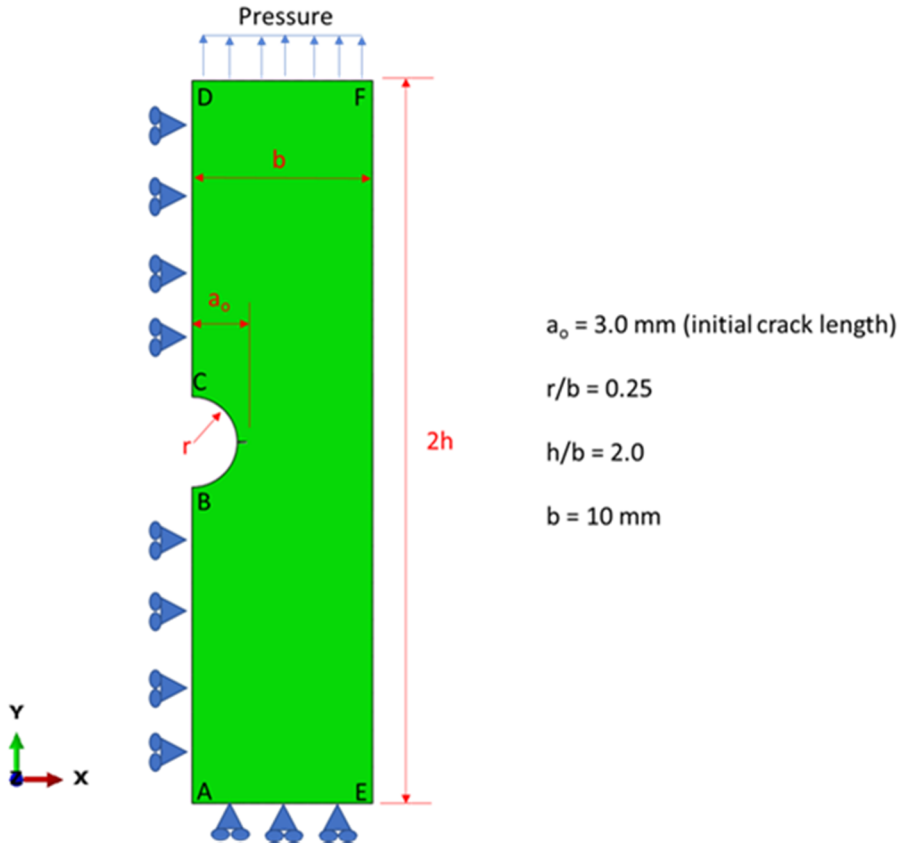

Units: N-mm-sec-MPa

FEA software: Abaqus 2020 (Build ID: 2019_09_13-12.49.31 163176)

Boundary Conditions: $u_x = 0$ along edges AB and CD to enforce a symmetry plane,
$u_y = 0$ along edge AE

Loading: Cyclic uniform pressure loading from 0.0 MPa to 79.40465 MPa along edge DF in each cycle (magnitude chosen to match cyclic stress range for Sink Hole geometry)

Material: Cold-rolled SAE 1020 steel.

Linear Elastic Material Properties were used with:

Young's Modulus = 2.07E5 MPa

Poisson's Ratio = 0.3

The da/dN fatigue properties for cold-rolled SAE 1020 steel are provided in Miranda [15]:

$$\frac{da}{dN} = 4.5 \cdot 10^{-10} \left(\Delta K - \Delta K_{th}\right)^{2.1}$$

where $\frac{da}{dN}$ is in m/cycle and ΔK is in MPa√m.

For simplicity, ΔK_{th} is set to zero for this problem.

We need to define the following Abaqus Paris-like relation:

$$\frac{da}{dN} = C_3 \left(\Delta G\right)^{C_4}$$

Converting between parameters and unit systems, we have the following for the plane strain condition:

		Plane Strain								
	da/dN	deltaK			deltaG			Modulus		
	Units	Units	C	n	Units	C3	C4	Units	Elastic	nu
input	m/cycle	MPa*m^0.5	4.50000E-10	2.1	N/m	9.5058E-11	1.05	MPa	2.07E+05	0.3
output	mm/cycle	MPa*mm^0.5	3.18576E-10	2.1	N/mm	1.2947E-04	1.05	MPa	2.07E+05	0.3

Hence,

$$\frac{da}{dN} = 1.2947 \cdot 10^{-4} \, \Delta G^{1.05}$$

with $\frac{da}{dN}$ in mm/cycle and ΔG n N/mm units.

Lastly, the critical strain energy release rate is required by the Abaqus fracture criterion. For this, we arbitrarily chose $G_{Ic} = G_{IIc} = G_{IIIc} = 45.5$ N/mm which is equivalent to a plane strain fracture toughness of 100 MPa√m. For this analysis, we remain far below this critical value.

	Plane Strain			
	Units	K	Units	G or J
Input	MPa*m^0.5	1.00000E+02	N/m	4.55000E+04
Output	MPa*mm^0.5	3.16228E+03	N/mm	45.5

To aid in the da/dN and fracture toughness parameter and unit conversions, Appendix F describes an Excel tool that interactively allows for such conversions. This tool is made available in the Supplemental Files associated with this report.

Analysis Steps:

Analysis is completed in two analysis steps:

1) *STATIC preload the structure to maximum value.

2) *FATIGUE, TYPE=SIMPLIFIED

Parameters Studied:

As tabulated below, independent analyses were used to evaluate mesh refinement (in-plane structural thickness and structural height), mesh type and element formulation. An additional analysis was completed to access the SIF solution for a crack orientation where the initial flaw was not aligned perpendicular to the maximum Principal Stress.

Hole in Plate	Mesh Refinement		Element	Mesh	Crack Growth	Crack Growth	Fatigue	Controls	Abaqus Input
	Structural Thickness	Structural Height (Fraction of Depth)	Formulation	Type	Position	ANGLEMAX	Tolerance	Disp Correction	File Name
Baseline	N	3/4th (No *TIE)	R	S	Default	85	0.1	0.01	**HolePlate_ 101**
Recommend Guidelines	N	Not less than 1/10th	R	S	Default	85	0.1	0.01	**HolePlate_ 111**
SIF Solution Comparison									
Reduced-Integration	C	3/4th (No *TIE)	R	S	Default	85	0.1	0.01	**HolePlate_ 112**
Full-Integration	C	3/4th (No *TIE)	F	S	Default	85	0.1	0.01	**HolePlate_ 113**
Focused Mesh									**FocusedMesh_Dir**
Mesh Refinement (Structural Thickness)									
Normal (58 elements)	N	3/4th (No *TIE)	R	S	Default	85	0.1	0.01	**HolePlate_ 101**
Fine (116 elements)	F	3/4th (No *TIE)	R	S	Default	85	0.1	0.01	**HolePlate_ 102**
Coarse (29 elements)	C	3/4th (No *TIE)	R	S	Default	85	0.1	0.01	**HolePlate_ 103**
Mesh Refinement (Structural Height)									
3/4th of Structural Depth (w/ o *TIE)	N	3/4th (No *TIE)	R	S	Default	85	0.1	0.01	**HolePlate_ 101**
3/4th of Structural Depth (w/ *TIE)	N	3/4th	R	S	Default	85	0.1	0.01	**HolePlate_ 104**
1/4th of Structural Depth (w/ *TIE)	N	1/4th	R	S	Default	85	0.1	0.01	**HolePlate_ 105**
1/10th of Structural Depth (w/ *TIE)	N	1/10th	R	S	Default	85	0.1	0.01	**HolePlate_ 106**
Element Formulation									
Full-Integration	N	3/4th (No *TIE)	F	S	Default	85	0.1	0.01	**HolePlate_ 107**
Reduced-Integration	N	3/4th (No *TIE)	R	S	Default	85	0.1	0.01	**HolePlate_ 101**
Mesh Type									
Structured	N	3/4th (No *TIE)	R	S	Default	85	0.1	0.01	**HolePlate_ 101**
Unstructured: In Plane	N	3/4th (No *TIE)	R	UnS	Default	85	0.1	0.01	**HolePlate_ 108**
	F	3/4th (No *TIE)	R	UnS	Default	85	0.1	0.01	**HolePlate_ 109**
	C	3/4th (No *TIE)	R	UnS	Default	85	0.1	0.01	**HolePlate_ 110**
	N	3/4th (No *TIE)	F	UnS	Default	85	0.1	0.01	**HolePlate_ 117**
	F	3/4th (No *TIE)	F	UnS	Default	85	0.1	0.01	**HolePlate_ 118**
	C	3/4th (No *TIE)	F	UnS	Default	85	0.1	0.01	**HolePlate_ 119**
Crack Orientation (Initially not aligned to be perpendicular to Principal Stress)									
Aligned	N	3/4th (No *TIE)	R	S	Default	85	0.1	0.01	**HolePlate_ 101**
30 deg off-axis	N	3/4th (No *TIE)	R	S	Default	85	0.1	0.01	**HolePlate_ 114**
30 deg off-axis	N	3/4th (No *TIE)	F	S	Default	85	0.1	0.01	**HolePlate_ 115**
30 deg off-axis	N	3/4th (No *TIE)	R	UnS	Default	85	0.1	0.01	**HolePlate_ 116**

Elements: 2D plane strain 4-node bilinear (CPE4) full integration and reduced integration (CPE4R) elements were used.

Meshes: Two mesh types (structured and unstructured) with three mesh densities (0.0625-mm, 0.125-mm and 0.250-mm) near the discontinuity.

Structured Mesh

Normal (0.125-mm mesh size) Fine (0.0625-mm) Coarse (0.250-mm)

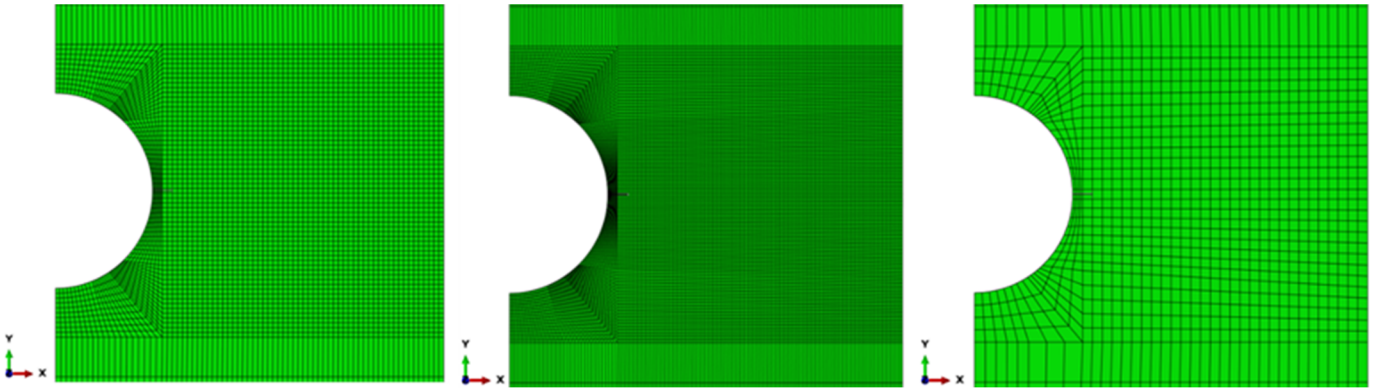

Unstructured Mesh

Normal (0.125-mm mesh size) Fine (0.0625-mm) Coarse (0.250-mm)

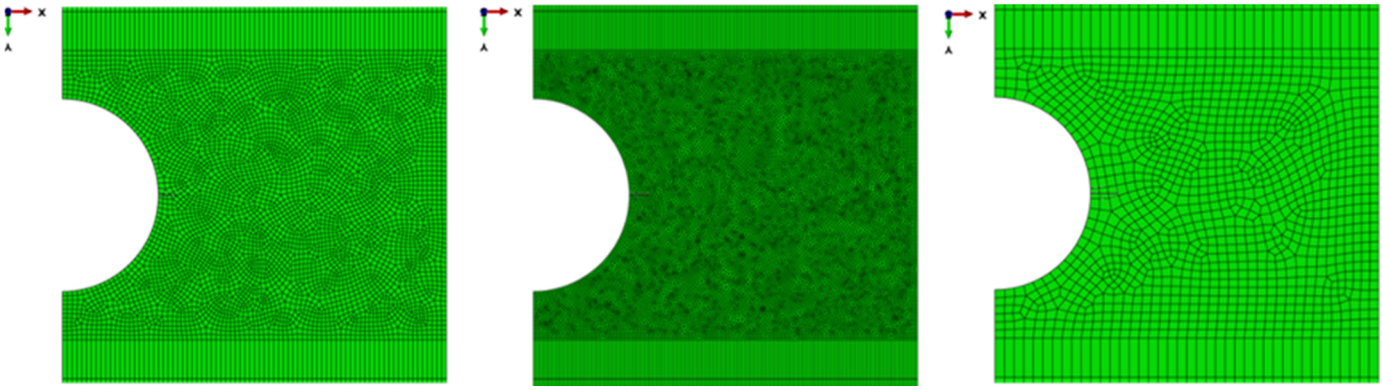

Results:

1) Comparison of SIF Geometry Correction Factors between Publication (Newman [22]), Focused Crack Tip Mesh in Abaqus and Structured Meshes with XFEM Crack Propagation

   The Abaqus XFEM built-in implementation does not require the mesh to conform to the crack geometry; however, the method does not permit a crack to lie along the element boundary in the structural thickness direction. Therefore, in simple problems such as this, where the crack is expected to propagate along a straight line; the mesh should be designed such that the expected crack propagation path does not lie along the element boundary in the structural thickness direction but is in the middle of the element for that direction. Hence, the initial crack is always away from the out-of-plane boundary in the structural height direction.

   As long as a crack propagates from one element edge to the opposite edge and is away from the side edges, the XFEM approach using the full-integrated element formulation is shown in Figure A1 to match published benchmark [22] and values obtained from traditional focused-mesh stationary cracks (available in Supplemental Files) for a given crack shape, geometry and loading up to a/b=0.7. The deviation occurs when there is a crack tip propagates to the element "top

edge" boundary at approximately a/b=0.7. By use of the slightly non-symmetric boundary condition (plane section remain plane) along the bottom edge of the model, this change illustrates the same crack turning issue for the more sophisticated Sink Hole geometry (Appendix C) that we will discuss later.

Seen in Figure A2, the full integration formulation was a better match for the analytical results for this 2D application. It was observed in the 3D PWSCC CT model (Appendix D) that the reduced integration formulation was the better match. In both models, the two element formulations, which differed by less than 10%, bounded the analytical result. Interestingly, the same "top edge" element boundary phenomenon is observed at a/b=0.8 for the reduced integration formulation.

Beta – Geometry Correction Factor

a/b	Newman	Abaqus Focused Mesh	Curve Fit Abaqus Focused Mesh	Abaqus XFEM Propagating Crack
0.30	1.078	1.076	1.090	1.097
0.3125		1.116	1.113	
0.325		1.143	1.134	1.153
0.35		1.177	1.168	1.186
0.40	1.216	1.215	1.219	1.224
0.45		1.246	1.255	1.256
0.50	1.285	1.284	1.289	1.294
0.55		1.333	1.330	1.344
0.60	1.397	1.395	1.389	1.406
0.65		1.475	1.471	1.487
0.70	1.580	1.579	1.581	1.661
0.75		1.715	1.724	1.816
0.80	1.904	1.903	1.899	2.007

$$K = \beta\sigma\sqrt{\pi a}$$

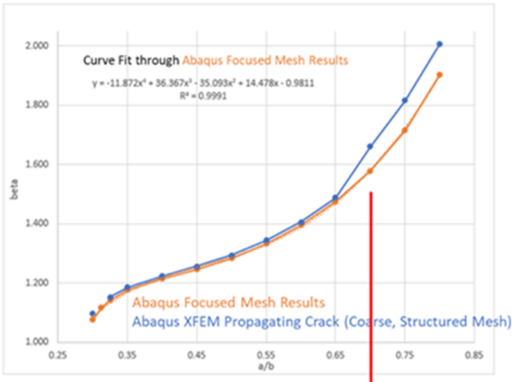

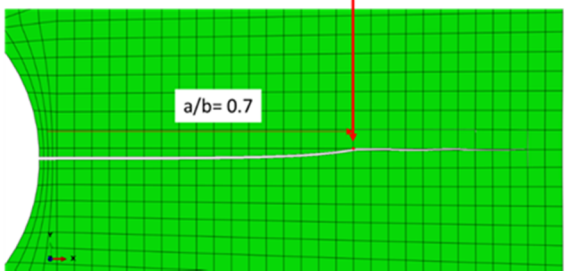

Figure A1 - Comparison of Stress Intensity Factor Solution for Two Cracks Emanating from a Hole in a Finite Plate under Uniform Uniaxial Far-Field Pressure Loading (HolePlate_113: Coarse, Full Integration). Analytical Solution is provided in Newman (16] and confirmed with Abaqus Focused Mesh Stationary Crack Evaluation (see Supplemental Files)

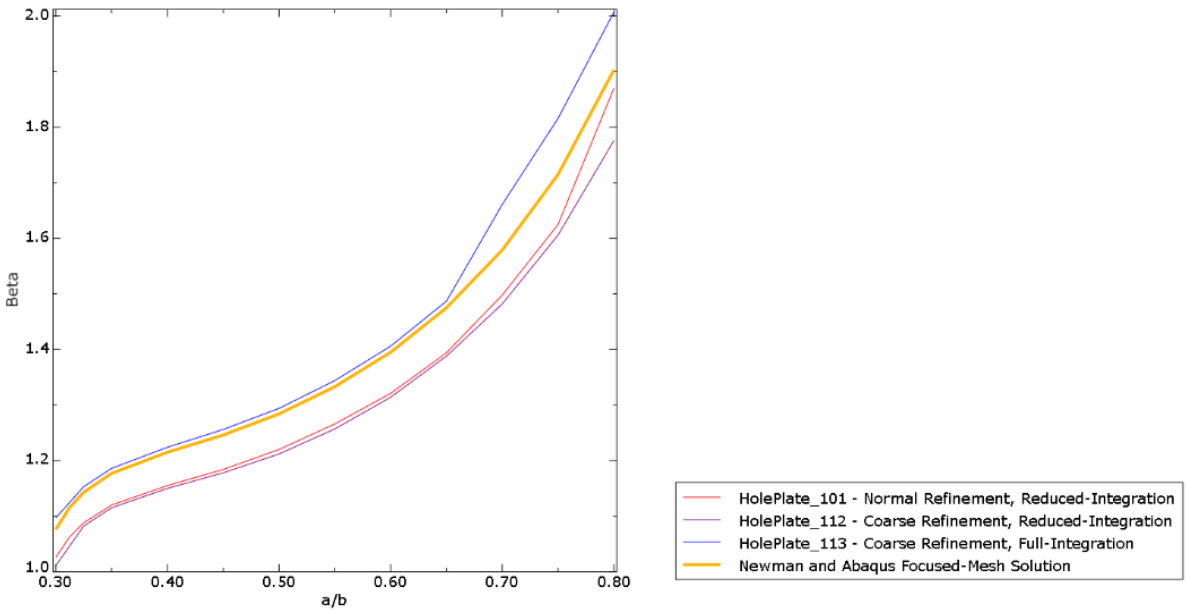

Figure A2 - Comparison of Stress Intensity Factor Solution for Two Cracks Emanating from a Hole in a Finite Plate under Uniform Uniaxial Far-Field Pressure Loading. Analytical Solution is provided in Newman (16] and confirmed with Abaqus Focused Mesh Stationary Crack Evaluation (see Supplemental Files)

2) Fatigue Crack Growth Predictions (Analytical Solution vs XFEM)

Figure A3 shows the fully-integrated formulation XFEM crack growth results after 50000 cycles for both the structured and unstructured meshes. Note, particularly on the structured meshes, the end of crack turning upon reaching the top edge (parallel to crack propagation) of the first element boundary. In short, this constrains the crack growth as additional curvilinear extension is precluded. As expected, the unstructured mesh shows greater deviation in crack growth propagation from a straight line.

Due to the limited number of data points available in Newman [22] for this geometry, thirteen individual finite element analyses were run to determine the non-dimensional geometry factors at different crack depths (a/b values ranging from 0.3 to 0.8) using stationary quarter-point elements with the contour integral extraction. For this linear elastic problem, J and G are equivalent. A fourth-order polynomial was then fit through the analysis data to provide an analytical SIF solution that was consistent with the Newman[16] data.

From there, the explicit time integration of the Paris Law was performed using this stress intensity factor solution. Using the constants and loadings described earlier in this Appendix, the crack locations were incremented in 1000-cycle increments.

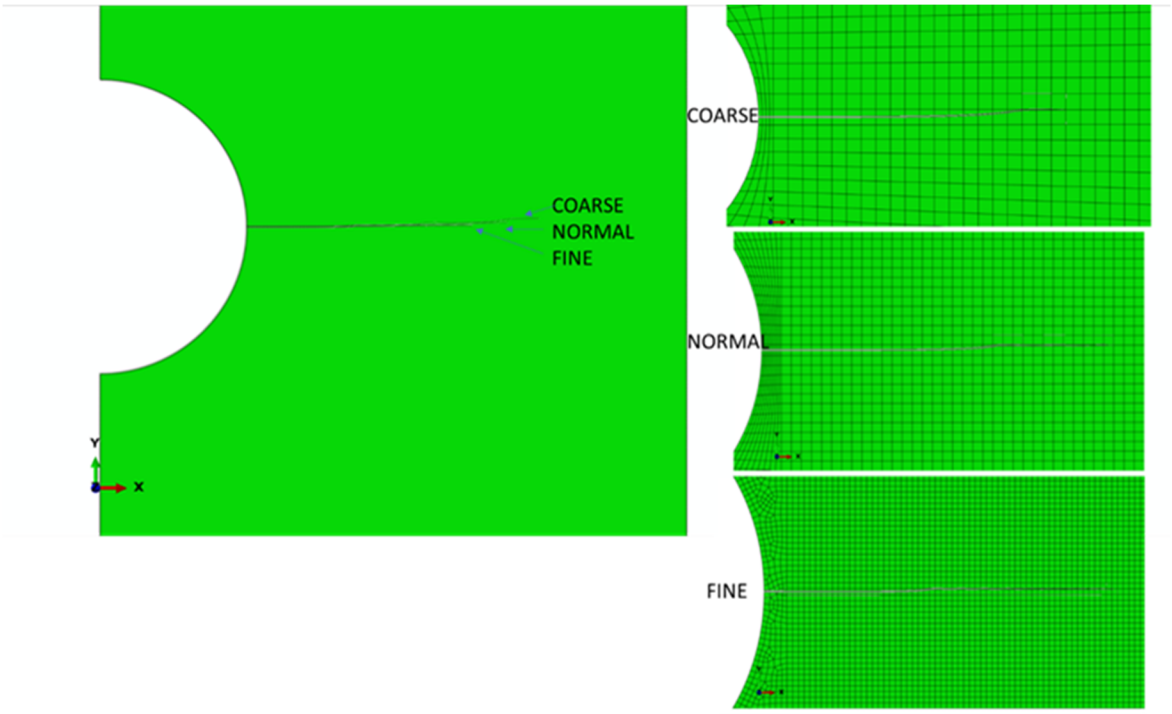

Figure A3 - Structured Crack Growth Paths at 50000 cycles (Full Integration)

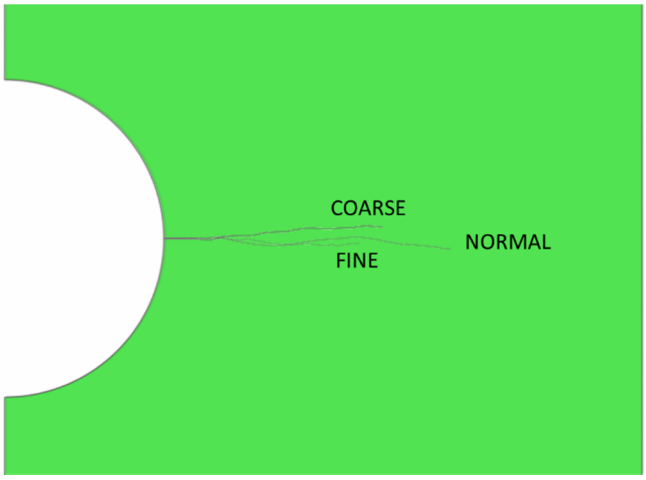

Figure A4 - Unstructured Crack Growth Paths at 50000 cycles (Full Integration)

Further, the crack growth rates are plotted below in Figure A5 for full integration elements. Perhaps, most troubling is the fact that for structured meshes with any deviation that the crack growth rates are seen to be below the analytical approach. In other words, non-conservative results are predicted. Further, *additional* mesh refinement is seen to cause a further deviation from the analytical solution.

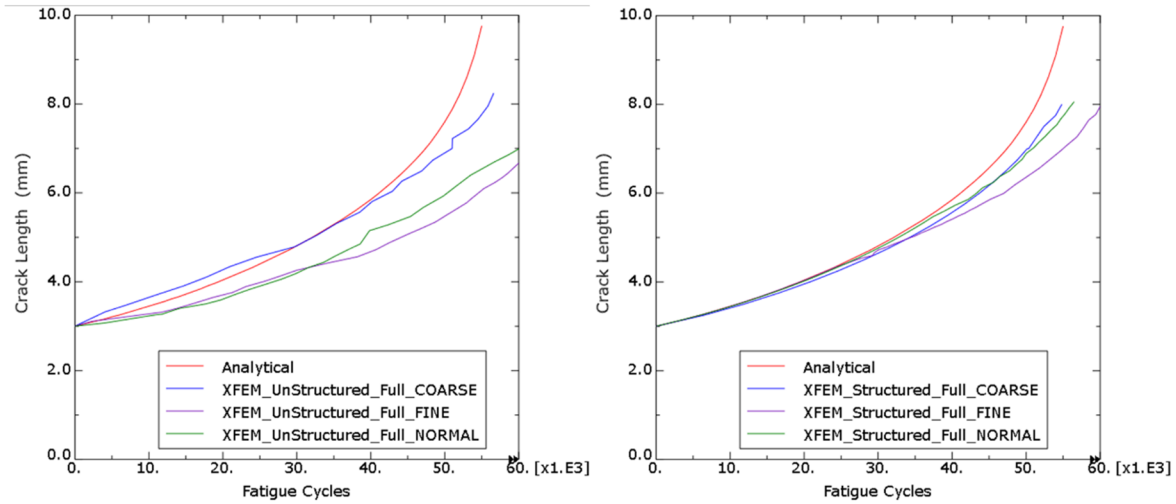

Figure A5 - Comparison of Crack Growth Rate for Two Cracks Emanating from a Hole in a Finite Plate under Uniform Uniaxial Far-Field Pressure Loading (Full Integration Elements)

As was shown previously with the lower strain energy release rate values, the reduced integration element formulation crack growth results (see Figure A6) are below the analytical values. For this formulation, additional mesh refinement does converge toward the analytical solution.

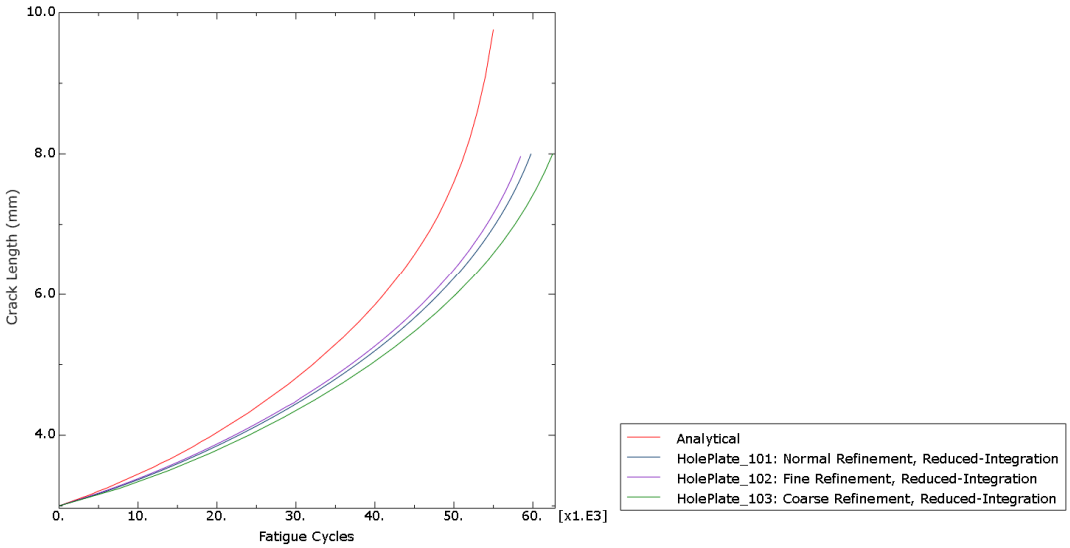

Figure A6 - Comparison of Effect of Mesh Refinement on Crack Growth Rate for Two Cracks Emanating from a Hole in a Finite Plate under Uniform Uniaxial Far-Field Pressure Loading (Reduced Integration Elements)

Overall, Figure A7 shows the best results with the normal refinement, structured meshes. For this 2D application, the full integration results provide the best solution up to an a/b=0.7 when the top edge of the element row containing the initial flaw is reached. The reduced integration results follow the intended analytical curve profile but is offset within the 10% difference in the strain energy release rate seen between the two element formulations.

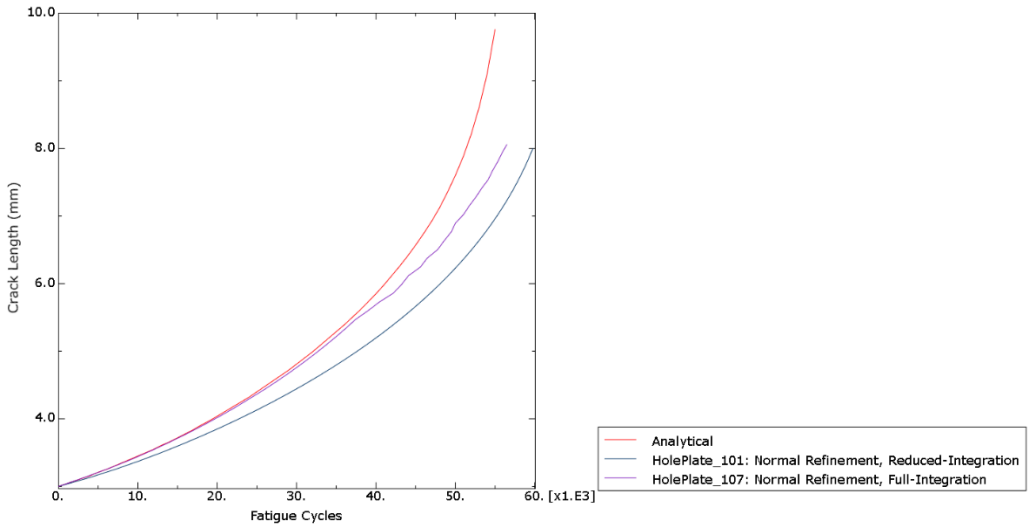

Figure A7 - Comparison of Effect of Element Integration Rule on Crack Growth Rate for Two Cracks Emanating from a Hole in a Finite Plate under Uniform Uniaxial Far-Field Pressure Loading (Normal Mesh Refinement)

3) Influence of Enrichment Region Structural Height

To ensure that the enrichment region height was of sufficient distance from the crack plane, a series of analysis runs were made varying the height as a function of the structural thickness. As was defined in Figure 2 of the main report, the structural thickness for this geometry was 10.0 mm. Analysis runs were made with the height set to 75%, 25% and 10% of the in-plane structural thickness. Further, these analysis runs were made with the structured quadrilateral element mesh tied to a triangular standard element region mesh. This was used to simulate a simple-to-generate coarse tetrahedral-like mesh in the far-field with a fine hex mesh in the enrichment region.

Shown in Figure A8, the influence of the enrichment region height on the calculated crack growth was insignificant down to and including the height set to 10% of the in-plane structural thickness. It was found that the strain energy release rate (Abaqus output variable ENTTRXFEM for propagating XFEM cracks) was not as sensitive to tie interfaces as the standard contour integral approach.

The general recommendation for the structural height is to set the structural height to 20% of the structural thickness to accommodate the potential for out-of-plane crack growth in practical applications such as reported in the VC Summer hot leg dissimilar weld axial flaw assessment which is documented in Appendix E.

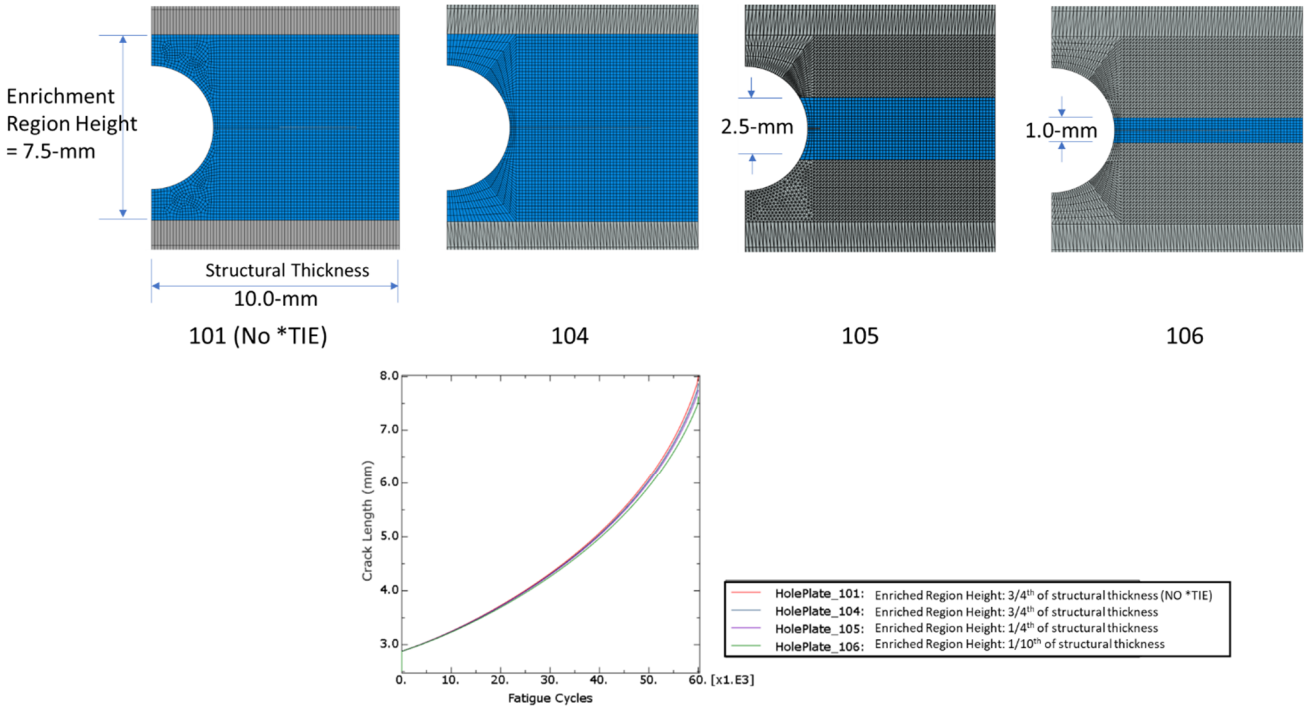

Figure A8 – Influence of Enrichment Region Height on Crack Growth Rate for Two Cracks Emanating from a Hole in a Finite Plate under Uniform Uniaxial Far-Field Pressure Loading (Structured Mesh, Normal Mesh Refinement, Reduced Integration Formulation)

4) Influence of Crack Orientation relative to Primary Loading

The Abaqus XFEM implementation has the ability to model mixed mode stationary and propagating cracks. As was first discussed in Section 2, the strain energy release rate, G, is directly computed for propagating flaws for XFEM in the linear elastic subcritical crack growth procedure via the modified VCCT method.[1] By directly computing the Mode I, II and III values, the crack extension occurs orthogonal to the maximum tangential stress when the crack growth criterion is met.[1]

Figure A9 shows the influence of a crack offset 30 degrees from the principal plane. Comparing with the analytical XFEM results from Daux [17], the initial mixed-mode cracks provide reasonable SIF values. Using the method discussed above, cracks change direction approximately normal to the loading direction when propagating under Mode I. This has been confirmed numerically and experimentally using the CT Shear specimen by Antunes [18]. Crack growth rates for the structured and unstructured mesh with full- and reduced integration follow the observations provided earlier in this Appendix.

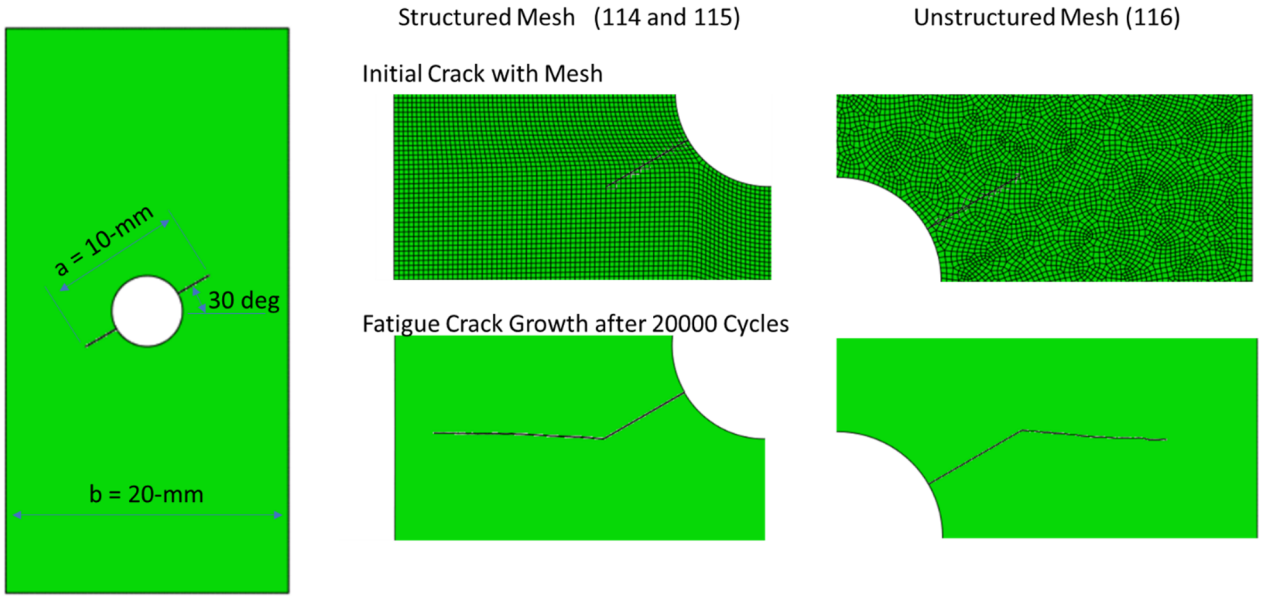

	Current Work			
HolePlate_<Run>	114	115	116	
Mesh Refinement:	Normal	Normal	Normal	Daux [17]
Mesh Type:	Structured	Structured	Unstructured	Table 7
Element Formulation:	Reduced	Full	Reduced	
Crack Angle:	30 deg	30 deg	30 deg	
Beta				
Mode I	0.975	0.948	0.927	0.943
Mode II	0.343	0.445	0.347	0.421

Figure A9– Influence of Initial Crack Orientation on Strain Energy Release Rate for Two Cracks Emanating from a Hole in a Finite Plate under Uniform Uniaxial Far-Field Pressure Loading (Normal Mesh Refinement)

5) Summary of Key Observations

- Full-integrated (CPE4) elements in structured meshes match published benchmark and values obtained from traditional focused-mesh stationary cracks for a given crack shape, geometry and loading up to a/b=0.7. A deviation occurs when there is a crack tip propagates to the element "top edge" boundary at approximately a/b=0.7.
- Reduced integration (CPE4R) elements in structured meshes underpredict the strain energy release rate and, subsequently, crack growth rates by approximately 10%.
- All unstructured meshes underpredict crack growth rates compared to structured meshes and analytical results.
- The influence of the in-plane enrichment region height on the calculated crack growth was insignificant down to and including the height set to 10% of the in-plane structural length.
- Mixed mode stationary XFEM cracks compare well with SIF values for structured and unstructured meshes. Upon growth, the cracks always adopt a direction approximately normal to loading direction propagating under mode I. The same observations regarding element formulation and mesh type apply to these initial mixed mode flaws.

APPENDIX B – XFEM FATIGUE MODEL: SURFACE FLAW IN FLAT PLATE

Description:

The Flat Plate geometry is a simple surrogate for a surface flaw in a pipe albeit with infinite radius.

The geometry chosen is aligned with the Raju-Newman SIF solution [16] where the finite dimension plate (2w=20-mm x t=10-mm x h=40-mm) has a 3:1 semi-elliptical flaw with an initial flaw depth of 2-mm. The structured mesh in the enriched region has a mesh seed size of 0.125 mm which was the same 'normal' mesh size used in the hole in plate geometry. For loading, a uniform far-field membrane stress of 100 MPa was used (no bending) and is assumed to cycle to zero for a complete fatigue cycle. Following Appendix A, the same SAE 1020 fatigue properties are used for this N-mm unit system model.

TABLE 9A.1 Taken from Anderson [13]

Stress Intensity Solution for a Semi-Elliptical Surface Flaw in a Flat Plate for $a \le c$

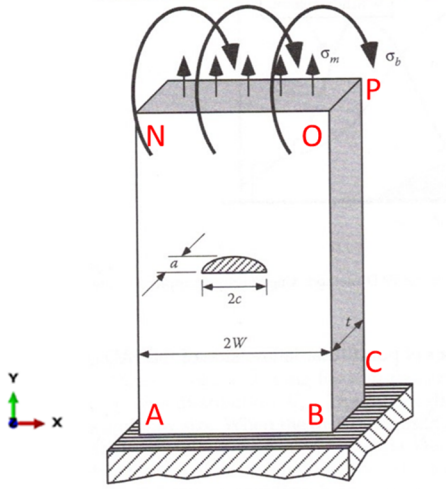

$$K_I = (\sigma_m + H\sigma_b)\sqrt{\frac{\pi a}{Q}}F\left(\frac{a}{t},\frac{a}{c},\frac{c}{W},\phi\right)$$

where

$$Q = 1 + 1.464\left(\frac{a}{c}\right)^{1.65}$$

$$F = \left[M_1 + M_2\left(\frac{a}{t}\right)^2 + M_3\left(\frac{a}{t}\right)^4\right] f_\phi f_w g$$

$$M_1 = 1.13 - 0.09\left(\frac{a}{c}\right)$$

$$M_2 = -0.54 + \frac{0.89}{0.2 + (a/c)}$$

$$M_3 = 0.5 - \frac{1.0}{0.65 + \left(\frac{a}{c}\right)} + 14\left(1.0 - \frac{a}{c}\right)^{24}$$

$$f_\phi = \left[\left(\frac{a}{c}\right)^2 \cos^2\phi + \sin^2\phi\right]^{1/4}$$

$$f_w = \left[\sec\left(\frac{\pi c}{2W}\sqrt{\frac{a}{t}}\right)\right]^{1/2}$$

$$g = 1 + \left[0.1 + 0.35\left(\frac{a}{t}\right)^2\right](1 - \sin\phi)^2$$

$$H = H_1 + (H_2 - H_1)(\sin\phi)^p$$

$$p = 0.2 + \frac{a}{c} + 0.6\left(\frac{a}{t}\right)$$

$$H_1 = 1 - 0.34\frac{a}{t} - 0.11\frac{a}{c}\left(\frac{a}{t}\right)$$

$$H_2 = 1 + G_1\left(\frac{a}{t}\right) + G_2\left(\frac{a}{t}\right)^2$$

$$G_1 = -1.22 - 0.12\left(\frac{a}{c}\right)$$

$$G_2 = 0.55 - 1.05\left(\frac{a}{c}\right)^{0.75} + 0.47\left(\frac{a}{c}\right)^{1.5}$$

σ_m—Membrane (tensile) stress

σ_b—Bending stress

$$\sigma_b = \frac{Mt}{2I}$$

where

$$I = \frac{Wt^3}{6}$$

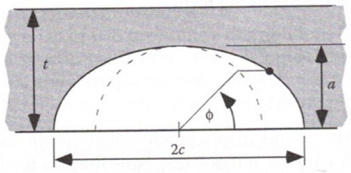

Source: Adapted from Newman, J.C. and Raju, I.S., Stress-intensity factor equations for cracks in three-dimensional finite bodies subjected to tension and bending loads. NASA Technical Memorandum 85793, NASA Langley Research Center, Hampton, VA, April 1984.

2w = 20-mm

t = 10-mm

h = 40-mm

a_i = 2-mm (initial crack depth)

$2c_i$ = 6-mm (initial crack length)

Units: N-mm-sec-MPa

FEA software: Abaqus 2020 (Build ID: 2019_09_13-12.49.31 163176)

Boundary Conditions: Plane A-B-C: $u_x = u_y = u_z = ur_x = ur_y = ur_z = 0$ (fully fixed)

Loading: Cyclic pressure (tensile) loading from 0.0 MPa to 100.0 MPa along Plane N-O-P in each cycle

Material: Cold-rolled SAE 1020 steel.

Linear Elastic Material Properties were used with:
Young's Modulus = 2.07E5 MPa
Poisson's Ratio = 0.3

Following Appendix A, the fatigue relation is:

$$\frac{da}{dN} = 1.2947 \cdot 10^{-4}\, \Delta G^{1.05}$$

with $\frac{da}{dN}$ in mm/cycle and ΔG in N/mm units.

Analysis Steps:

Analysis is completed in two analysis steps:

1) *STATIC preload the structure to maximum value.

2) *FATIGUE, TYPE=SIMPLIFIED

Elements: 3D 8-node continuum elements with full- (C3D8) and reduced integration (C3D8R) were used.

Meshes: Two mesh types (structured and unstructured) with two mesh densities (0.125-mm and 0.250-mm) near the discontinuity.

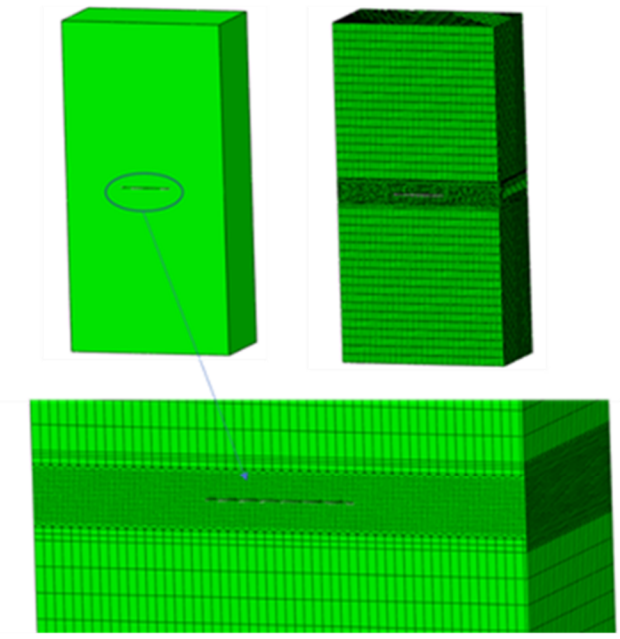

102 – Structured Mesh

101 – Structured Mesh in Enriched Region

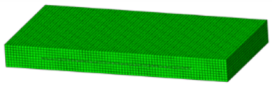

104 – In-Plane Unstructured Mesh in Enriched Region

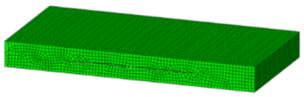

105 – Out-of-Plane Unstructured Mesh in Enriched Region

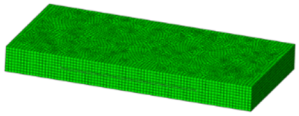

Flat Plate		Mesh Refinement	Element Formulation	Mesh Type	Crack Growth Position	Crack Growth ANGLEMAX	Fatigue Tolerance	Controls Disp Correction	Abaqus Input File Name
Baseline		Normal	Reduced	Structured	Default	85	0.1	0.01	FlatPlate_101
Mesh Refinement									
Normal (40-elements)		N	R	S	Default	85	0.1	0.01	FlatPlate_101
Fine (80-elements)		Fine	R	S	Default	85	0.1	0.01	FlatPlate_102
Element Formulation									
Reduced-Integration		N	R	S	Default	85	0.1	0.01	FlatPlate_101
Full-Integration		N	Full	S	Default	85	0.1	0.01	FlatPlate_103
Mesh Type									
Structured		N	R	S	Default	85	0.1	0.01	FlatPlate_101
Unstructured: In Plane		N	R	UnS_InPlane	Default	85	0.1	0.01	FlatPlate_104
Unstructured: Out-of-Plane		N	R	UnS_OutPlane	Default	85	0.1	0.01	FlatPlate_105
Crack Growth Controls									
*FRACTURE CRITERION, POSITION=									
Default		N	R	S	Default	85	0.1	0.01	FlatPlate_101
Nonlocal		N	R	S	Nonlocal	85	0.1	0.01	FlatPlate_106
*FRACTURE CRITERION, POSITION=NONLOCAL, ANGLEMAX=									
85 (default)		N	R	S	Nonlocal	85	0.1	0.01	FlatPlate_106
45		N	R	S	Nonlocal	45	0.1	0.01	FlatPlate_107
*FATIGUE tolerance									
0.1 (Default)		N	R	S	Default	85	0.1	0.01	FlatPlate_101
0.175		N	R	S	Default	85	0.175	0.01	FlatPlate_108
0.25		N	R	S	Default	85	0.25	0.01	FlatPlate_109
0.01		N	R	S	Default	85	0.01	0.01	FlatPlate_111
General Solution Controls									
*Controls displacement correction									
0.01 (Default)		N	R	S	Default	85	0.1	0.01	FlatPlate_101
1		N	R	S	Default	85	0.1	1	FlatPlate_110
Initial Flaw Size									
ai/t	ai/ci								
0.2	0.67	N	R	S	Default	85	0.1	0.01	FlatPlate_101
0.2	0.67	N	R	S	Default	85	0.01	0.01	FlatPlate_111
0.1	0.67	N	R	S	Default	85	0.1	0.01	FlatPlate_113
0.1	0.67	N	R	S	Default	85	0.01	0.01	FlatPlate_115
0.05	0.67	N	R	S	Default	85	0.1	0.01	FlatPlate_112
0.05	0.67	N	R	S	Default	85	0.01	0.01	FlatPlate_114

Parameters Studied:

As tabulated below, fifteen (15) independent analyses were used to evaluate mesh refinement, mesh type, element formulation, crack growth controls and general solution controls.

Results:

1) Comparison of Crack Driving Force between Full- and Reduced Integration XFEM runs with Analytical Solution

Table B1 compares the analytical solution for the stress intensity factor with results from the full- and reduced integration baseline models with normal, structured mesh for different initial flaw sizes. In order to compare, the Abaqus XFEM propagating strain energy release variable, ENTRRXFEM, is converted to the stress intensity factor using the standard plane strain conversion at the deepest and surface locations of the flaw. It should be noted that the analytical solution involved the explicit time integration of the Paris Law using the stress intensity factor provided by Raju-Newman [16]. Using the constants and loadings described earlier in this Appendix, the surface and deepest crack locations were incremented in 1000-cycle increments such that an elliptical shape is maintained.

For this 3D problem, the reduced integration element formulation values were found to match the analytical values within 1% at the deepest point while the full integration values differed by ~7.8%. These values are consistent with findings of the PWSCC CT model (Appendix D). For the surface location, more variation is seen and expected (~7.8%) for the reduced integration case compared to the analytical solution as even with focused-mesh contour integral evaluations near surface calculations see higher variations.

Table B1 – Comparison of the XFEM Calculated Stress Intensity Factor Compared to the Analytical Newman [16] Solution for the Initial 2-mm Deep x 3-mm Long Semi-Elliptical Surface Flaw in a Flat Plate Subjected to Uniform Membrane Loading

Analysis	ai / t (a/c = 0.667)	SIF (MPa*mm^.5) Crack Location Deepest a	Surface c
FlatPlate_101	0.2	210.9	204.5
Analytical [16]		208.7	189.8
FlatPlate_113	0.1	149.8	143.7
Analytical [16]		144.2	129.9
FlatPlate_112	0.05	112.2	103.1
Analytical [16]		101.5	91.2

2) Influence of Element Formulation on Crack Growth Rate and Shape

While the strain energy release rates were essentially matching between the reduced integration structured mesh XFEM models and the analytical solution [16], the predicted crack lengths as a function of exposure time were found to conservatively differ as the crack extension progressed as shown in Figure B1. Crack shapes were found to be similar at the 50000-cycle mark (see Figure B2).

As will be discussed detail in 6), the damage extrapolation parameter, ΔD_{Ntol}, at the default value of 0.1 ensures a conservative crack growth rate. A tighter value of 0.01 will be shown to better match the crack depth and length analytical solutions for the reduced integration, normal structured mesh model.

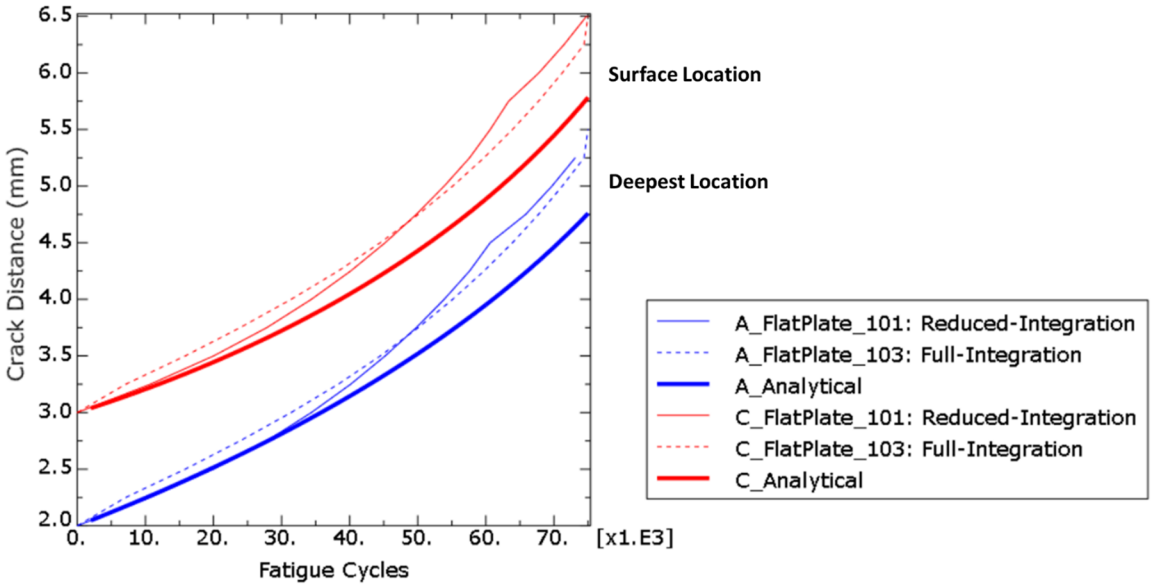

Figure B1– Influence of Element Formulation on Crack Growth Rate for Semi-Elliptical Surface Flaw in a Finite Width Flat Plate under Uniform Uniaxial Far-Field Pressure Loading (Normal Mesh Refinement)

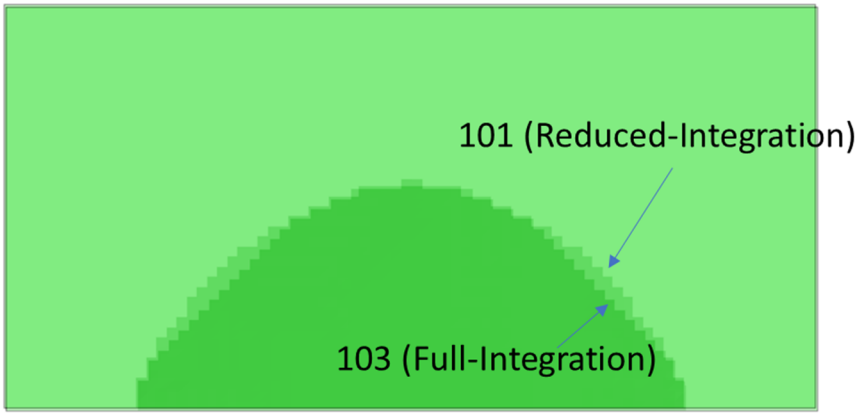

Figure B2– Influence of Element Formulation on Crack Shape at 50000 cycles for Semi-Elliptical Surface Flaw in a Finite Width Flat Plate under Uniform Uniaxial Far-Field Pressure Loading (Normal Mesh Refinement)

3) Influence of Mesh Refinement on Crack Growth Rate and Shape

Increased mesh refinement (80 elements versus 40-elements for the in-plane structural length) for a structured mesh shows a clear trend toward the analytical solution. This increase in accuracy is offset by an increase in computational time. 39 solver iterations in 906 seconds for FlatPlate_101 and 191 solver iterations in 24045 seconds for FlatPlate_102 were required for the runs on a six-core Intel i7-8750H cpu at 2.2 GHz. In fairness, the FlatPlate_102 computational requirements could be drastically reduced via the use of a *TIE between a refined enriched region and coarse standard element mesh. Still, the more refined mesh would have higher computational requirements.

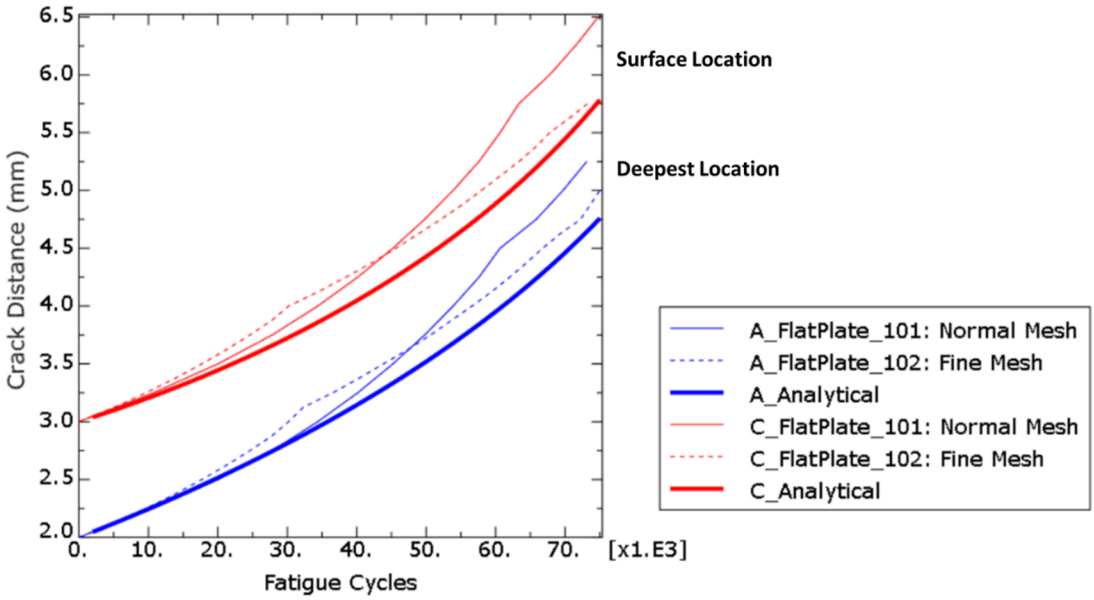

Figure B3– Influence of Mesh Refinement on Crack Growth Rate for Semi-Elliptical Surface Flaw in a Finite Width Flat Plate under Uniform Uniaxial Far-Field Pressure Loading (Reduced Integration)

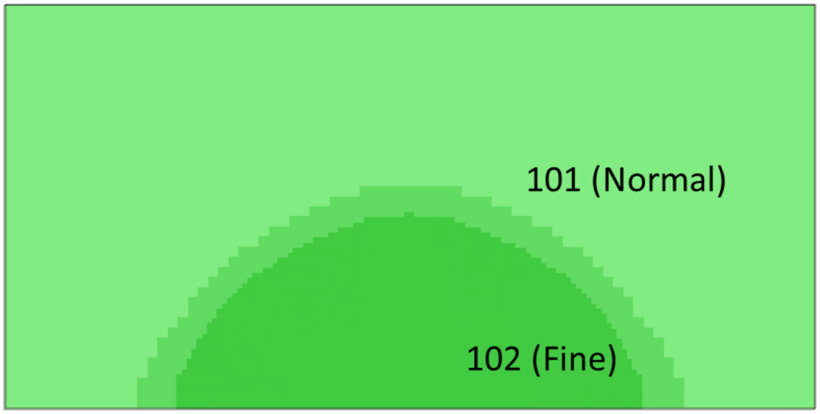

Figure B4 – Influence of Mesh Refinement on Crack Shape at 50000 cycles for Semi-Elliptical Surface Flaw in a Finite Width Flat Plate under Uniform Uniaxial Far-Field Pressure Loading (Reduced Integration)

4) Influence of Mesh Type on Crack Growth Rates and Shape

The crack growth rate (Figure B5) and crack shape (Figure B6) were run for structured, in-plane unstructured and out-of-plane unstructured meshes using a common mesh seed of 0.25mm. Overall, the unstructured mesh results were found to be somewhat erratic as higher crack growth rates were observed at lower rates and slower rates as the cracks progressed.

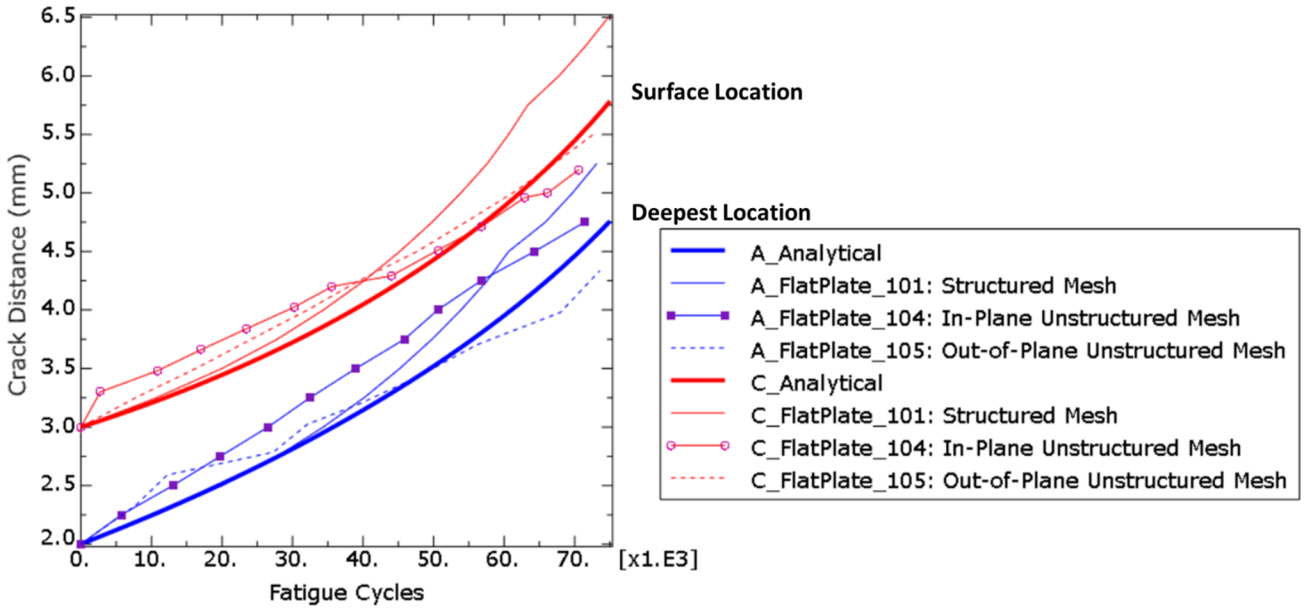

Figure B5– Influence of Mesh Type on Crack Growth Rate for Semi-Elliptical Surface Flaw in a Finite Width Flat Plate under Uniform Uniaxial Far-Field Pressure Loading (Reduced Integration)

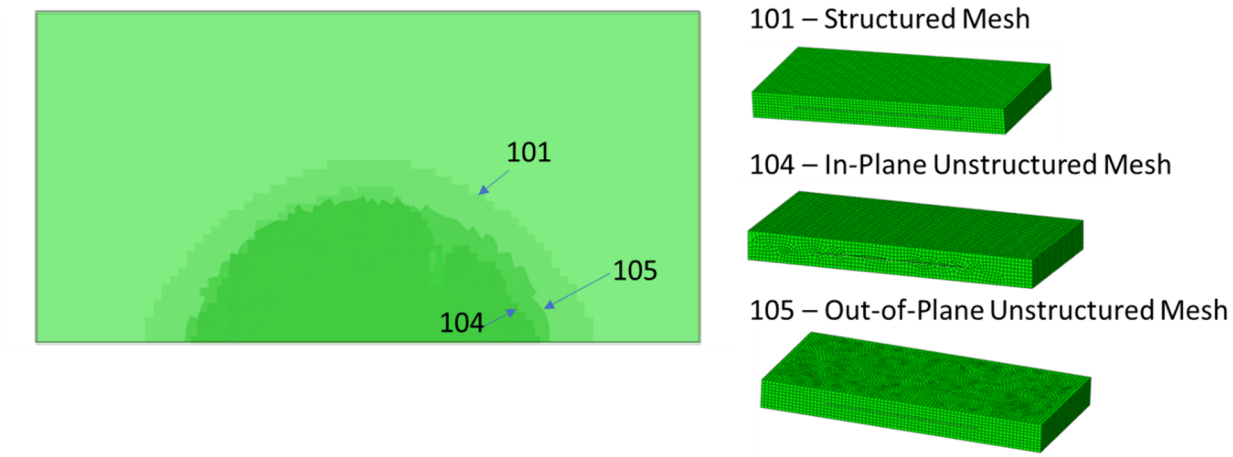

Figure B6 – Influence of Mesh Type on Crack Shape at 50000 cycles for Semi-Elliptical Surface Flaw in a Finite Width Flat Plate under Uniform Uniaxial Far-Field Pressure Loading (Reduced Integration)

5) Influence of *FRACTURE CRITERION parameters on Crack Growth Rate

To provide some improvement in regards to a smooth crack front during curvilinear crack growth, the nonlocal approach (*FRACTURE CRITERIA,POSITION=NONLOCAL,ANGLEMAX=) can be specified where the nonlocal stress/strain fields ahead of the crack tip over a region is intended to improve the computed crack propagation direction. Seen in Figure B7, for this planar deformation problem, no appreciable difference is noted in the crack growth shape or crack growth rate.

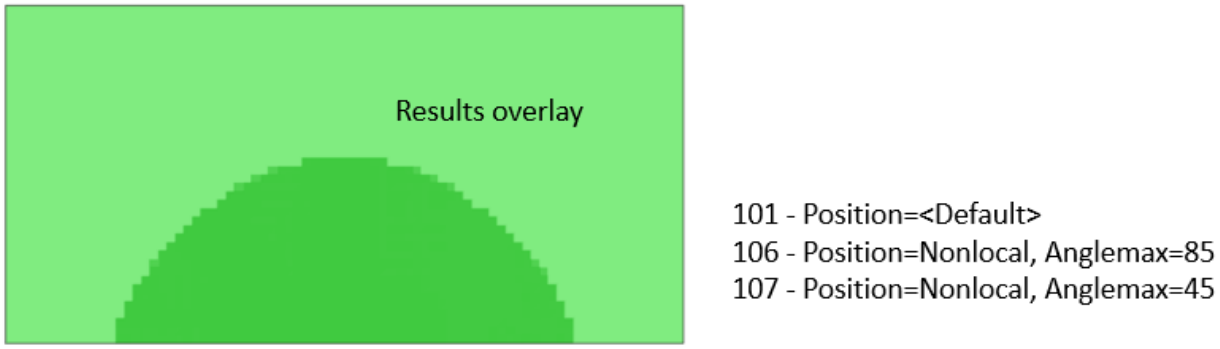

Figure B7 – Influence of Crack Growth POSITION Parameter on Crack Shape at 50000 cycles for Semi-Elliptical Surface Flaw in a Finite Width Flat Plate under Uniform Uniaxial Far-Field Pressure Loading (Reduced Integration)

6) Influence of Crack Growth Controls on Solution Accuracy and Computational Resources

While the strain energy release rates were essentially matching between the baseline reduced integration model (FlatPlate_101) and the analytical solution, the predicted crack lengths as a function of exposure time were found to differ significantly as shown in Figure D3.

While this capability precisely accounts for the number of cycles needed to cause fatigue crack growth over that length, it may be computationally intensive. To accelerate the subcritical crack growth analysis and to provide a smooth solution for the crack front, you can specify a nonzero tolerance, ΔD_{Ntol}, for the least number of cycles to fracture an enriched element.

As was explained in Section 2.2.3, the near-tip asymptotic singularity is not considered in the Abaqus XFEM implementation, and only the displacement jump across a failed element is considered. so Therefore, the crack has to propagate across an entire element at a time to avoid the need to model the stress singularity. So, some accommodation must be made as to what to do with the elements next to the element that has reached the subcritical crack growth extension criterion. To accelerate the subcritical crack growth analysis and to provide a smooth solution for the crack front, Abaqus uses a default tolerance, ΔD_{Ntol}, of 0.1.

In Figures B8 and B9, the ΔD_{Ntol} to 0.175. the FlatPlate_108 model is seen to provide a conservative estimate compared to the analytical crack growth curve. However, as the crack propagates, the crack shape is seen to change from the semi-elliptical shape crack front to a more non-intuitive triangular shape.

In Figure B10, the ΔD_{Ntol} is tightened to 0.01. The FlatPlate_111 model results initially follow the analytical crack growth curve very closely. However, as the analysis continues the model begins to deviate from the analytical solution resulting in non-conservative crack growth. It was hoped that the curve would follow the analytical solution more closely, and as a result of this trend toward non-conservative behavior it still recommended that the default ΔD_{Ntol} of 0.1 be utilized in general modeling conditions to achieve a bounding conservative solution.

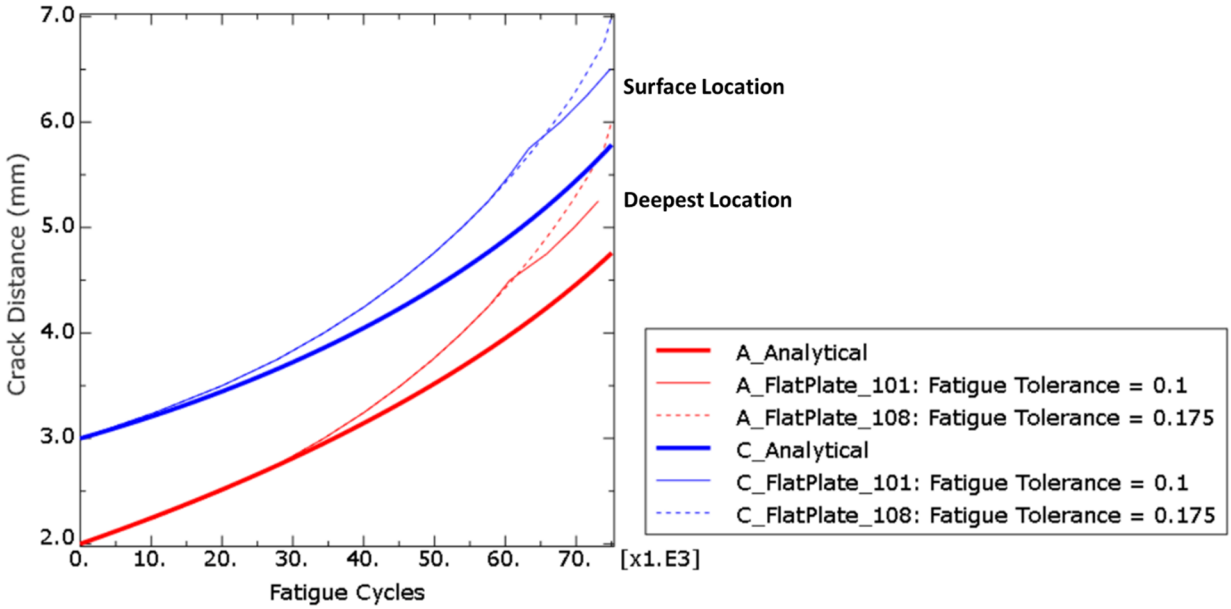

Figure B8 – Influence of "Loose" Crack Growth Damage Extrapolation Tolerance Parameter on Crack Growth Rate for Semi-Elliptical Surface Flaw in a Finite Width Flat Plate under Uniform Uniaxial Far-Field Pressure Loading (Reduced Integration)

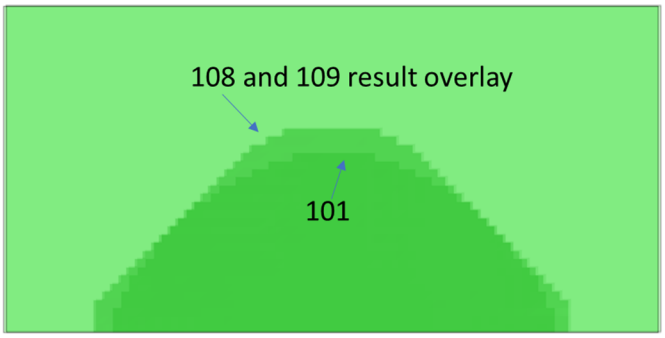

*FATIGUE 2nd line, 5th entry
101 – 0.1
108 – 0.175
109 – 0.25

Figure B9 – Influence of "Loose" Crack Growth Damage Extrapolation Tolerance Parameter on Crack Shape at 50000 cycles for Semi-Elliptical Surface Flaw in a Finite Width Flat Plate under Uniform Uniaxial Far-Field Pressure Loading (Reduced Integration)

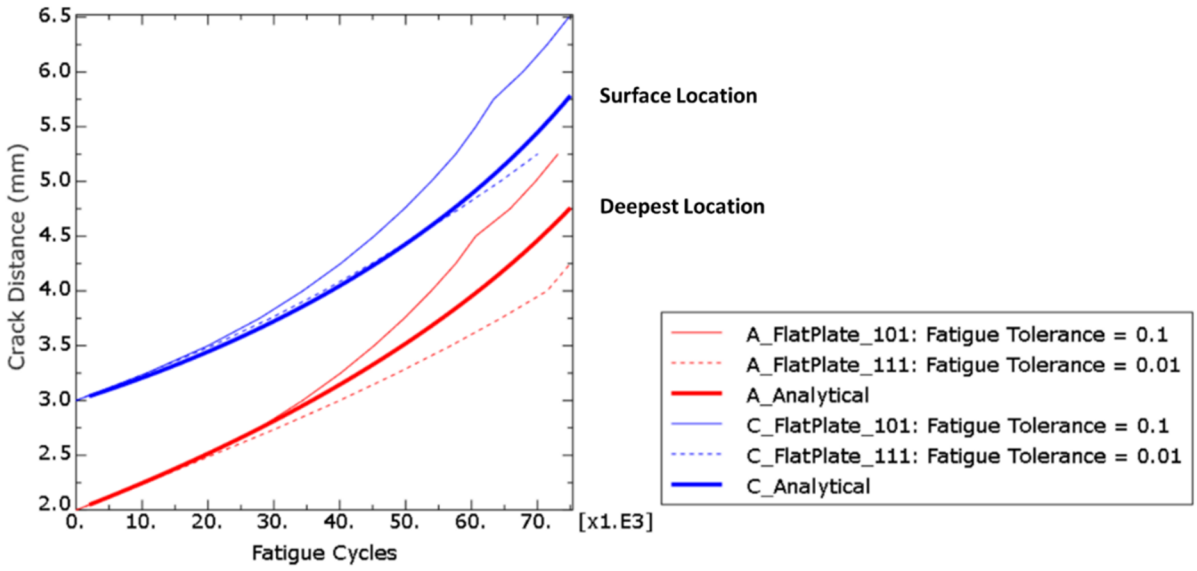

Figure B10 – Influence of "Tight" Crack Growth Damage Extrapolation Tolerance Parameter on Crack Growth Rate for Semi-Elliptical Surface Flaw in a Finite Width Flat Plate under Uniform Uniaxial Far-Field Pressure Loading (Reduced Integration)

Table B1 – Computational Resources for the PWSCC CT Model for Different Subcritical Damage Extrapolation Tolerance (ΔD_{Ntol}), Parameters

	FlatPlate		
Analysis Run:	101	111	108
ΔD_{Ntol}:	0.1	0.01	0.175
Computer Wallclock Time* (min)	15.1	97.8	13.9
Increments	39	259	35
Iterations	39	259	35

* All computer runs were made on a six-core Intel i7-8750H cpu at 2.2 GHz.

7) General Solution Controls: *CONTROLS

An XFEM crack propagation analysis can sometimes fail to converge, in spite of reasonable damage properties and a suitably refined mesh in the enriched region. For example, as the fracture criterion for subcritical crack growth is achieved, the crack front is released with typically small displacements and displacement corrections.

Figure B11 shows that for this linear elastic problem that loosening the displacement correction factor by an order of magnitude does not affect solution quality.

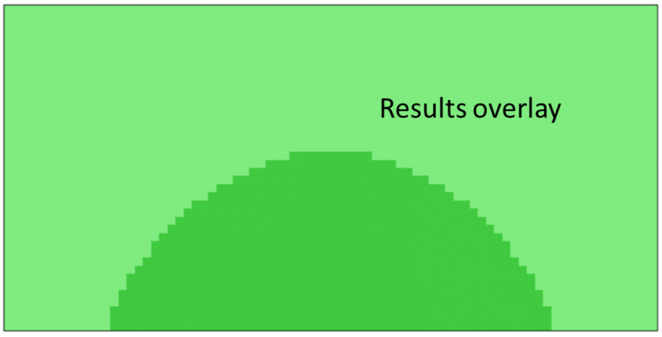

*controls, parameters=field, field=displacement
2nd line, 2nd entry
101 – 0.01
110 – 1.0

Figure B11 – Influence of "Loose" General Solution Displacement Correction Parameter on Crack Shape at 50000 cycles for Semi-Elliptical Surface Flaw in a Finite Width Flat Plate under Uniform Uniaxial Far-Field Pressure Loading (Reduced Integration)

8) Effect of Initial Flaw Size Using Minimum Mesh Size Recommendations

A logical question could be asked whether the minimum mesh refinement recommendations would be satisfactory for smaller initial flaw sizes. To address this concern, a sensitivity study was developed to include a_i/t values of 0.2 (baseline), 0.1, and 0.05 using the minimum mesh refinement (40-elements in structural thickness direction).

Shown below in Figure B12, it is quite obvious that for both the initial a_i/t flaws of 0.1 and 0.05 that the crack shape is rather poorly captured with this level of refinement. However, by the time that the crack reaches an a/t=0.4 that the crack shape is reasonably captured and at the end of the simulation that crack front is captured quite well. This is expected as the crack front is passing through more and more elements.

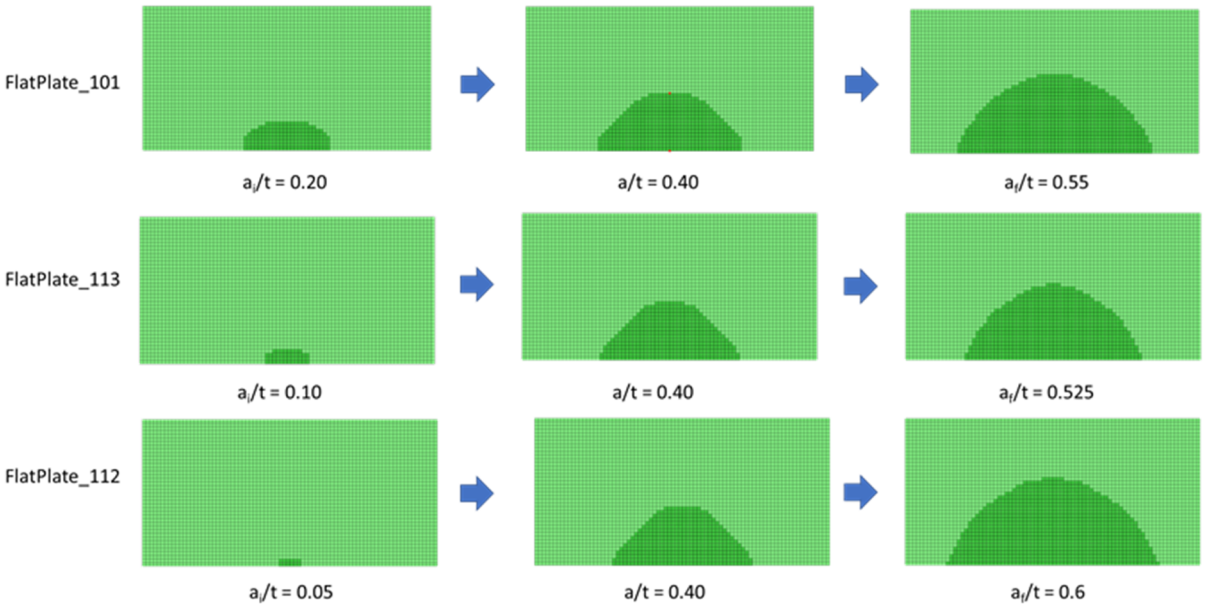

Figure B12 – Effect of Initial Flaw Size using Minimum Mesh Recommendations

Perhaps more importantly, the crack growth rates at the surface and deepest points are conservative compared to the analytical solution using the general mesh size recommendations for smaller initial crack sizes in Figure B13. This is seen below for each of the initial flaws studied. For completeness, when the ΔD_{Ntol} is set down to 0.01, unfortunately, the crack growth rate does not conservatively bound the analytical solution at higher crack depths.

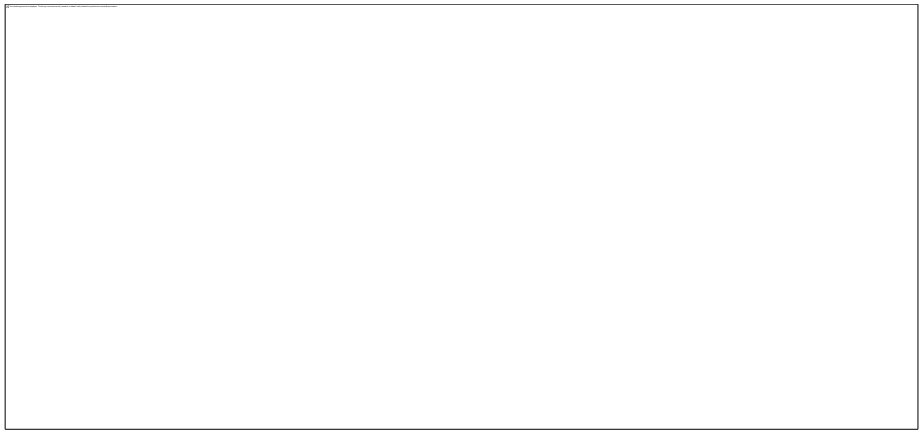

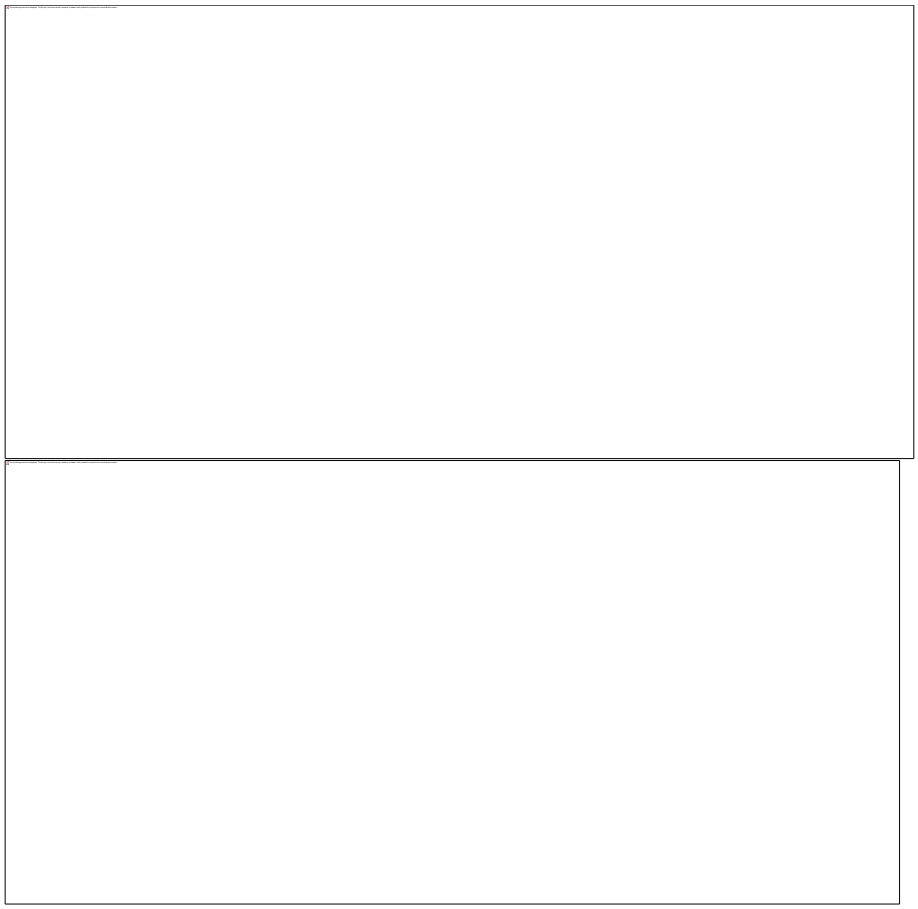

Figure B13 – Small Initial Flaw Size Crack Growth Results compared to Analytical Results using Minimum Recommended Mesh Sizes for Semi-Elliptical Surface Flaw in a Finite Width Flat Plate under Uniform Uniaxial Far-Field Pressure Loading (Reduced Integration)

To reinforce this observation, the plane strain SIF values (converted strain energy release rate ENRRTXFEM output variable) for the initial flaw sizes are shown in Table B2 to be quite good compared to the analytical solution even down to the a/t=0.05 at the deepest point and surface locations. For the a/t=0.05 XFEM mesh specification, stress intensity factor values are ~12% higher than the analytical solution. This is deemed as acceptable and could serve as a bound for other geometries that may be considered.

Table B2 – Stress Intensity Factor Solution for Small Initial Semi-Elliptical Surface Flaw in a Finite Width Flat Plate under Uniform Uniaxial Far-Field Pressure Loading using Minimum Mesh Size Recommendations

Analysis	ai / t (a/c = 0.667)	SIF (MPa*mm^.5) Crack Location	
		Deepest a	Surface c
FlatPlate_101	0.2	210.9	204.5
Analytical [16]		208.7	189.8
FlatPlate_113	0.1	149.8	143.7
Analytical [16]		144.2	129.9
FlatPlate_112	0.05	112.2	103.1
Analytical [16]		101.5	91.2

To summarize, the general minimum mesh refinement is applicable down to practical initial flaw sizes of a_i/t =0.05. Of course, more mesh refinement will lead to more accurate results (see Figure B3) but this will need to be balanced with additional computational cost.

9) Summary of Key Observations
   - For this 3D model, a structured, hexahedral first-order continuum element with a reduced integration formulation was the best match for the analytical crack growth and crack shape results along the curved crack front.
   - In order to better match the analytical results in terms of crack growth rate and crack shape, the damage extrapolation tolerance term, ΔD_{Ntol}, was tightened to 0.01. This does result in ~6x longer run times.
   - For this model, the default ΔD_{Ntol} was not the most accurate but it will always achieve a conservative result at a reasonable computational cost. For this reason, it was chosen to be used as the general recommendation.
   - The general minimum mesh refinement is applicable down to practical initial flaw sizes (a_i/t =0.05). Of course, more mesh refinement will lead to more accurate results but this will need to be balanced with additional computational cost.

APPENDIX C – XFEM FATIGUE MODEL: SINKHOLE GEOMETRY

Description:

Following the work of Miranda [15], this model considers a standard CT specimen that has been modified with an additional hole. The presence of the additional hole perturbs the crack path, resulting in a curvilinear crack growth but still keeps the crack front itself nearly straight. Two geometries were investigated which include (1) “Sink Hole” where the crack propagates into the additional hole and (2) “Miss Hole” where the crack path is modified but does propagate into the additional hole. Both geometries were confirmed by experimentation.

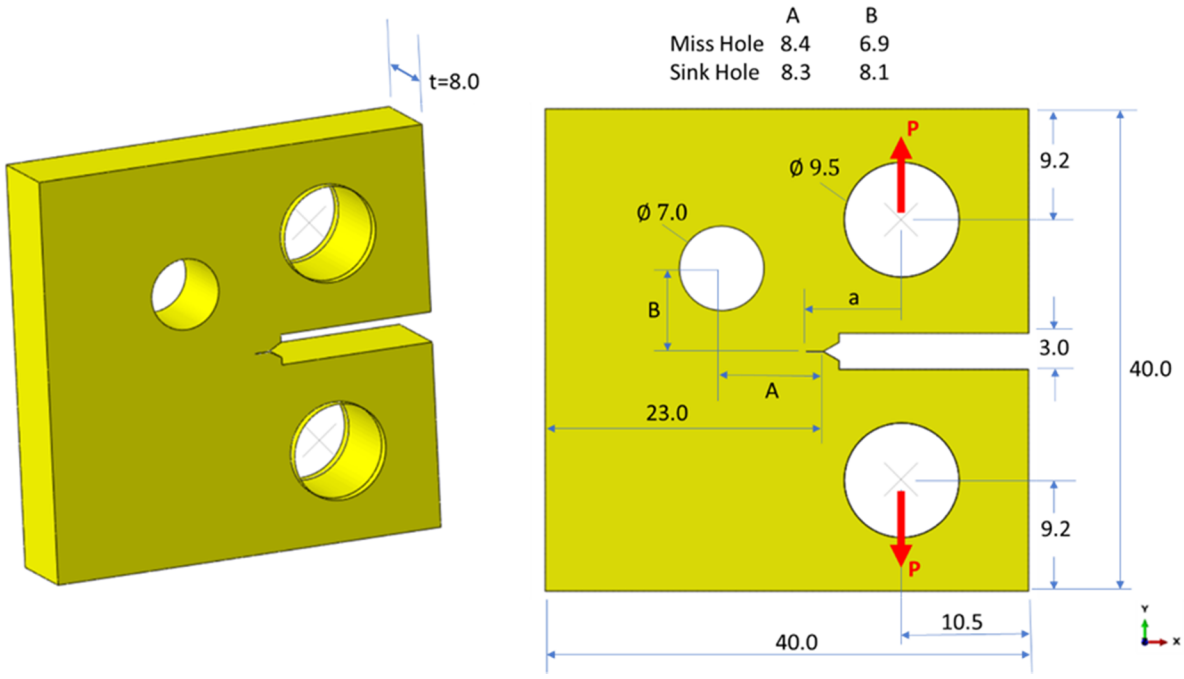

Units: N-mm-sec-MPa

FEA software: Abaqus 2020 (Build ID: 2019_09_13-12.49.31 163176)

Boundary Conditions: Surface-to-Surface Contact Pairs between rigid pins and CT specimen with a coulomb friction coefficient of 0.1.

Top Pin Reference Node: $u_x=u_z=ur_x=ur_y=ur_z=0$ (y-translation free)

Bottom Pin Reference Node: $u_x= u_y=u_z=ur_x=ur_y=ur_z=0$ (fully fixed)

Loading: Top Pin Reference Node: P_y = 2000 N

This was chosen to obtain a $K_{max} \approx 8.0$ MPa to achieve the proper ΔK for the simplified fatigue procedure. It is appreciated that constant loading is applied as opposed to the feedback-control constant K that was used during the testing. As a result, crack growth rates will not be reasonable; however, crack shape prediction will be accurate.

Material: Cold-rolled SAE 1020 steel.

Linear Elastic Material Properties were used with:
Young's Modulus = 2.05E5 MPa
Poisson's Ratio = 0.3

Following Appendix A, the fatigue relation is:

$$\frac{da}{dN} = 1.2947 \cdot 10^{-4}\, \Delta G^{1.05}$$

with $\frac{da}{dN}$ in mm/cycle and ΔG in N/mm units.

Analysis Steps:

Analysis is completed in two analysis steps:

1) *STATIC preload the structure to maximum value.

2) *FATIGUE, TYPE=SIMPLIFIED

Elements: 3D 8-node first-order continuum elements with full- (C3D8) and reduced integration (C3D8R) were used.

Meshes: Two mesh types (structured and unstructured) with three mesh densities (coarse, normal and fine) were used with the "Miss Hole" and "Sink Hole" geometries.

Parameters studied:

As tabulated below, twelve (12) independent analyses were used to evaluate the geometry type, mesh refinement, mesh type, element formulation and crack growth controls.

Sink and Miss Hole Geometries	Geometry	Mesh Refinement	Element Formulation	Mesh Type	Crack Growth Position	Crack Growth ANGLEMAX	Fatigue Tolerance	Controls Disp Correction	Abaqus Input File Name
Baseline	Sink Hole	Normal	Reduced	Structured	Default	-	0.1	0.01	SinkHole_101
Baseline	Miss Hole	N	R	S	Default	-	0.1	0.01	MissHole_101
Mesh Refinement									
Normal (45-elements; 0.6-mm mesh seed)	Sink Hole	N	R	S	Default	-	0.1	0.01	SinkHole_101
Normal (45-elements; 0.6-mm mesh seed)	Miss Hole	N	R	S	Default	-	0.1	0.01	MissHole_101
Coarse (45-elements; 0.6-mm x 1.0-mm Height direction)	Sink Hole	Coarse	R	S	Default	-	0.1	0.01	SinkHole_102
Fine (90-elements; 0.3-mm mesh seed)	Sink Hole	Fine	R	S	Default	-	0.1	0.01	SinkHole_105
Element Formulation									
Full-Integration	Sink Hole	N	Full	S	Default	-	0.1	0.01	SinkHole_103
	Sink Hole	C	F	S	Default	-	0.1	0.01	SinkHole_104
	Sink Hole	Coarse #2							
Reduced-Integration	Sink Hole	N	R	S	Default	-	0.1	0.01	SinkHole_101
Mesh Type									
Structured	Sink Hole	N	R	S	Default	-	0.1	0.01	SinkHole_101
	Miss Hole	N	R	S	Default	-	0.1	0.01	MissHole_101
Unstructured: In Plane	Miss Hole	N	R	UnS (7 in Notch Width)	Default	-	0.1	0.01	MissHole_102
	Miss Hole	N	R	UnS (5 in Notch Width)	Default	-	0.1	0.01	MissHole_105
	Miss Hole	N	R	UnS (11 in Notch Width)	Default	-	0.1	0.01	MissHole_106
Crack Growth Controls									
*FRACTURE CRITERION, POSITION=									
Default	Miss Hole	N	R	UnS	Default	-	0.1	0.01	MissHole_102
Nonlocal	Miss Hole	N	R	UnS	Nonlocal	85	0.1	0.01	MissHole_103
	Sink Hole	N	R	S	Nonlocal	85	0.1	0.01	SinkHole_106
*FRACTURE CRITERION, POSITION=NONLOCAL, ANGLEMAX=									
30	Miss Hole	N	R	UnS	Nonlocal	30	0.1	0.01	MissHole_104

Results:

1) Baseline Recommendations

Figure C1 shows the baseline results achieving the desired crack paths while using a 3D structured, hexahedral first-order continuum element mesh with reduced integration. This is further reinforced when the experimental results are overlaid on respective crack paths as shown on in Figure C2 (Sink Hole) and C3 (Miss Hole). However, as seen in Figure C3, it should be noted that asymmetric deformation is observed on the Miss Hole geometry despite no physical or mesh-dependent mechanism that should have led to this behavior. For this isotropic material, all loading is symmetric while the in-plane mesh is extruded through-the-thickness.

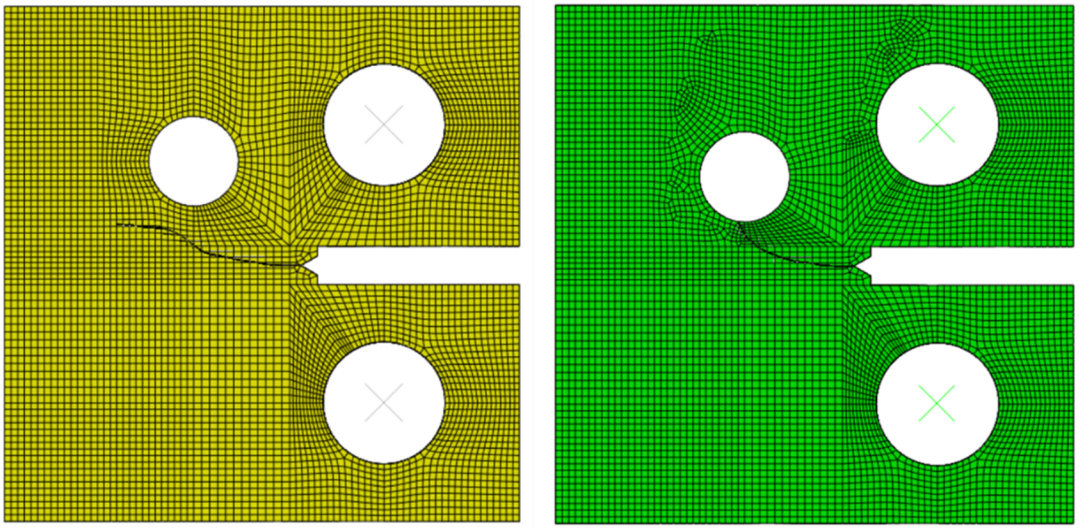

Figure C1 – Final Crack Shape for Baseline Miss Hole and Sink Hole Assessments
(Structured Mesh with 3D Hexahedral Continuum Elements using Reduced Integration)

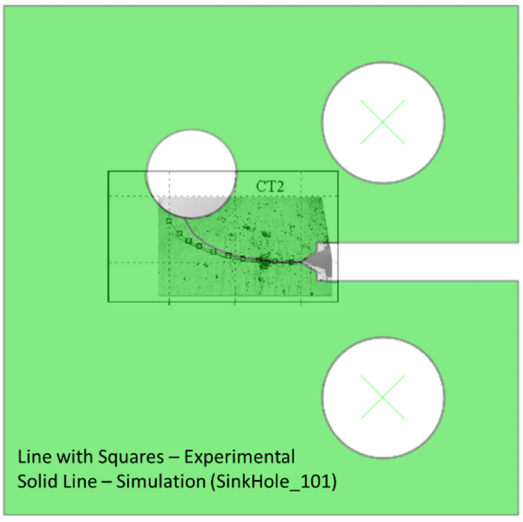

Figure C2 – Final Crack Shape for Baseline Sink Hole XFEM Assessment overlaid on Experimental Crack Growth Path Reported by Miranda [15]

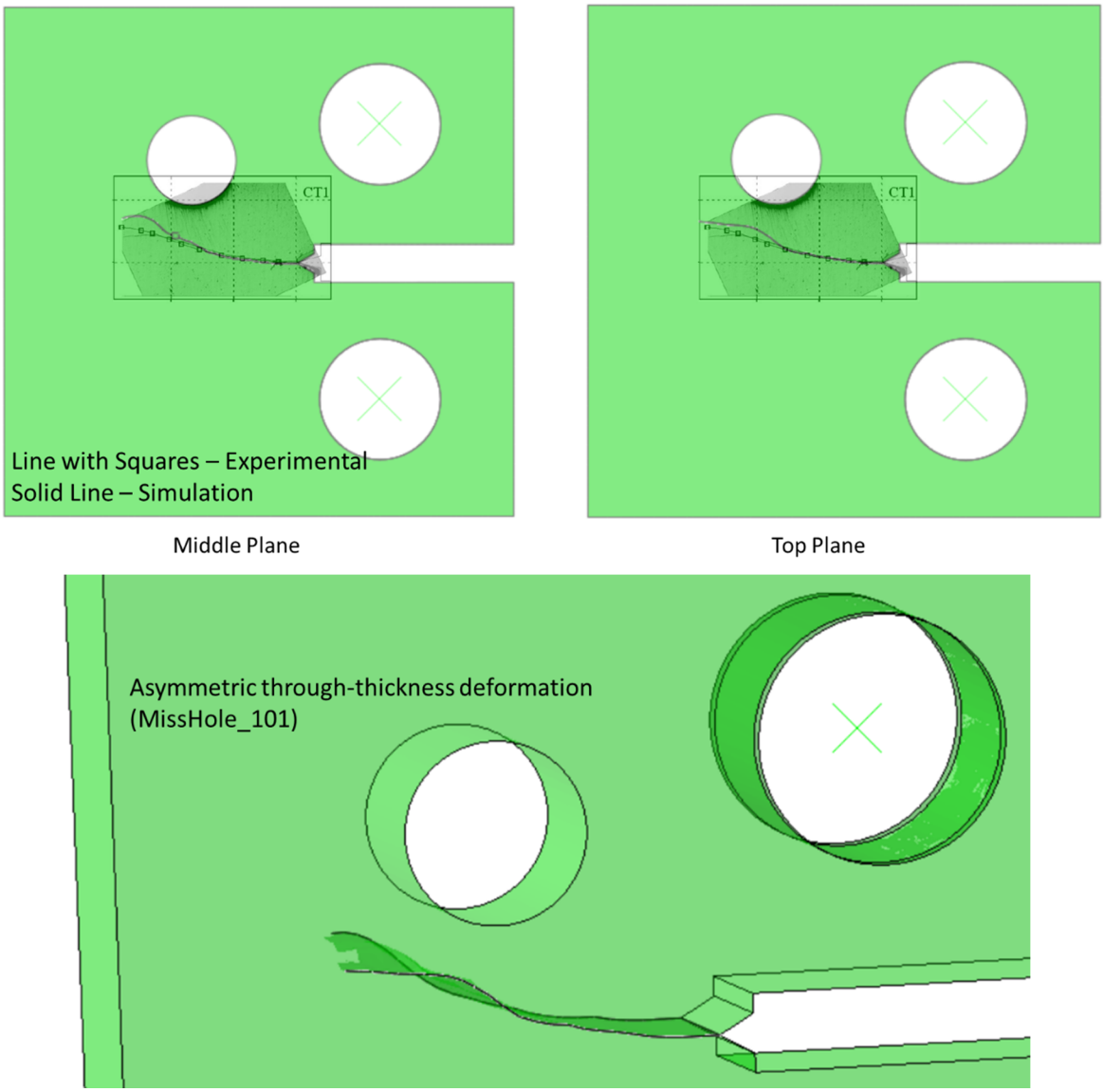

Figure C2 – Final Crack Shape for Baseline Miss Hole XFEM Assessment overlaid on Experimental Crack Growth Path Reported by Miranda [15]

2) Element Formulation: Full Integration Effect on Crack Turning

When full integration elements are used, Figure C3 shows non-physical crack growth.

Essentially, as curvilinear cracks propagate up to an element interface, the crack turns and then extends further along the element boundary that is parallel to the original crack orientation. In this way, the anticipated crack trajectory into the sink hole is not obtained. Various other *FRACTURE CRITERION functionality options were attempted but no fundamental changes in analysis results were seen when full integration elements were used. These findings are consistent with results provided with the hole in plate (Appendix A) XFEM model.

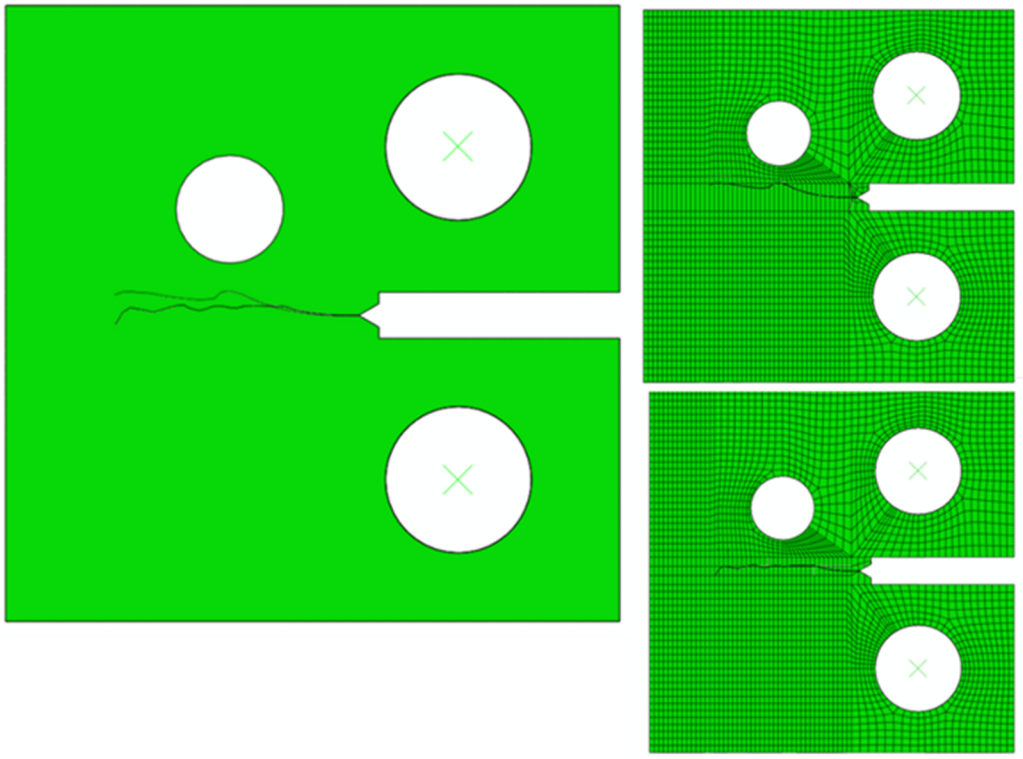

Figure C3 – Influence of Mesh Refinement for Fully-Integrated, Structured "Sink Hole" Meshes (SinkHole_104)

3) Mesh Refinement: Sink Hole (SinkHole_101 vs. SinkHole_102 vs. SinkHole_105)

Using reduced integration elements with a structured mesh as our baseline, a mesh refinement study comparing variations in the vertical mesh while keeping the in-plane mesh density the same (SinkHole_101: 0.6-mm x 0.6-mm mesh seed vs. SinkHole_102: 0.6 x 1.0-mm mesh seed) as well as a more refined model (SinkHole_105: 0.3-mm x 0.3-mm mesh seed) was performed.

Shown in Figure C4, the crack trajectories are similar between the coarse and normal meshes. Figure C5 illustrate the crack length as a number of fatigue cycles. This correlation between the normal and fine meshes indicate the normal mesh (0.6-mm x 0.6-mm mesh; 58 elements in the structural thcikness direction) is sufficient from a mesh refinement perspective.

It should be noted that the crack growth cycles are not comparably to experimental results as the current XFEM run is run under constant load cycles as opposed to the experimental feedback-controlled constant K (driving force) loading. For a precise comparison, a sensor element via Abaqus user subroutines would need to be implemented in the XFEM model.

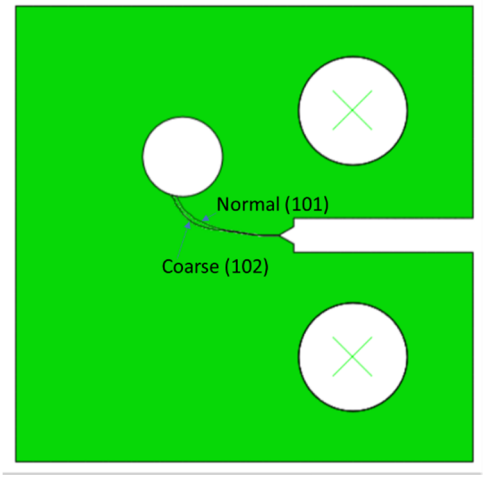

Figure C4 – Influence of Mesh Refinement for Reduced integration, Structured "Sink Hole" Meshes

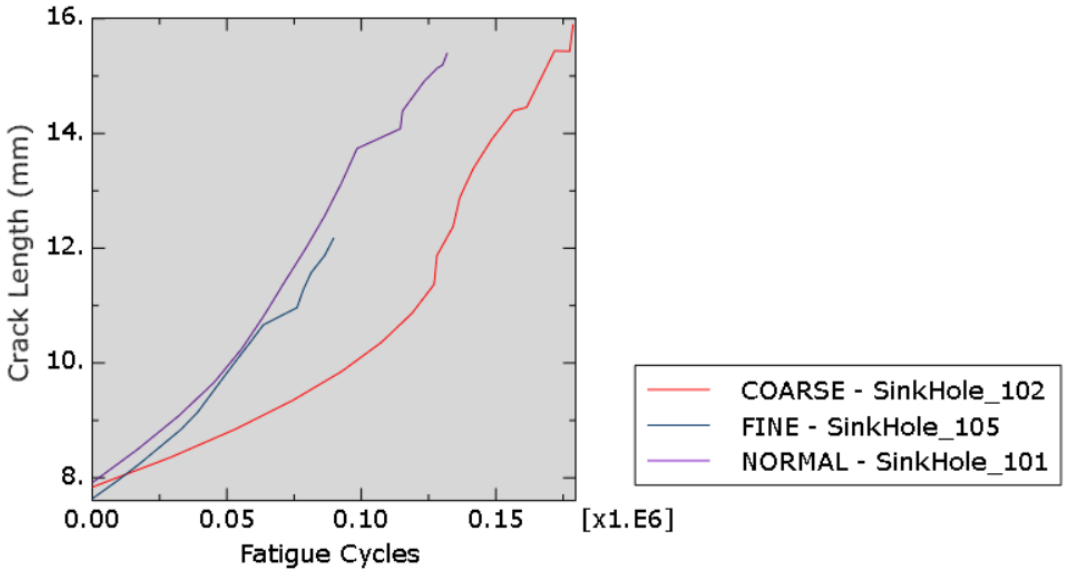

Figure C5 – Influence of Mesh Refinement on Crack Growth Rate for Reduced Integration, Structured "Sink Hole" Meshes

4) Mesh Type: Structured vs Unstructured

Even with reduced integration elements, it is still possible to obtain an incorrect solution when modeling curvilinear crack growth. Figure C6 shows that when crack turning occurs in an unstructured portion of the mesh (MissHole_102) that an incorrect crack trajectory can be seen.

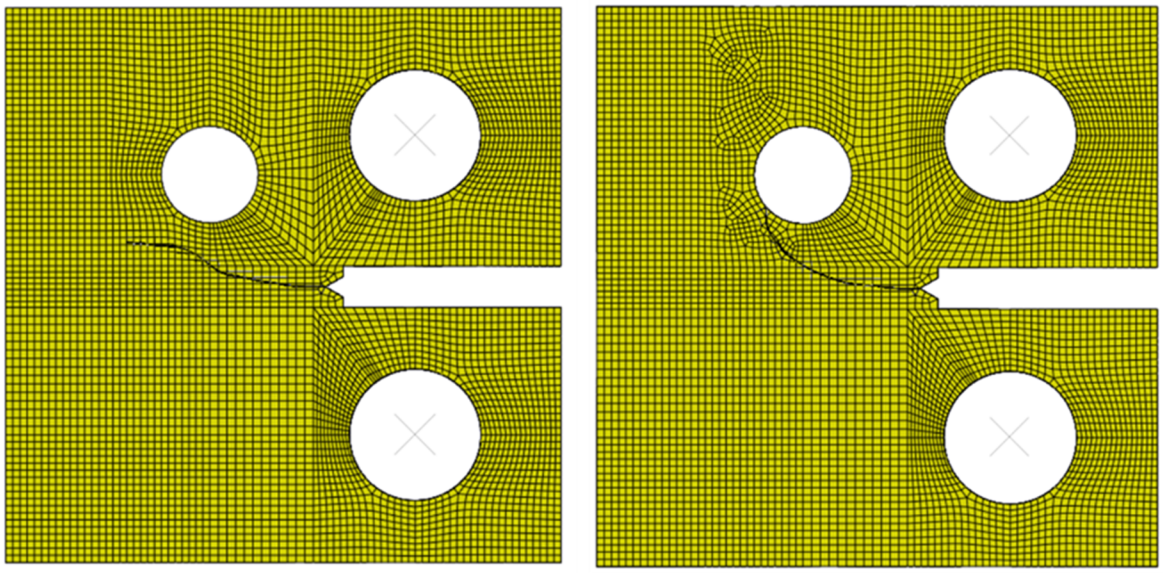

Figure C6 – Influence of Mesh Type on Crack Growth Shape for Reduced integration "Miss Hole" Meshes

5) Fracture Criterion: Default versus POSITION=Nonlocal

in the case of unstructured or relatively coarse meshes, it becomes extremely challenging to maintain a smooth, continuous three-dimensional crack front during curvilinear crack propagation with the current XFEM method. To provide some improvement, the nonlocal approach (*FRACTURE CRITERIA, POSITION=NONLOCAL) can be specified where the nonlocal stress/strain fields ahead of the crack tip over a region is intended to improve the computed crack propagation direction.

Figure C7 shows that an unstructured mesh with the nonlocal approach (MissHole_103) is able to obtain the desired crack trajectory. The sink hole geometry with the nonlocal averaging (SinkHole_106) follows the same trajectory as the default option (SinkHole_101).

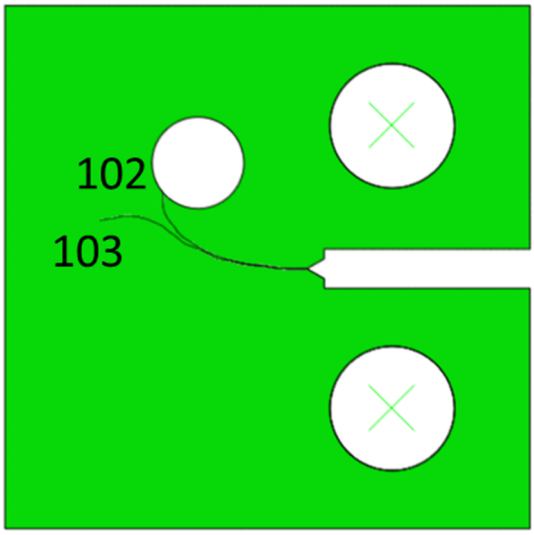

Figure C7 – Influence of Crack Growth POSITION Parameter on Crack Growth Shape for Reduced integration “Miss Hole” Meshes

6) Fracture Criterion: POSITION=Nonlocal, ANGLEMAX=85 versus POSITION=Nonlocal, ANGLEMAX=30

As expected, controlling the maximum crack turn within one element from the default of 85 degrees (MissHole_103) to values as low as 30 degrees were found to cause no appreciable difference in results (MissHole_104).

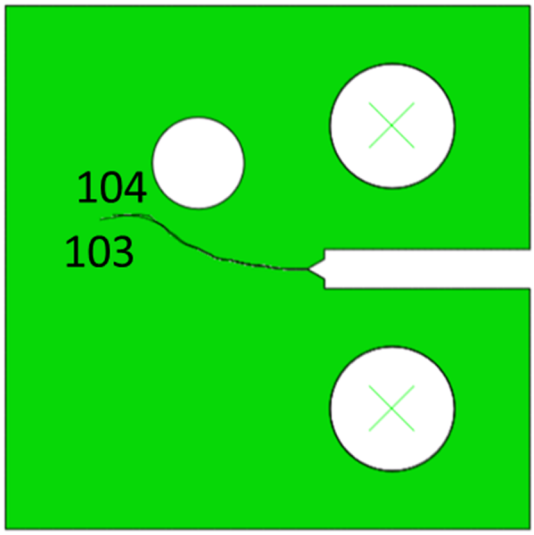

Figure C8 – Influence of Crack Growth POSITION=NONLOCAL,ANGLEMAX= Parameter on Crack Growth Shape for Reduced Integration “Miss Hole” Meshes

Figure C9 provides a summary of the observed behavior for the reduced integration Miss Hole geometry analyses.

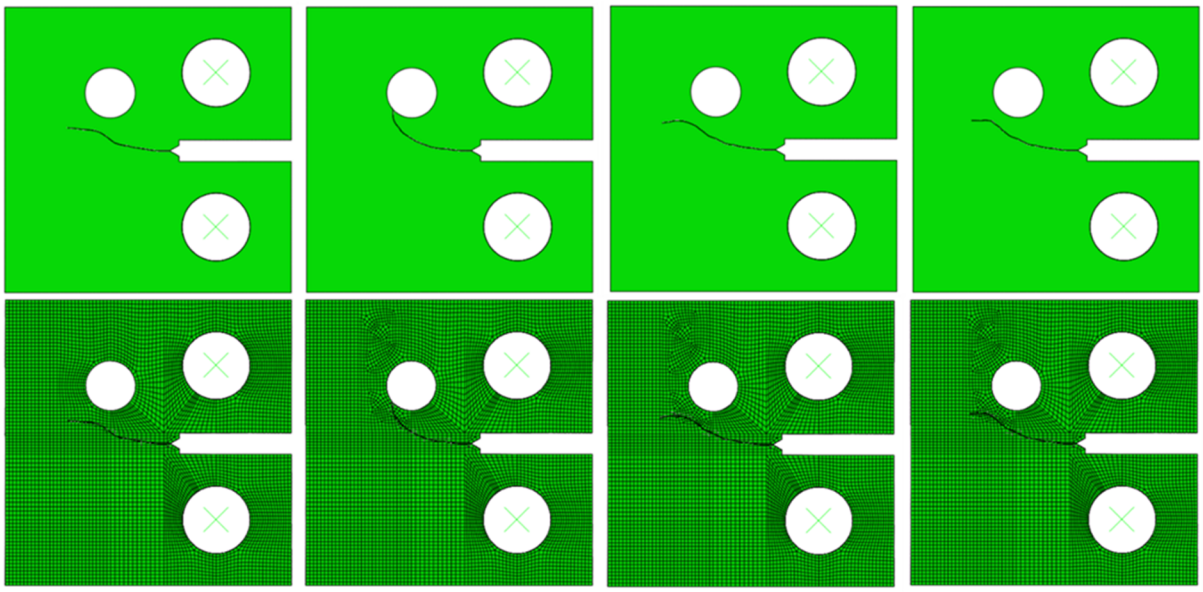

Miss Hole:	101	102	103	104
Mesh:	Structured	Unstructured	Unstructured	Unstructured
El Formulation:	Reduced	Reduced	Reduced	Reduced
*FC POSITION:	Default	Default	Nonlocal	Nonlocal
*FC ANGLEMAX:	-	-	85 degrees	30 degrees

Figure C9 – comparison of mesh type and crack growth parameters on crack growth shape for reduced integration "Miss Hole" Meshes

Seen in Figure C10 for all Miss Hole geometries studied, structured meshes were utilized up to the width of the "Notch Width" which seems to greatly influence the crack turning. As was discussed with the hole in plate model, the crack turning is impeded when the crack is essentially parallel and close to an element edge. This is true for the reduced integration elements even though not as severe as the full integration. Comparing five- (105) vs seven- elements(101 and 102) for the notch width but otherwise using the same mesh seed, a clear deviation is seen as related to this phenomenon.

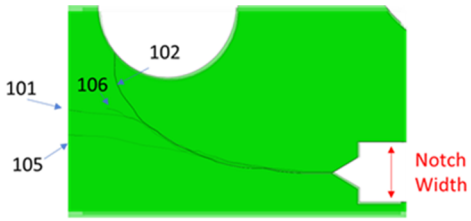

MissHole:	101	102	105	106
Mesh:	Structured	Unstructured	Unstructured	Unstructured
Mesh Seed:	0.6	0.6	0.6	0.3
Notch Width Elements:	7	7	5	11

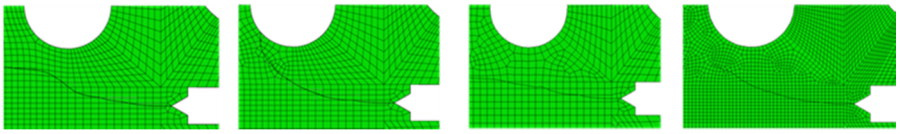

Figure C10 – Comparison of Mesh Type and Crack Growth Parameters on Crack Growth Shape for Notch Width Refinement for "Miss Hole" Meshes

7) Key Observations from this XFEM Model

- When the general modeling recommendations (structured mesh with reduced integration) are followed, the experimentally-validated crack growth trajectories are obtained for both the Sink Hole and Miss Hole geometries.
- Non-physical crack growth is observed with curvilinear crack extension when fully-integrated elements are utilized.
- An incorrect crack trajectory is seen for the Miss Hole geometry when an unstructured mesh is used with reduced integration elements. However, an unstructured reduced integration mesh with the nonlocal approach is able to obtain the desired crack trajectory.
- Crack trajectory was observed to be impeded for both reduced- and full integration element formulations.

APPENDIX D – XFEM PWSCC MODEL: COMPACT TENSION

Description:

As an extension of the quasi-2D PWSCC modeling of a CT specimen performed by Facco [**Error! Reference source not found.**], a full 3D analysis was undertaken to verify the non-uniform SIF solution along the crack front along with the corresponding non-uniform through-the-thickness crack extension as a function of the *FATIGUE damage extrapolation tolerance term.

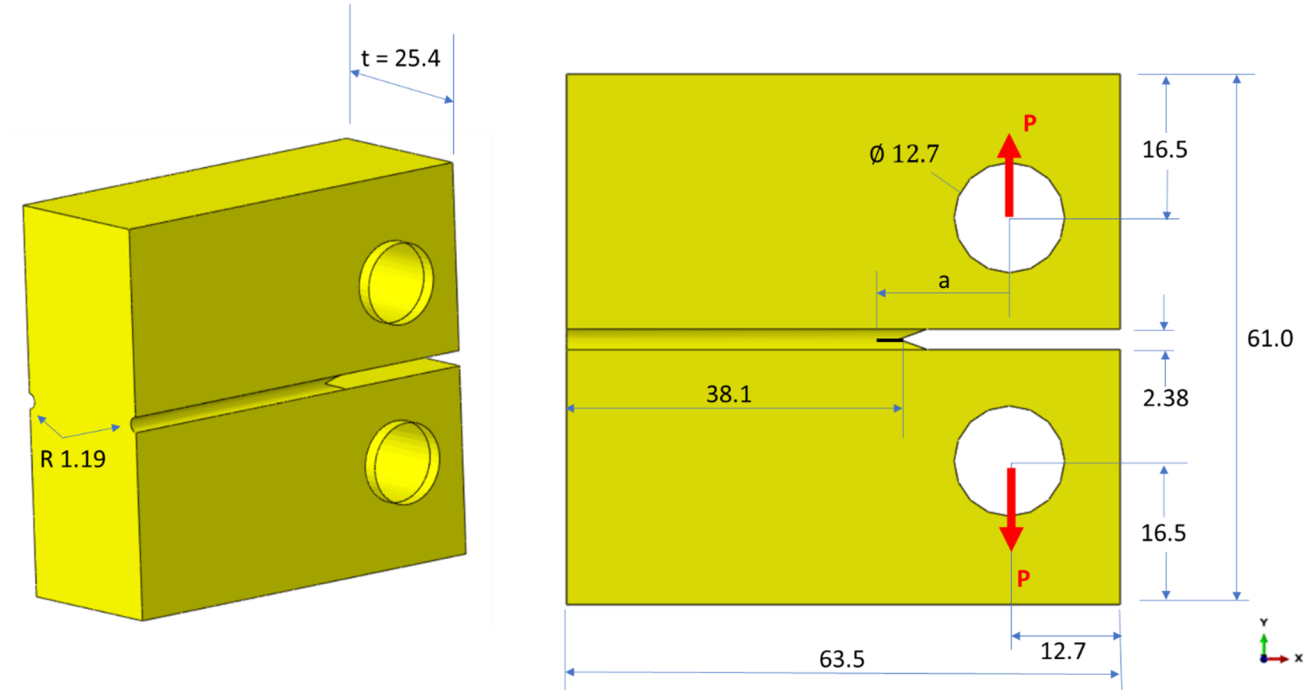

Units: N-mm-sec-MPa

FEA software: Abaqus 2020 (Build ID: 2019_09_13-12.49.31 163176)

Boundary Conditions: Surface-to-Surface Contact Pairs between rigid pins and CT specimens with a coulomb friction coefficient of 0.1.

Top Pin Reference Node: $u_x=u_z=ur_x=ur_y=ur_z=0$ (y-translation free)

Bottom Pin Reference Node: $u_x= u_y=u_z=ur_x=ur_y=ur_z=0$ (fully fixed)a

Loading: Top Pin Reference Node: P_y = 26500 N

This was chosen to obtain a K_i = 33.5 MPa√m which was used in Test Period 4 of the Alloy 182 shielded metal arc weld material in PWR water as outlined in Section 4.1 of Alexandreanu [15]. It is appreciated that constant loading is applied as opposed to the feedback-control constant K that was used during the testing.

Material: Welded (SMA) Alloy 182 in PWR water conditions

Linear Elastic Material Properties were used at 320 C:

Young's Modulus = 2.0E5 MPa

Poisson's Ratio = 0.3

The PWSCC crack growth rate for Alloy 182 based on data reported in Table 4 of Alexandreanu [19]:

$$\frac{da}{dt} = 2.847 \cdot 10^{-13}\, G^{0.8}$$

with $\frac{da}{dt}$ in m/sec and G is in N/m units.

Using the Appendix F Excel tool to convert between unit systems, the following equation was then used for the required strain energy release rate crack growth relation:

$$\frac{da}{dt} = 7.15134 \cdot 10^{-8}\, G^{0.8}$$

with $\frac{da}{dt}$ in mm/sec and G is in N/mm units.

Analysis Steps:

Analysis is completed in two analysis steps:

1) *STATIC preload the structure to maximum value.

2) *FATIGUE, TYPE=SIMPLIFIED

Elements: 3D 8-node continuum elements with full- (C3D8) and reduced integration (C3D8R) were used in different analysis runs.

Mesh: A structured mesh type with nominal mesh density (0.125-mm mesh seed; 60 elements in the in-plane structural depth direction) near the discontinuity.

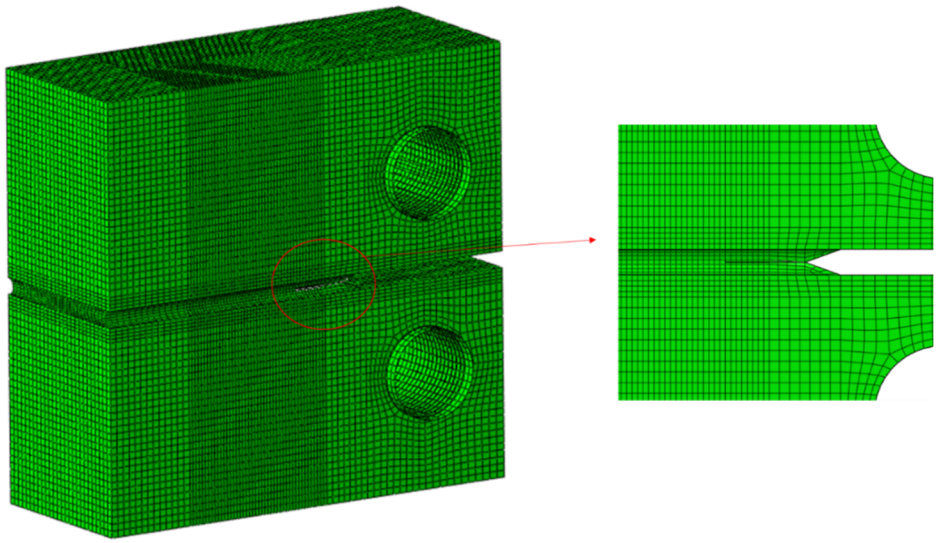

Parameters Studied:

Independent analyses were used to evaluate the element formulation (reduced- and full integration) and crack growth damage extrapolation tolerance controls.

PWSCC CT	Mesh Refinement	Element Formulation	Mesh Type	Crack Growth Position	Crack Growth ANGLEMAX	Fatigue Tolerance	Controls Disp Correction	Abaqus Input File Name
Baseline	Normal (60-elems)	R	Structured	Default	-	0.1	0.01	PWSCC_CT_ 101
Element Formulation								
Reduced-Integration	Normal (60-elems)	R	Structured	Default	-	0.1	0.01	PWSCC_CT_ 101
Full-Integration	Normal (60-elems)	F	Structured	Default	-	0.1	0.01	PWSCC_CT_ 102
Crack Growth Controls								
*FATIGUE tolerance								
0.01 (Tight)	Normal (60-elems)	R	Structured	Default	-	0.01	0.01	PWSCC_CT_ 103

Results:

1) Comparison of Strain Energy Release Rate Between Full- and Reduced Integration XFEM Runs with Analytical Solution [19]

The purpose of this model was to apply the general modeling recommendations that had been based on loading of a standard PWSCC compact tension specimen. To ensure that the proper crack driving force relation was obtained, the analytical stress intensity factor solution for this CT geometry from ASTM E1681 is detailed in Equation 7 of NUREG/CR-6964 [19]:

$$K = \frac{P}{B\sqrt{W}} \cdot \frac{\left(2+\frac{a}{W}\right)}{\left(1-\frac{a}{W}\right)^{\frac{3}{2}}} \left(0.886 + 4.64\left(\frac{a}{W}\right) - 13.32\left(\frac{a}{W}\right)^2 + 14.72\left(\frac{a}{W}\right)^3 - 5.6\left(\frac{a}{W}\right)^4\right)$$

The analytical K was converted to G via the standard plane strain conversion to aid in the comparison with the propagating strain energy rate output variable from Abaqus, ENRRTXFEM. The analytical solution involved the explicit time integration of the Paris Law using this stress intensity factor using the constants and loadings described earlier in this Appendix. The surface and deepest crack locations were incremented in 1E6-second increments such that an elliptical shape was maintained.

Figure D1 shows the through-thickness variation of the strain energy release rate for the full- (PWSCC_CT_102) and reduced integration (PWSCC_CT_101) at the initial crack length (20-mm) as compared to the analytical solution. For this 3D model, there are variations through-the-thickness with the most noticeable effect as the free edges are approached. This should lead to some variation in PWSCC growth rates through-the-thickness. The reduced integration formulation was a better match for the analytical results at the constrained (plane strain) location in the center of the specimen thickness. It was previously observed in the 2D plane strain hole in plate model (Appendix A) that the full integration formulation was the better match. In both models, the two element formulations, which differed by less than 10%, bounded the analytical result.

Figure D2 shows the trends continue for the observed strain energy crack release rate as a function of crack extension at the mid-thickness of the crack front.

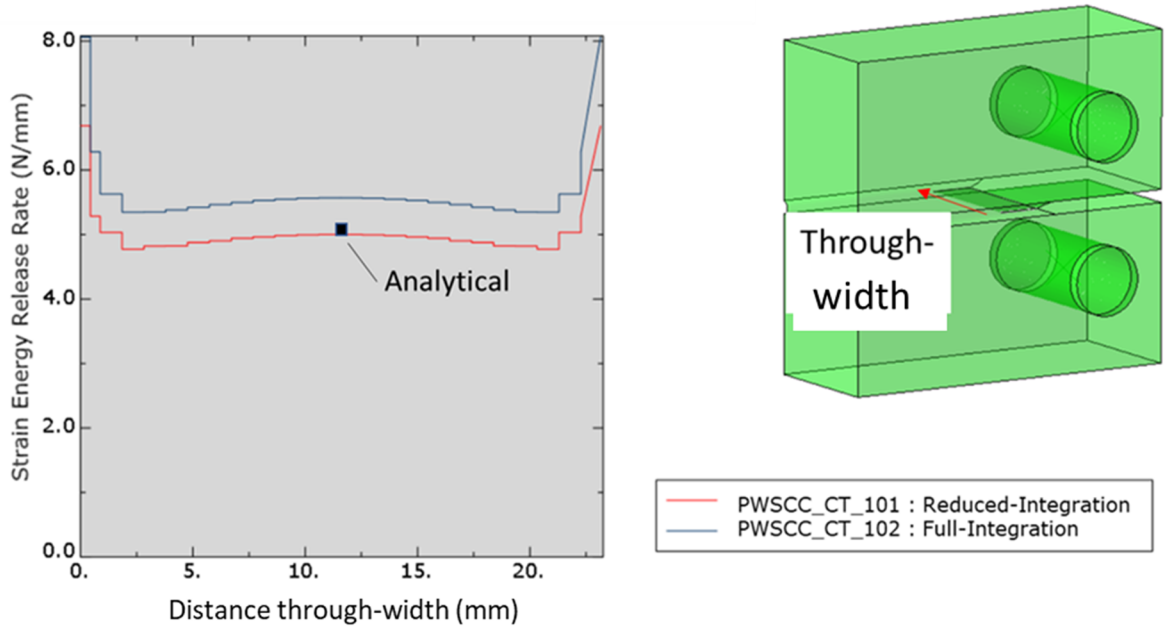

Figure D1 – Through-Thickness Variation of the Strain Energy Release Rate for the Full- (102) and Reduced integration (101) at Initial Crack Length (20-mm) as Compared to Analytical Solution

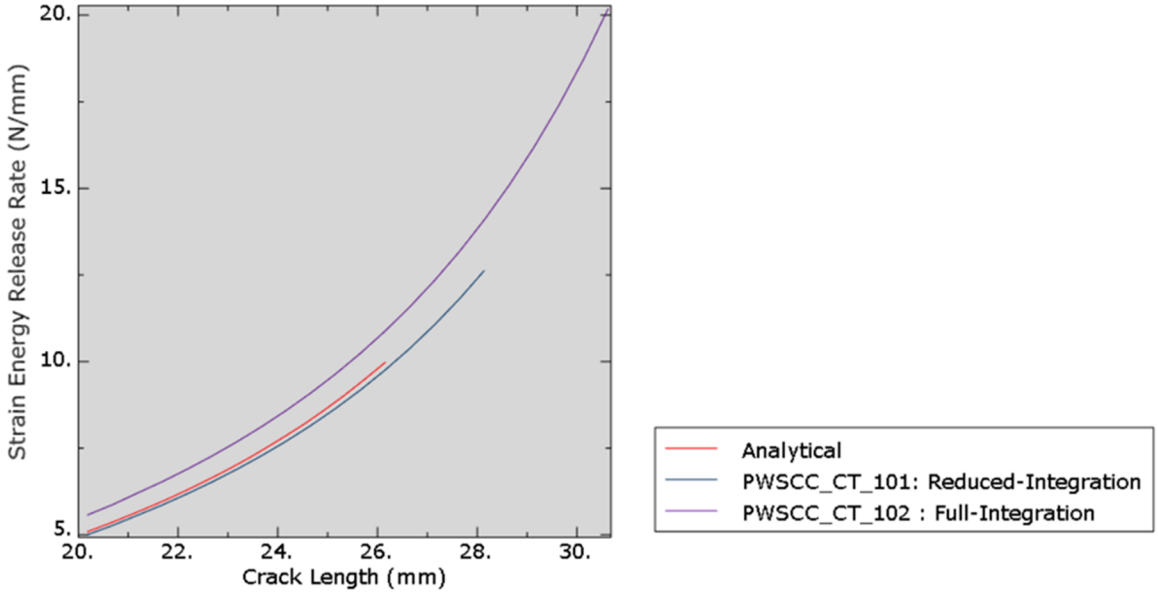

Figure D2 – Strain Energy Release Rates as a Function of Crack Length for Different Element Formulations at the Mid-Thickness Location of Crack Front

2) Influence of Crack Growth Controls on Solution Accuracy and Computational Resources

While the strain energy release rates were essentially matching between the baseline reduced integration model (PWSCC_CT_101) and the analytical solution, the predicted crack lengths as a function of exposure time were found to differ significantly as shown in Figure D3.

As was explained in Section 2.2.3, the near-tip asymptotic singularity is not considered in the Abaqus XFEM implementation, and only the displacement jump across a failed element is considered.

Therefore, the crack has to propagate across an entire element at a time to avoid the need to model the stress singularity. So, some accommodation must be made as to what to do with the elements next to the element that has reached the subcritical crack growth extension criterion. To accelerate the subcritical crack growth analysis and to provide a smooth solution for the crack front, Abaqus uses a default tolerance, ΔD_{Ntol}, of 0.1. For this application, we tighten the ΔD_{Ntol} to 0.01. As seen in Figure D3, the PWSCC_CT_103 model is seen to follow almost exactly the analytical crack growth curve. Further, a non-uniform crack front is seen in Figure D4 as compared to the perfectly straight crack front observed with the default ΔD_{Ntol} value. It is believed that the tighter controls is a numerical artifact of the tighter control whereas the default (and looser) crack growth tolerance results in a more averaged crack front.

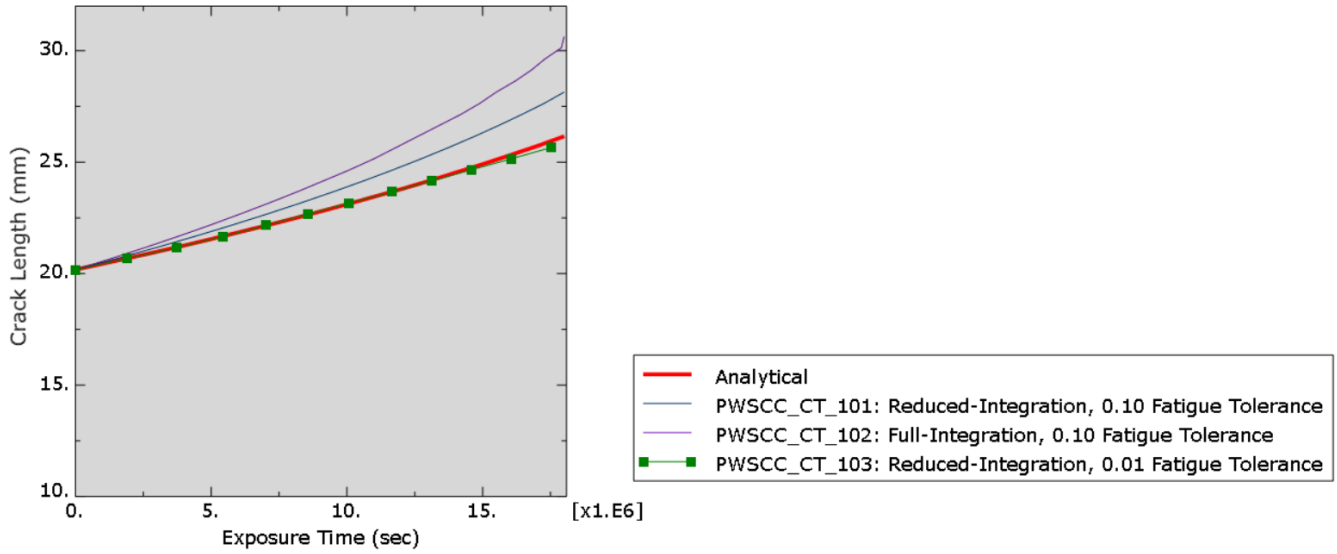

Figure D3 – Crack Length as a Function of Exposure Time for Fatigue Damage Extrapolation Tolerance Parameters

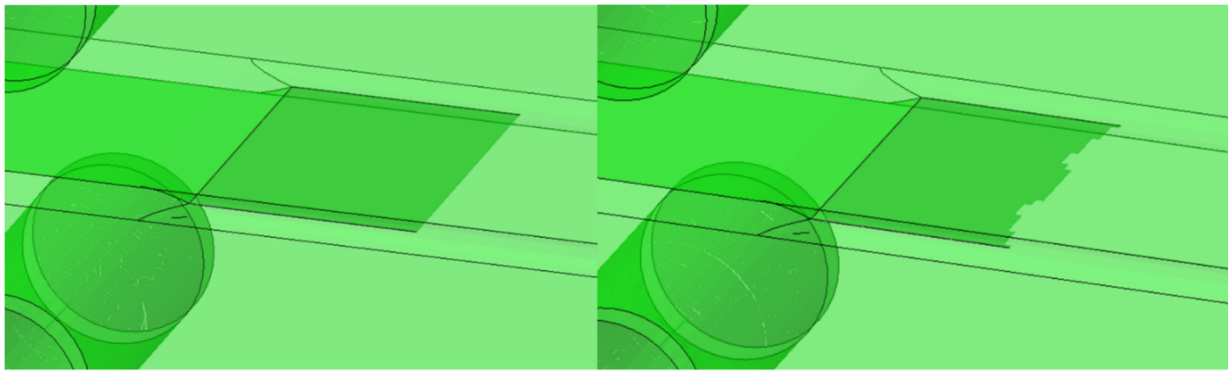

PWSCC_CT_101

PWSCC_CT_103
(Tighter Crack Growth Control)

Figure D4 – Contour Plot of Deformation showing the Influence of the Subcritical Damage Extrapolation Tolerance Parameter

There is a computational cost associated with the tighter tolerance on the damage extrapolation tolerance term. Table D1 shows that a 2.3x longer run was found to obtain the most accurate results.

Table D1 – Computational Resources for the PWSCC CT Model for Different Fatigue Damage Extrapolation Tolerance Parameters

	PWSCC_CT	
Analysis Run:	101	103
Fatigue Tolerance:	0.1	0.01
Computer Wallclock Time* (min)	45.6	104.7
Increments	35	114
Iterations	102	234

* All computer runs were made on a six-core Intel i7-8750H cpu at 2.2 GHz.

3) Key Observations from this XFEM model assessment
   - The built-in Abaqus XFEM capability can be used to model PWSCC.
   - For this 3D model, a structured, hexahedral first-order continuum element with a reduced integration formulation was the best match for the analytical results at the constrained (plane strain) location in the center of the specimen thickness.
   - In order to better match the analytical results in terms of crack growth rate and crack shape, the subcritical damage extrapolation tolerance term, ΔD_{Ntol}, was tightened to 0.01. This does result in 2.3x longer run times.
   - For this model, the default ΔD_{Ntol} was not the most accurate for crack growth rate but it will always achieve a conservative result at a reasonable computational cost. For this reason, it was chosen to be used as the general recommendation.

APPENDIX E – XFEM PWSCC MODEL: VC SUMMER AXIAL SURFACE FLAW IN HOT LEG

Description:

To provide some level of assurance with the modeling recommendations for a practical axial crack XFEM approach developed in this report, an analysis was performed for the axial PWSCC flaw (see below) that was found in the reactor pressure vessel hot leg of the V. C. Summer plant [20]. The purpose of this assessment was to examine the effect of different weld repair procedures on the resultant weld residual stresses and their potential impact on PWSCC.

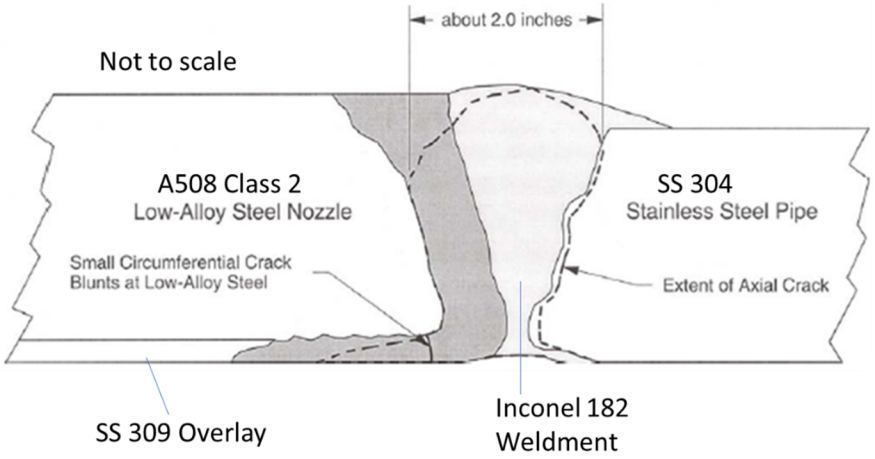

Using an axisymmetric finite element model, the weld residual stresses in the vicinity of the hot leg to reactor pressure vessel (RPV) nozzle bimetallic weld was obtained. The entire history of fabrication of the weld was included in the analysis, including the Inconel buttering, post-weld heat treatment (PWHT), weld deposition, weld grind-out and inside-out weld repair, hydro-testing, service temperature heat-up, and finally service loads. The results were then mapped onto a 360 deg finite element model of the weld joint. Within the model, a refined enrichment region, within a 5 degree slice, was defined such that an internal semi-elliptical axial flaw could be propagated using XFEM with PWSCC properties within the Alloy 182 weldment.

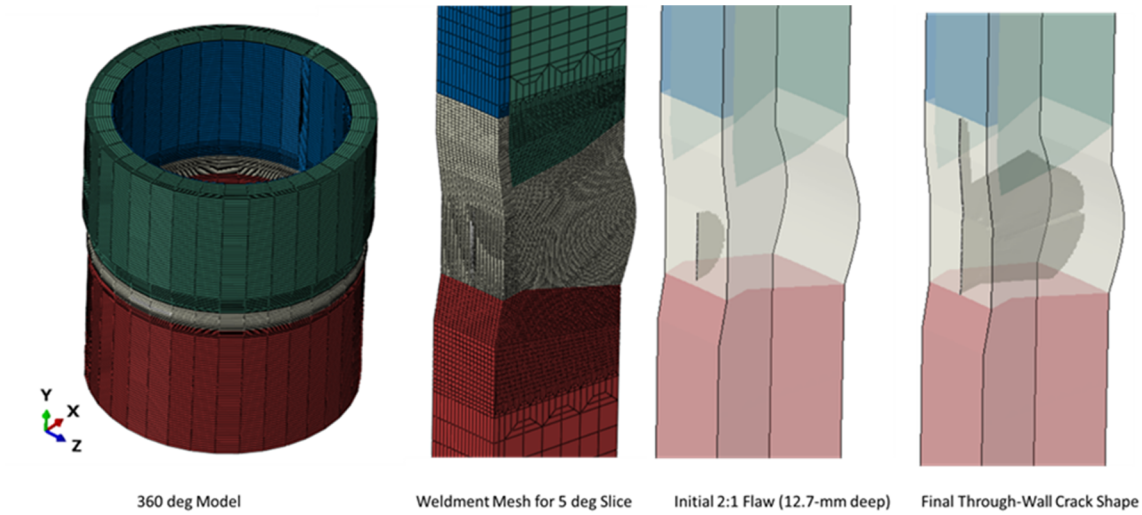

Units: N-mm-hour-MPa

FEA software: Abaqus 2020 (Build ID: 2019_09_13-12.49.31 163176)

Boundary Conditions: "Plane Sections Remain Plane" constraints were enforced at both ends of the piping via a cylindrically-oriented kinematic coupling which allowed radial dilation/contraction of the planes but constrained the other DOF.

Centered References Points control the motion for each constrained plane:

SS304 material Reference Node: $u_x=u_z=ur_x=ur_y=ur_z=0$ (y-translation free)

A508 C2 material Reference Node: $u_x= u_y=u_z=ur_x=ur_y=ur_z=0$ (fully fixed)

A tie constraint is applied to contain the 355-deg coarse mesh to the 5 deg refinement mesh which contains the XFEM enrichment region.

Loading: The residual stress profile is mapped onto the 360 deg model via the use of the *MAP SOLUTION capability. Below, the primary driving force hoop stress is shown mapped onto the refined region which contains the XFEM enrichment region.

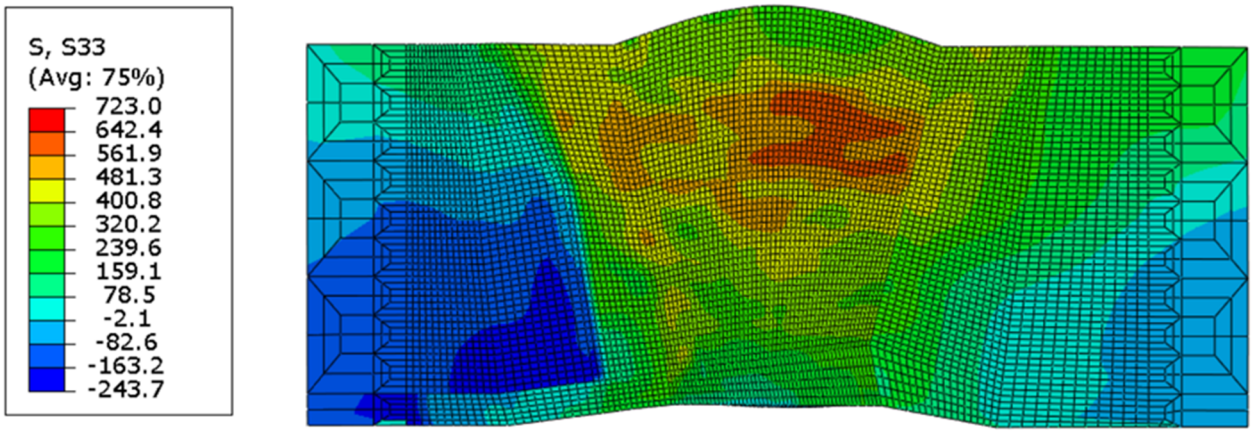

The internal faces of the pipe, including the crack face, are exposed to an internal pressure of 15.513 MPa (2250 psig).

A corresponding end cap (thrust) loading of P_y = 6734573.29 N is applied to the A508 C2 material Reference Node.

The hot leg assembly was set to a uniform temperature of 324 C.

Material: Temperature-dependent Linear Elastic Material Properties were used at 324 C for the Welded (SMA) Alloy 182, SS 309, SS 304 and A508 Class 2 materials.

For the Welded (SMA) Alloy 182 in PWR water conditions which is subject to the PWSCC mechanism, the MRP-115 [21] crack growth rate (75th percentile) for Alloy 182 was adopted in the present study at 324 C.

$$\frac{da}{dt} = 2.0611 \cdot 10^{-3}\, K^{1.6}$$

when $\frac{da}{dt}$ is in in/year and K is in ksiVin units. In this particular work, no K threshold is utilized and hence,

Using the Appendix F Excel tool to convert between unit systems and parameters, the following equation was then used for the required strain energy release rate crack growth relation:

$$\frac{da}{dt} = 4.0516 \cdot 10^{-4}\, G^{0.8}$$

when $\frac{da}{dt}$ is in mm/hour and G is in N/mm units.

Analysis Steps:

As a precursor to the XFEM assessment, the axisymmetric welding residual model was provided followed by 360 deg model generation and results transfer. As these modeling details are of secondary importance for the XFEM assessment, only the necessary restart files are provided in the Supplemental Files. Then, with the use of the *MAP SOLUTION capability, the solution was mapped onto a new 360 deg 3-D model that contained a 5 deg slice refined section with the enriched region with a 2:1 initial XFEM flaw size (12.7-mm deep). Using the relationship between the simplified fatigue procedure and PWSCC to establish modified constants depicted in Section 2.2.3 of this report, a *FATIGUE,TYPE=SIMPLIFIED procedure was then used to grow the crack in an Abaqus/Standard simulation.

The XFEM analysis is completed in two analysis steps:

1) *STATIC preload the structure to maximum value.

2) *FATIGUE, TYPE=SIMPLIFIED

Elements: C3D8R - 3D first-order 8-node continuum elements with reduced integration were used.

Meshes: A single highly refined structured mesh (1.0-mm x 1.0-mm in the plane of the crack) was utilized within the 5 deg mesh region that contains the enrichment zone and initial flaw. In the remaining of the model, a 5-mm x 5-mm in-plane mesh was used with 36 elements in the circumferential direction.

Parameters Studied:

In addition to the baseline assessment which incorporated the general recommendations, independent analyses were used to evaluate fracture control and crack growth damage extrapolation tolerance controls influences on the run times, crack growth rates and shapes.

VC Summer Hot Leg DWM Nozzle	Mesh Refinement	Element Formulation	Mesh Type	Crack Growth Position	Crack Growth ANGLEMAX	Damage Extrapolation Tolerance	Controls Disp Correction	Abaqus Input File Name
Baseline	Normal (60-elems)	Reduced	Structured	Default	-	0.1 (Default)	0.01 (Default)	VCSummer_ 101
Crack Growth Controls								
*FRACTURE CRITERION, POSITION=								
Nonlocal	N	R	S	Nonlocal	85	0.1	0.01	VCSummer_ 102
*FATIGUE damage extrapolation tolerance								
0.175	N	R	S	Default	-	0.175	0.01	VCSummer_ 103
0.01	N	R	S	Default	-	0.01	0.01	VCSummer_ 104
Mesh Refinement (Structural Height)								
Coarse (2x Mesh seed Size)	N	R	S	Default	-	0.1	0.01	VCSummer_ 105

	Crack Type	Mesh Type	Driving Force Extraction	Material	Loading	Abaqus Input File Name
SIF Solution Comparison (stationary intial flaw with a/t=0.2)						
	Stationary	Focused-Mesh FEA	J-Integral	Inco 182	Pressure Only	VCSummer_ 201
	Propagating	Structured-Mesh XFEM	modified VCCT	Inco 182	Pressure Only	VCSummer_ 202
	Stationary	Structured-Mesh XFEM	modified VCCT	Inco 182	Pressure Only	VCSummer_ 203
	Propagating	Structured-Mesh XFEM	modified VCCT	All	Pressure Only	VCSummer_ 204

Available Benchmark Result:

The V.C. Summer hot leg dissimilar metal v-groove weld axial crack evaluation was evaluated using the Advanced Finite Element Analysis (AFEA) methodology following the work of Shim [22].

As first introduced in the Task 1 report, the so called Advanced Finite Element Analysis (AFEA) has been developed and used to model the 'natural crack growth' in simple geometries such as pipe components. AFEA consists of calculating stress intensity factors at numerous points along the crack, growing the crack at each point, development of a new automatic finite element mesh to produce the next crack size and shape, calculating the stress intensity factor along the crack front, and growing the crack further. The AFEA process requires an automated finite element mesh generator and the entire process is managed with a controlling script (e.g. Python). The script develops a mesh for the current crack size, produces a finite element model based input file, submits the finite element job, extracts results (especially stress intensity factors along the crack front), grows the crack at points along the crack, develops next mesh, and so on until the crack grows through-thickness. This growth process typically requires tens of focused 'spider' crack meshes to be developed and often takes insignificant solution to model crack growth to a through-wall. Because each solution is elastic, the solution time is manageable. The ability of AFEA to handle the elastic stress intensity factor that PWSCC is characterized by along with a mapped welding residual stress as an elastic field was key in developing this for production-capable assessments.

In this benchmark, the axisymmetric weld residual stress field described previously for the actual configuration was mapped onto a simplified 180-degree pipe with a uniform thickness and three distinct regions representing the A508C2 pipe, Alloy 182 weldment and SS 304 pipe. Seen in Figure E1, eleven distinct time points were used to evaluate planar crack extension of this axial flaw. The time to reach through-wall was estimated to be 1.18 years.

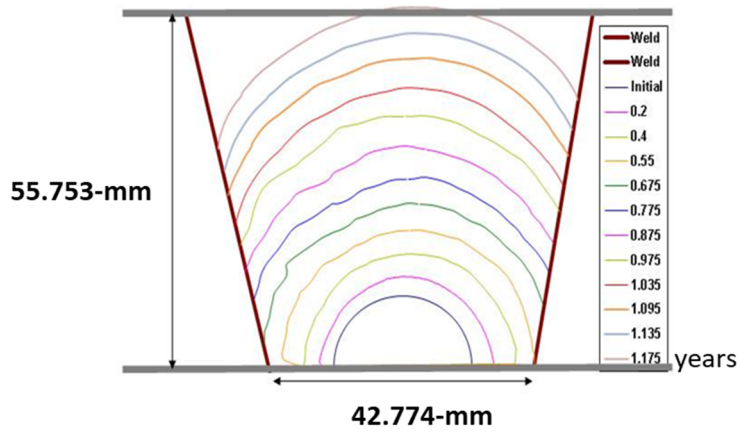

Figure E1 - Crack Shape Evolution as Function of Time for the Advanced Finite Element Analysis (AFEA) of the PWSCC VC Summer Axial Surface Flaw in DWM Hot Leg

Results:

1) Comparison of SIF Geometry Correction Factors between Publication (API-579 [24]), AFEA Focused Crack Tip Mesh in Abaqus and Structured Meshes with XFEM Crack Propagation

   To verify the general modeling recommendations in terms of crack driving force, a stress energy release rate sensitivity study was undertaken. Since the VC Summer DWM hot leg is a multi-material geometrically complex component, some simplifications were required. Fortunately, the API-579 [24] regulatory fitness-for-service code provides a standard weight-function based stress intensity factor benchmark in Section 9B.5.10 for a semi-elliptical internal, surface flaw subjected to pressure in a straight pipe. For our needs, a one-hour fatigue check for the VC Summer XFEM model was performed with the entire component being modeled as Inconel 182 and without the residual stress but still maintaining the internal pressure including the crack face pressure. Table E1 summarizes the results as a function of position along the crack front for the initial flaw (a/t=0.2 with 2c/a=2). As can be seen, the XFEM ENRRTXFEM output variable shows reasonable correlation (within 8% away from the surface) along the crack front when compared to the regulatory fitness-for-service benchmark. When the simplified subcritical crack growth procedure is changed to a static procedure such that the contour integral could be evaluated for a stationary crack, the strain energy release rates are also seen to be comparable. In addition, the initial flaw size was evaluated in a second-order, reduced-integration model with a 1/r-singularity employed at the crack tip in a manner that is consistent with the AFEA solution. Similar to the stationary-crack XFEM contour integral model, strain energy release rates are seen to correlate well with the published benchmark and XFEM solutions.

Table E1 : Comparison of Strain Energy Release Rate (units: N/mm) for an internal axial elliptical flaw (2c/2=2, a/t=0.2) utilizing a Published Benchmark[24] along with Stationary and Propagating Crack Extraction Techniques in Abaqus with Pressure Loading Only

Analysis Run:	VCSummer_	202	203	201
	Published	**XFEM**		**AFEA**
	Benchmark	**Propagating**	**Stationary**	**Stationary**
Crack	**API-579**	**ENRRTXFEM**	**J-Integral**	**J-Integral**
Front	Straight Pipe	VCSummer	VCSummer	Straight Pipe
Angle	Pressure Only	Pressure Only	Pressure Only	Pressure Only
(deg)	INCO only	INCO only	INCO only	INCO only
0	1.456	1.382	1.317	1.308
45		1.125	1.068	1.067
90	1.064	0.976	0.995	1.062
135		1.103	1.084	1.104
180	1.456	1.025	1.349	1.307

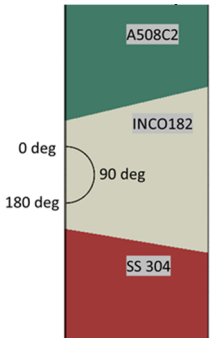

To continue the calculated driving force work in a generalized sense, the inclusion of the different materials as opposed to just a single material (Inconel 182) and the inclusion of welding residual stress values are tabulated as seen in Table E2. With the influence of single versus multi-material differences being minimal, the weld residual stresses are seen to be the dominant load at smaller crack sizes.

Table E2: Comparison of Strain Energy Release Rate for an internal axial elliptical flaw (2c/a=2, a/t=0.2) in the VC Summer DWM Surge Nozzle illustrating influence of Weld Residua Stress

Analysis Run:	202	204	101
		XFEM	
	Propagating	**Propagating**	**Propagating**
Crack	**ENRRTXFEM**	**ENRRTXFEM**	**ENRRTXFEM**
Front	VCSummer	VCSummer	VCSummer
Angle	Pressure Only	Pressure Only	WRS+Press
(deg)	INCO only	4-material	4-material
0	1.382	1.493	4.350
45	1.125	1.394	5.570
90	0.976	1.149	6.900
135	1.103	1.208	7.090
180	1.025	1.193	6.000

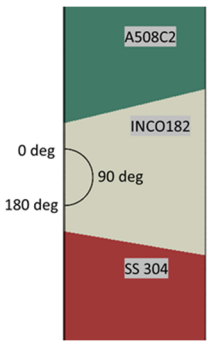

To summarize, acceptable crack driving force correlation (G values within ~8%) is seen between a published benchmark (API-579 [24]), AFEA-type focused crack-tip mesh in Abaqus and structured meshes with XFEM crack propagation. Further, the welding residual stress have been confirmed to be the dominant loading for smaller crack sizes.

2) Baseline Results Compared with Advanced Finite Element Analysis (AFEA) and Post-Mortem Crack Shape from Actual Defect

Figure E2 shows the crack shape evolution as a function of time for the PWSCC VC Summer axial surface flaw in the DWM hot leg XFEM assessment. As expected, the shape of the XFEM crack growth was driven by the hoop weld residual stress (WRS). This is seen in the figure as the early-stage crack growth at a given time is in the depth direction vs the in-plane length. Further, the location of the actual wall penetration (Figure E3) coincides with the high stress location of the XFEM predicted results.

Also, in Figure E3, results from the linear elastic natural crack growth (AFEA) analysis are shown overlaid on the final XFEM results. The AFEA approach shows the time to reach through-wall is 1.18 years while the baseline XFEM analysis is 1.20 years. Of course, there are differences between the two approaches. This includes such geometrical differences where XFEM uses the actual non-uniform thickness piping along with a crown on the weldment whereas the AFEA solution uses a straight pipe. Furthermore, while the initial flaw depth ratio (a/t) of 0.2 was used for both assessments, the actual depth value of 12.7-mm is used for the XFEM model and 11.15-mm is used for the AFEA. Other numerical differences exist such as the crack driving force extraction procedure (modified VCCT for the propagating XFEM analysis versus the contour integral extraction for instantaneous AFEA analysis). Despite the differences in the approaches, the overall comparison is seen to be quite good.

Still, there is some level of concern with the XFEM simulations associated with slight out-of-plane oscillatory deformations. Figure E4 demonstrates the observed slight out-of-plane deformations which occurred primarily, but not exclusively, at the edge of the enriched regions. As indicated in this figure, Abaqus is seen to abort at 99% of the through-wall thickness for the baseline analysis (VCSummer_101) at an element near the edge of the enriched region. As noted in the figure, some of the other sensitivity analyses also encountered premature failure of the analysis.

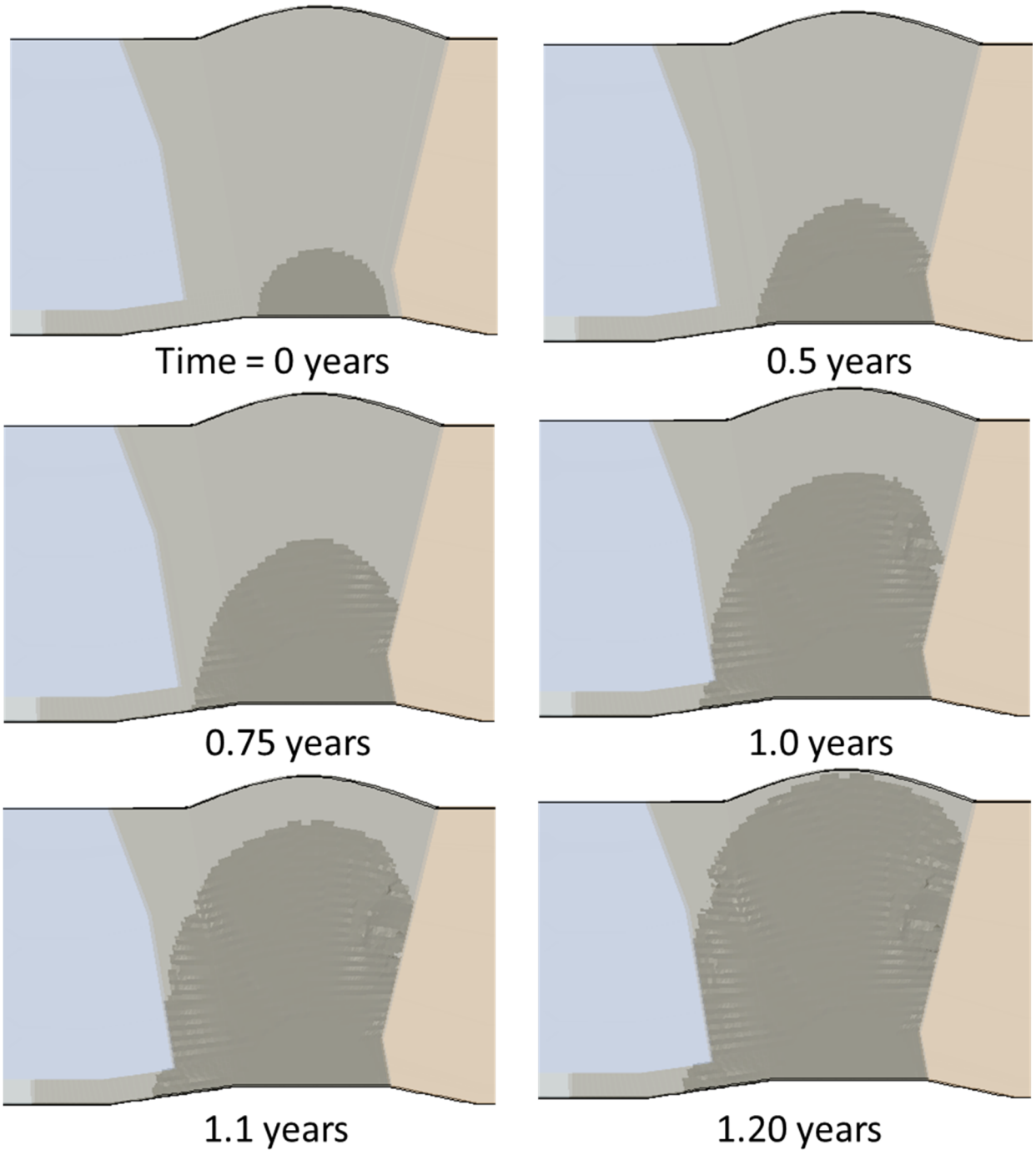

Figure E2 - Crack Shape Evolution as Function of Time for Baseline PWSCC VC Summer Axial Surface Flaw in DWM Hot Leg XFEM Assessment

Figure E3 - Overlay of Natural Crack (Advanced FEA approach) Shape on the Baseline XFEM assessment along with Post-Mortem Crack Shape [20] for PWSCC VC Summer Axial Surface Flaw in DWM Hot Leg

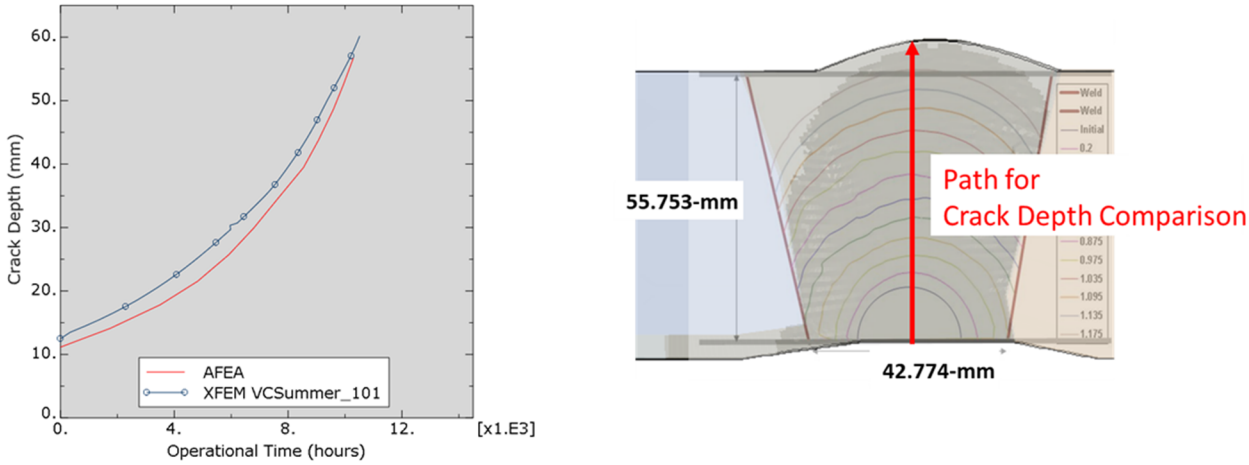

Figure E4 - Comparison of Crack Growth at Deepest Point as a Function of Time between Advanced Finite Element Analysis (AFEA) [23] and XFEM for PWSCC VC Summer Axial Surface Flaw in DWM Hot Leg

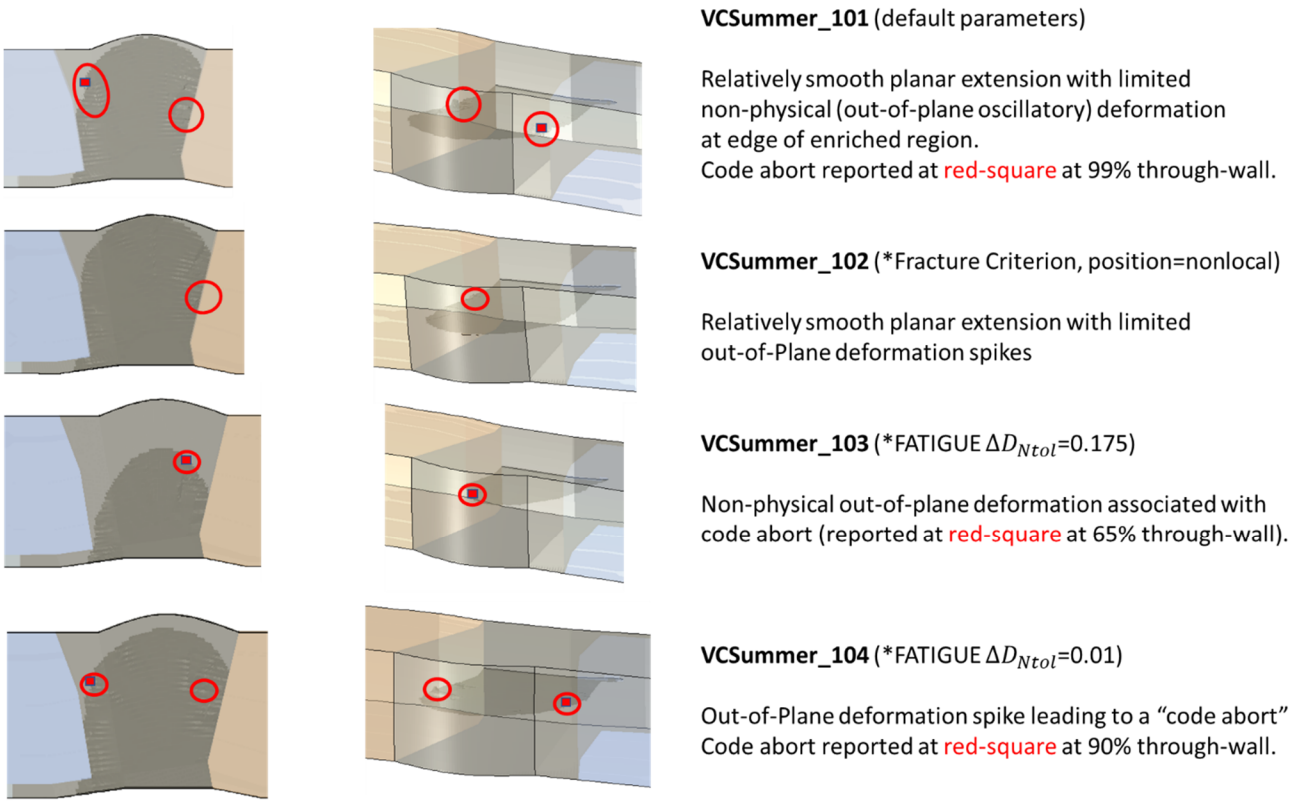

Figure E5 - Observed Out-of-Plane Crack Growth for PWSCC VC Summer Axial Surface Flaw in DWM Hot Leg XFEM Assessments

3) Crack Extension (*Fracture Criterion : Default versus POSITION=Nonlocal)

In attempt to maintain a smooth, continuous three-dimensional crack front, the nonlocal averaging was used in VCSummer_102. However, minimal changes were observed in the crack shape (Figure E5) and crack growth rate (Figure E6) for this near planar crack extension problem.

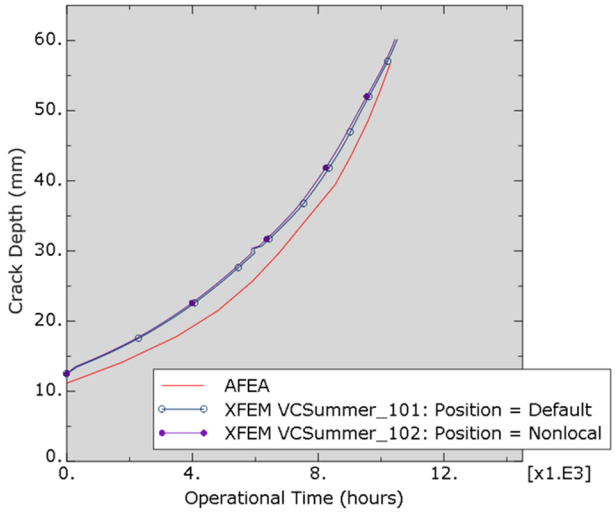

Figure E6 - Influence of Crack Growth POSITION Parameter on Crack Growth at Deepest Point as a Function of Time for PWSCC VC Summer Axial Surface Flaw in DWM Hot Leg

4) Subcritical Damage Extrapolation Tolerance Parameter

For longer running analyses, the damage extrapolation tolerance parameter, ΔD_{Ntol}, can be used to accelerate the subcritical crack growth analysis and to provide a smooth solution for the crack front. Figure E7 shows that increasing ΔD_{Ntol} to 0.175 from the default of 0.1 does increase the crack growth rate while crack shapes at the same crack depth are seen to be deviated significantly from the baseline XFEM analysis. Further, when ΔD_{Ntol} is set to 0.175, a code abort is observed at an out-of-plane oscillatory (numerical artifact) deformation near the edge of the enrichment region at approximately the 60% of through-wall crack depth . When ΔD_{Ntol} is set to a tight value of 0.01, minimal changes are noted with baseline analysis in terms of crack growth rate and crack shape.

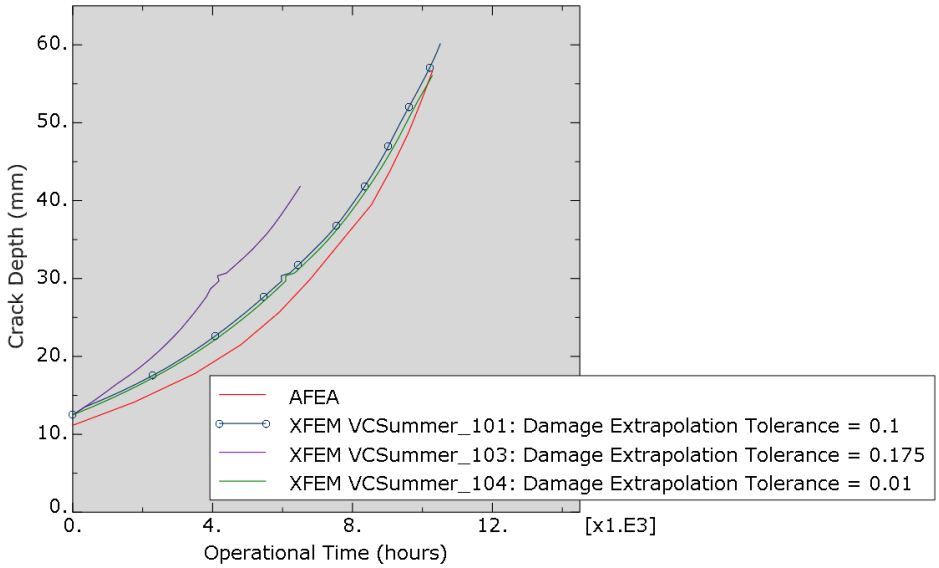

Figure E7 - Influence of Crack Growth Damage Extrapolation Tolerance Parameter on Crack Growth at Deepest Point as a Function of Time for PWSCC VC Summer Axial Surface Flaw in DWM Hot Leg

5) Importance of Mesh Seed Size in Structural Height Direction

As was defined in the main body of the report in Figure 7(c), the enriched region structural height (hoop-direction) region mesh seed was investigated using the recommended 1-mm mesh seed (baseline) and a coarser 2-mm mesh seed. Figure E8 shows the importance of maintaining the recommended mesh refinement in the structural height direction as the time to reach through-wall is predicted to increase by over 30% with the coarse mesh seed. Unlike the stationary crack contour integral (J-Integral) and interaction integral (stress intensity factor, K) where fairly coarse meshes are able to capture path independent driving force values, the propagating crack values are calculated for each crack front element with the linear-elastic strain energy release rate, G, directly using the modified VCCT method, and, hence, require a nearly perfect cube shape as provided in the recommended meshing parameters.

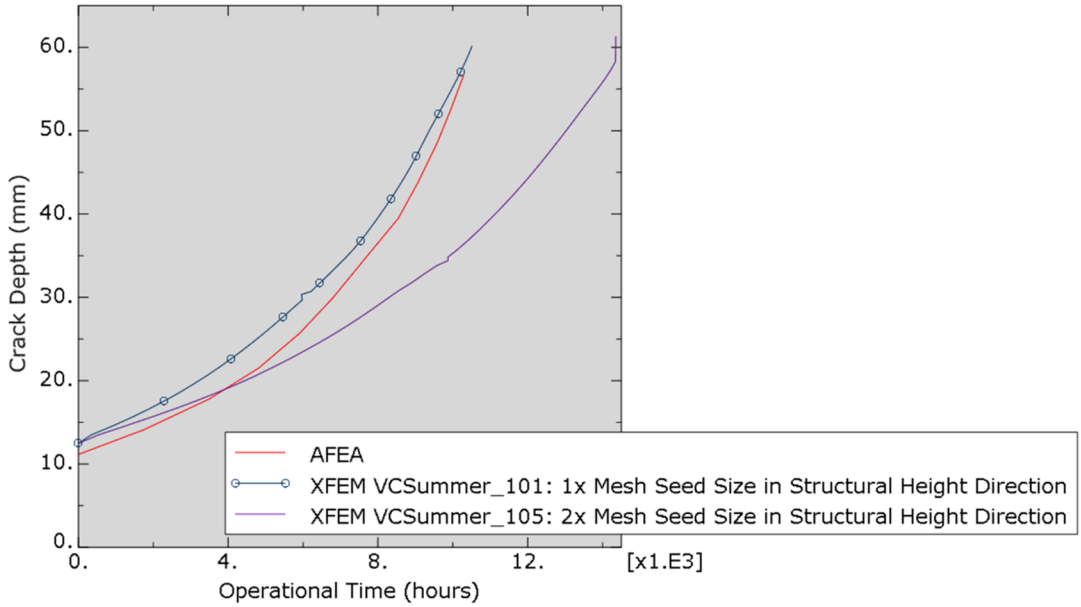

Figure E8 - Influence of Mesh Seed Size in Structural Height Direction on Crack Growth at Deepest Point as a Function of Time for PWSCC VC Summer Axial Surface Flaw in DWM Hot Leg

6) Computational Cost

In terms of computational cost, Table E3 shows the XFEM capability is computationally expensive. With the current Abaqus XFEM implementation, it is possible to achieve analysis runs in under one-day by utilizing multi-core simulations. Further, by increasing the ΔD_{Ntol} to increased values (e.g. 0.175 or 0.25), the runtimes can by reduced by approximately 2x while ensuring that a more conservative crack growth rate is obtained. This may be of benefit when a rough estimate, but not necessarily the most accurate, solution is required. However, it was seen in this final set of runs for the VC Summer analysis, that premature failure of the Abaqus simulation due to an internal code error did occur when the ΔD_{Ntol} was set to 0.175.

Table E3 – Computational Resources for the PWSCC VC Summer Axial Surface Flaw in DWM Hot Leg XFEM for Different Crack Extension Parameters

	VC_Summer	
Analysis Run:	101	102
Position:	Default	Nonlocal
Damage Extrapolation Tolerance:	0.1	0.1
Computer Wallclock Time* (hrs)	19.15	19.58
Increments	4415	4531
Iterations	4415	4531

* All computer runs were made with 10-cores with an Intel® Xeon® Gold 6148 2.4GHz chip on RHEL 7.5

In relation to other numerical techniques, such as the linear elastic natural crack growth approach, those solutions will be faster from a processor time perspective (on the order of a dozen solver passes). However, unless proper scripting algorithms exist, the setup time will likely reduce the total analysis time advantage.

7) Key Observations from this XFEM model assessment

- Using the general XFEM modeling recommendations, the built-in Abaqus XFEM capability has shown to be robust for modeling a relatively complex PWSCC application. The final through-wall crack shape was found to be similar to the experimentally reported crack shape.
- The importance of maintaining the recommended mesh refinement in the structural height direction was shown during this study.
- While using essentially the same linear elastic modeling assumptions associated with crack growth, the XFEM approach was found to conservatively bound the AFEA solution.

APPENDIX F – PARAMETER AND UNIT CONVERSION EXCEL TOOL

Provided in the Supplemental Files is a unit and parameter conversion tool for driving force (K-to-G and G-to-K) and Paris Law (ΔK-to-ΔG and ΔG-to-ΔK) coefficients. This tool can be used for cycle-dependent (i.e. fatigue) and time-dependent (e.g. PWSCC) Paris-like crack growth relations.

For this capability, we have coded a Visual Basic macro within Excel. Step-by-Step instructions are provided within the spreadsheet. This tool can be used as a standalone spreadsheet or embedded within a website. Please note that there are limited error checks in place to trap data input errors.

As an example for the crack growth relation, we can review the Miranda [15] work where the SAE 1020 fatigue constants were given in the same general form as:

$$\frac{da}{dN} = 4.5 \cdot 10^{-10} \Delta K^{2.1}$$

with $\frac{da}{dN}$ in m/cycle and ΔK in $MPa\sqrt{m}$.

Going through the necessary plain-strain conversion for a pure N-m unit system, the Paris Law-like ΔG relation required by Abaqus becomes:

$$\frac{da}{dN} = 9.1685 \cdot 10^{-11} \Delta G^{1.05}$$

with $\frac{da}{dN}$ in m/cycle and ΔG in $\frac{N}{m}$.

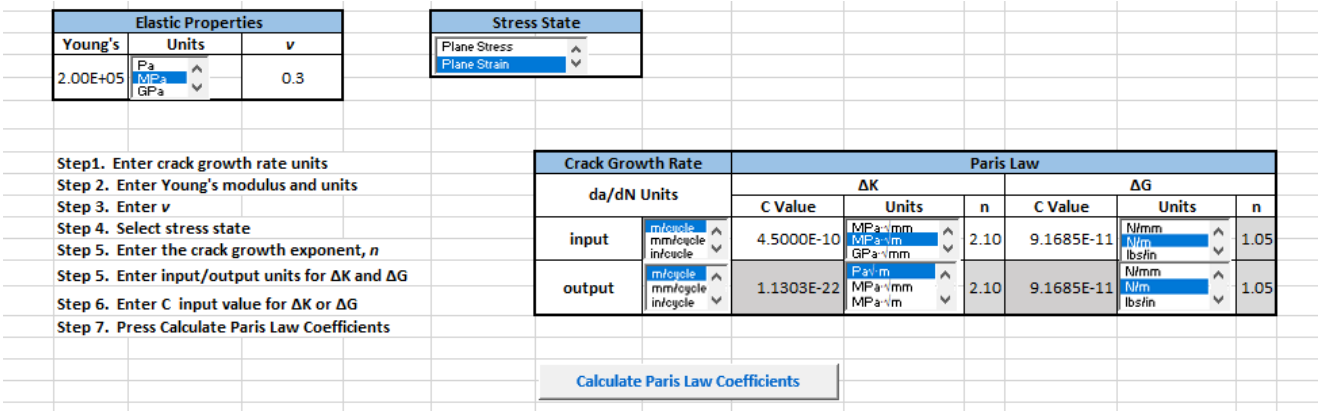

In an analogous manner, the fracture driving force (or toughness) can be converted between common units of K and G. Shown below, a fracture toughness of K=100 $MPa\sqrt{m}$ is converted to K=91.0 $ksi\sqrt{in}$, G=4.55E4 N/m and G=259.81 lbsf/in.